Ecosystem and Large-Scale Climate Impacts of Plant Leaf Dynamics

Marlies Kovenock

A dissertation
submitted in partial fulfillment of the
requirements for the degree of

Doctor of Philosophy

University of Washington

2019

Reading Committee:

Abigail L.S. Swann, Chair

Janneke Hille Ris Lambers

Curtis A. Deutsch

Program Authorized to Offer Degree:
Biology

University of Washington

Abstract

Ecosystem and Large-Scale Climate Impacts of
Plant Leaf Dynamics

Marlies Kovenock

Chair of the Supervisory Committee:
Chair Abigail L.S. Swann
Atmospheric Sciences and Biology

Vegetation modifies Earth's climate by controlling the fluxes of energy, carbon, and water. Of critical importance is a better understanding of how vegetation responses to climate change will feedback on climate. Observations show that plant leaf traits respond to elevated carbon dioxide concentrations. These leaf trait responses have the potential to modify plant functioning and competitive dynamics, and could therefore alter carbon cycling and surface energy fluxes with implications for regional and global climate. Yet the climate impacts of changes in leaf structural traits — such as increases in leaf mass per area and leaf carbon to nitrogen ratio — in response to elevated carbon dioxide are not included in most climate projections and remain to be tested and quantified.

Here we show that one leaf trait response to elevated carbon dioxide — a one-third increase in leaf mass per area — significantly impacts climate and carbon cycling in Earth system model simulations. Higher leaf mass per area enhances warming in response to elevated carbon dioxide by reducing the increase in leaf area, which lowers carbon uptake and evapotranspirative cooling by plants and leads to enhanced solar radiation absorbed at the Earth's surface. Our results suggest that leaf trait responses to carbon dioxide should be considered in climate projections and provide additional motivation for ecological and physiological experiments that improve our mechanistic understanding of plant responses to

environment.

Tropical forests exert extensive control over global energy, carbon, and water fluxes and thus play a critical role in determining future climate. Using an ensemble of demographic vegetation model simulations we quantify the influence of two leaf trait responses to elevated carbon dioxide — increases in leaf mass per area and leaf carbon to nitrogen ratio — on tropical forest functioning and competitive dynamics. We find that consideration of these leaf trait responses reduces projected carbon uptake and evapotranspirative cooling when plant type abundance is held invariant with time. However, given that more competitively advantageous leaf trait responses also maintain higher levels of plant productivity and evapotranspiration, including changes in plant type abundance may mitigate these decreases in ecosystem functioning. Models that explicitly represent competition between plants and leaf responses to elevated carbon dioxide are needed to capture these influences on tropical forest functioning and large-scale climate.

Lastly, we improve the simulation of present-day tropical forest functioning and structure in a demographic vegetation model by including a gradient of leaf mass per area with canopy depth, following observations. By benchmarking the modified model's performance against observations at a tropical forest test site across nearly 300 plausible plant trait parameterizations, we identify high-performing parameter sets and areas for further model development.

TABLE OF CONTENTS

LIST OF FIGURES

LIST OF TABLES

ACKNOWLEDGMENTS

This dissertation would not have been possible without the support of many people. Foremost, I wish to thank my advisor Abigail Swann for her exceptional mentorship. I am truly fortunate to have been her student. Thank you also to the Ecoclimate Lab, in particular Jennifer Hsiao, Marysa Laguë, Greg Quetin, and Elizabeth Garcia; my co-authors Charles Koven, Ryan Knox, and Rosie Fisher; and my graduate committee members Elizabeth Van Volkenburgh, Soo-Hyung Kim, Janneke Hille Ris Lambers, and Curtis Deutsch for helping me to craft this work. From nascent ideas to peer review, I have truly valued our discussions and your support. My sincere thanks also goes to the many colleagues at the University of Washington who provided interesting discussions, sounding boards, and friendships over the years — Will King, Katie Dobkowski, Amber Hageman, Johanna Cantillo Polo, Darshi Banan, Leander Anderegg, Ian Breckheimer, Leonard Jones, Katrina Van Raay, Isabel McCoy, Sam Pennypacker, Lucas Zeppetello, and many others. Thank you also to the terrestrial sciences group at the National Center for Atmospheric Research, particularly Gordon Bonan, Dave Lawrence, and Danica Lombardozzi, for many interesting discussions and creating a welcoming community. I also want to thank my pre-graduate school colleagues at the University of California and the California Institute of Technology — Paul Tarr for his mentorship and Jiwon Gwak, Rachel Li, Adam Krantz, and Patrick Pearce for their camaraderie. Thank you also to Kristen Laskaris for excellent career advice and encouraging me to pursue my interests and to Jan Hendrickson-Smith for unparalleled guidance across a breadth of fields over many years.

Last but certainly not least, I wish to thank my family. To my husband and best friend, Evan Tuck, thank you from the bottom of my heart for your encouragement and partnership.

I would not have done this without you. An enormous amount of gratitude also goes to my parents, Renate Mallus-Médot and Dan Kovenock; grandmother, Judy Kovenock; sister, Hanna Kovenock; mother-in-law, Joanmarie Curran; and dear friends Leanne Greenberg, Francesca Baldassano, Michelle Dennis, and Melissa Lacey for continually inspiring me to dream and backing it up with encouragement and loving support. Lastly, thank you to Adi for bringing me tremendous joy and the extra bit of motivation needed to complete this dissertation.

DEDICATION

To my grandmother, Judith Kovenock

Chapter 1
INTRODUCTION

This dissertation examines the interaction between vegetation and climate. That plants respond to environmental drivers is widely appreciated. Nearly everyone has noticed plants responding to their environment, whether it is flowers blooming with the coming of spring or grass browning at the end of a dry summer. That plants also strongly influence large-scale climate — by modifying the fluxes of energy, carbon, and water at the Earth's surface [e.g., Bonan, 2008] — is less widely considered. The cyclical nature of the plant-climate relationship means that plant responses to environmental change have the potential to feedback on, and alter, large-scale climate.

Feedbacks between vegetation and climate change are of critical importance to future climate projections but remain highly uncertain [e.g., Friedlingstein et al., 2014]. Rising atmospheric carbon dioxide concentrations, due to human activities such as fossil fuel burning, are causing climate change by enhancing radiative warming of the Earth's surface. Climate change policy, mitigation, and adaptation strategies rely on Earth system model projections of 21st century climate. However, these projections are highly variable. Even for the same carbon dioxide emissions scenario, there is large uncertainty across these models about the amount of carbon dioxide that will remain in the atmosphere and, thus, the resulting amount of expected warming. This uncertainty stems in large part from differences in how these models represent plants and their responses to changes in environmental drivers, such as rising atmospheric carbon dioxide concentrations. Identifying which plant responses to environmental drivers matter most for future climate and how to accurately include them in Earth system models can help reduce this uncertainty.

Incorporating observations of plant trait distributions and their responses to environmental drivers into Earth system models has been proposed as a way to improve predictions of plant influences on climate [e.g., Kattge et al., 2011, Verheijen et al., 2013, 2015, Reich et al., 2014, Fisher et al., 2015]. Previous studies have found that the responses of leaf-level rates of carbon and water fluxes (i.e., photosynthesis and stomatal conductance) to elevated carbon dioxide have profound effects on large-scale climate [e.g., Sellers et al., 1996, Pu and Dickinson, 2012]. Other studies have shown that changes in climate can shift the relative abundance of different plant types within an ecosystem with implications for overall ecosystem functioning and, thus, large-scale climate [e.g., Cox et al., 2000, Levine et al., 2016].

The response of leaf structural traits to elevated carbon dioxide could similarly influence ecosystem functioning and large-scale climate. However, to date, the potential climate impacts of these leaf structural trait responses are not fully understood. Among the most widely observed changes in leaf structural traits in response to elevated carbon dioxide are increases in the ratios of leaf mass to area and leaf carbon to nitrogen. These leaf trait responses have been observed in a wide range of plant types across biomes and continents [e.g., Poorter et al., 2009, Ainsworth and Long, 2005, Medlyn et al., 2015] and could therefore have wide-ranging influences on plant functioning and climate. Leaf structural trait changes could directly alter climate by modifying leaf-level carbon and water fluxes, as well as leaf area, which provides the surface area over which these leaf-level processes are summed. These leaf structural changes may also indirectly modify climate. Changes in plant functioning and leaf area could impact competition among plants for light, which may influence the relative abundance of different plant types. Since plant types differ in their rates of functioning, changes in the relative abundance of plant types could alter the influence of plants on climate.

Despite the wide observance of changes in leaf structural traits in response to elevated carbon dioxide, the influence of these leaf dynamics on climate is not included in many climate projections and remains to be tested and quantified. This dissertation contributes to this line of research by investigating how the responses of three leaf structural traits — leaf

mass per area, leaf carbon to nitrogen ratio, and leaf nitrogen per area — to elevated carbon dioxide impact ecosystems and large-scale climate. We consider both the direct and indirect impacts on ecosystems and climate using Earth system model and demographic vegetation model simulations.

The remainder of this introductory chapter provides background information on how plants influence climate; how vegetation responses to elevated carbon dioxide are expected to alter the influence of plants on climate; and the three leaf trait responses examined in this dissertation and their potential effect on climate. This chapter also discusses the tools we use to study the influences of leaf trait changes on ecosystems and climate.

1.1 Plant influences on climate

Plants influence climate by modifying the fluxes of carbon, water, and energy at the Earth's surface. This dissertation focuses on two ways in which plants control these fluxes: the uptake of carbon dioxide from the atmosphere through photosynthesis (net primary productivity) and the cooling of the Earth's surface through evapotranspiration. The remainder of this chapter may also refer to these two processes (net primary productivity and evapotranspiration) as ecosystem functioning.

1.1.1 Carbon uptake

Plants remove carbon dioxide from the atmosphere through the process of photosynthesis. Some of the carbon captured through photosynthesis is stored as biomass, some is respired back into the atmosphere as plants use sugars to fuel their metabolic processes. The amount of carbon dioxide captured during photosynthesis minus the amount respired back into the atmosphere is referred to as net primary productivity. We use net primary productivity in this dissertation to quantify the amount of carbon dioxide vegetation removes from the atmosphere. Greater net primary productivity means that plants remove more carbon dioxide from the atmosphere, which reduces radiative warming of the Earth and thus has a cooling effect.

1.1.2 Evapotranspirative cooling

Evapotranspiration is the flux of water from the Earth's surface to the atmosphere. Evapotranspiration is comprised of three terms: transpiration, the evaporation of water from the surface of leaves, and the evaporation of soil water. Transpiration is the biologically controlled flux of water from soil through plants into the atmosphere. It occurs as plants open pores on their leaves to allow carbon dioxide in for photosynthesis, simultaneously allowing water vapor inside the leaf to move through these pores into the atmosphere. Vegetation also exerts control over the amount of water evaporating from the surface of leaves, as evaporation from leaf surfaces depends on the amount of leaf area present. Evapotranspiration of water removes energy from the Earth's surface and therefore has a cooling effect.

1.2 Scaling from leaf to ecosystem

Scaling leaf-level photosynthesis and transpiration to ecosystem measures of net primary productivity and evapotranspiration requires information about the total amount of leaves present and the relative abundance of different plant types. We use leaf area index as a measure of the total amount of leaves present. Leaf area index is defined as the total amount of leaf area covering a given area of ground (m^2 leaf area / m^2 ground area). Greater leaf area index enhances the surface area over which photosynthesis and transpiration occur and thus has the potential to increase ecosystem carbon uptake and evapotranspirative cooling.

The capacity for photosynthesis and transpiration varies among plant types. Therefore, information about the relative abundance of plant types is also necessary to scale photosynthesis and transpiration to the ecosystem and global scales.

1.3 Expected plant responses to elevated carbon dioxide

Observations suggest that plant functioning is sensitive to atmospheric carbon dioxide concentrations. At the leaf-level, elevated carbon dioxide is expected to stimulate photosynthesis and reduce transpiration, as an abundance of carbon allows plants to close their

leaf pores more often and conserve water. Greater net primary productivity in response to elevated carbon dioxide is expected to enhance leaf area index. Higher leaf area index could further enhance carbon uptake and offset leaf-level reductions in transpiration by increasing the surface area over which photosynthesis and transpiration occur.

The sensitivity of plant functioning to elevated carbon dioxide varies among plant types. This variation in responses could mean that elevated carbon dioxide enhances leaf area and biomass more in some plant types than in others. As these properties influence the ability of plants to compete for limiting resources such as light, changes in leaf area and biomass have the potential to alter competitive dynamics between plants and, thus, the relative abundance of different plant types.

1.4 Expected climate impacts of plant responses to elevated carbon dioxide

Changes in carbon uptake and evapotranspiration due to elevated atmospheric carbon dioxide concentrations have the potential to alter the influence of vegetation on Earth's climate. Elevated carbon dioxide is expected to enhance net primary productivity. This response would remove more carbon dioxide from the atmosphere and have a cooling effect. At the same time, elevated carbon dioxide is expected to reduce evapotranspiration, which would warm the Earth's surface. However, the magnitude, and even the sign, of changes in net primary productivity and evapotranspiration in response to elevated carbon dioxide remains uncertain. These ecosystem level measures of plant functioning are influenced by many smaller scale processes, each of which may also respond to changing environmental drivers. A better understanding of which plant responses to climate matter for net primary productivity and evapotranspiration, and how to include these responses in Earth system models, is urgently needed to improve projections of future climate. Changes in leaf structural traits in response to elevated carbon dioxide are one such plant response that may influence ecosystem functioning, and thus feedback on climate, but their influence remains poorly understood.

1.5 Leaf trait dynamics

Observations show that plants change structural aspects of their leaves in response to elevated carbon dioxide concentrations. These leaf trait changes have the potential to directly alter climate by modifying carbon uptake (net primary productivity) and evapotranspirative cooling. They could also indirectly influence climate by altering competitive dynamics between plants and, thus, the relative abundance of different plant types.

This dissertation focuses on the responses of three leaf traits: leaf mass per area, leaf carbon to nitrogen ratio, and leaf nitrogen per area. Leaf mass per area describes the carbon cost of building a unit of leaf area (g C / m^2 leaf area). This trait can also be referred to by its inverse, specific leaf area (m^2 leaf area / g C). Leaf carbon to nitrogen ratio describes the mass-based amount of carbon relative to nitrogen within the leaf (g C / g N). Together these two leaf traits determine the amount of nitrogen per leaf area (g N / m^2 leaf area) as follows:

$$N_{area} = \frac{LMA}{C{:}N_{leaf}} \tag{1.1}$$

where N_{area} is the leaf nitrogen per area (g N / m^2 leaf), LMA is the leaf mass per area (g C / m^2 leaf), and $C{:}N_{leaf}$ is the leaf carbon to nitrogen ratio (g C / g N). As nitrogen is a critical component of photosynthetic enzymes, nitrogen per area is an important determinant of photosynthetic capacity per leaf area.

Observations suggest that leaf mass per area and leaf carbon to nitrogen ratio increase by as much as one third in response to a doubling of carbon dioxide in a wide range of C_3 plants across ecosystems and continents. The leading hypothesis for why these leaf trait changes occur in response to elevated carbon dioxide is that the abundance of carbon causes non-structural carbohydrates (i.e., carbon) to accumulate in leaves as other resources, such as nitrogen, begin to limit plant growth.

1.6 Potential climate impacts of leaf trait dynamics

1.6.1 Direct influences

The direct influence of these leaf trait responses to elevated carbon dioxide on ecosystem functioning and climate is challenging to predict as they present trade-offs between enhancing leaf area and increasing photosynthetic rates per leaf area. Higher leaf carbon to nitrogen ratio reduces leaf nitrogen per area following Equation 1.1 and thus reduces photosynthetic capacity per leaf area in the absence of other leaf changes. Such lowering of photosynthetic capacity per leaf area has the potential to reduce net primary productivity and evapotranspiration. However, greater leaf carbon to nitrogen ratio also makes leaf area less expensive in terms of nitrogen to build. Making leaves cheaper to build in terms of nitrogen could allow plants to enhance leaf area under nitrogen limitation of growth. Higher leaf area could enhance net primary productivity and evapotranspiration. Whether increasing leaf carbon to nitrogen ratio will enhance ecosystem functioning by increasing leaf area, or diminish functioning by reducing photosynthesis per leaf area is not immediately apparent.

Increasing leaf mass per area also presents trade-offs for plant functioning that make predicting its influence on ecosystems and climate challenging. Greater leaf mass per area makes leaf area more expensive in terms of carbon for plants to build. As such, consideration of this leaf trait change has the potential to reduce the expected increase in leaf area in response to elevated carbon dioxide. However, greater leaf mass per area also increases the amount of nitrogen per leaf area (following Equation 1.1) and, thus, could enhance photosynthetic capacity per leaf area in the absence of other leaf trait changes. Whether leaf mass per area will diminish net primary productivity and evapotranspiration by reducing leaf area, or increase these functions by enhancing photosynthesis per area is uncertain prior to experimental testing.

1.6.2 Indirect influences

Leaf trait responses to elevated carbon dioxide could also indirectly alter ecosystem functioning and climate by modifying plant competitive dynamics, and thus the relative abundance of different plant types. Leaf area and biomass allow plants to shade neighboring plants and, thus, exert control over competition for light in the canopy. Changes in leaf mass per area and leaf carbon to nitrogen ratio could alter leaf area and biomass (through their influence on net primary productivity) as described above. The magnitude of these leaf trait changes in response to elevated carbon dioxide has been observed to differ by species and could therefore differentially alter competitive ability and, thus, modify the relative abundance of different plant types. As plant types differ in their capacities for photosynthesis and transpiration such changes in plant type abundance could modify the influences of vegetation on ecosystem functioning and climate.

1.7 Tools for studying plant influences on climate

This dissertation uses Earth system model and demographic vegetation model simulations to test how leaf trait responses to elevated carbon dioxide directly and indirectly impact ecosystems and large-scale climate. Observations of plant responses to elevated carbon dioxide reported in the literature inform the leaf trait changes we make in our modeling experiments.

1.7.1 Earth system model simulations

We use Earth system model simulations to quantify the direct influences of leaf trait changes on global vegetation and climate. The National Center for Atmospheric Research's Community Earth System Model, used herein, simulates global land, atmosphere, ocean, sea ice, and carbon cycling processes, as well as the coupling between these processes. The land component of the model includes plants whose properties and functioning have the potential to influence simulated climate by modifying the fluxes of energy, water, and car-

bon between the Earth's surface and the atmosphere. Broad plant functional types (e.g., broadleaf evergreen tropical trees, needleleaf evergreen temperate trees) represent variation across plant types and differ in properties including leaf mass per area, leaf carbon to nitrogen ratio, and maximum photosynthetic rates. In the model, photosynthesis responds to environmental conditions (e.g., carbon dioxide concentration, temperature, water availability, and sunlight) and net primary productivity controls the amount of plant growth and leaf area simulated. As leaf mass per area and leaf carbon to nitrogen are used to calculate leaf area and photosynthetic rates, changes in these leaf traits have the potential to alter leaf area, carbon uptake, and evapotranspiration and, thus, influence climate in our simulations. As our Earth system model simulations hold the spatial distribution of plant functional types invariant with time, these experiments test the direct influence of changes in leaf traits on ecosystems and climate.

1.7.2 Demographic vegetation model simulations

We use demographic vegetation model simulations to investigate how leaf trait responses to elevated carbon dioxide alter plant competitive dynamics in a tropical forest ecosystem. Specifically, we use the Functionally Assembled Terrestrial Ecosystem Simulator (FATES) embedded within the National Center for Atmospheric Research's Community Land Model. This model mechanistically simulates ecological dynamics and ecosystem assembly through processes including plant growth, competition for light and water, recovery from disturbance, reproduction, mortality, and recruitment. Height structured vegetation is explicitly represented, allowing us to test how leaf trait changes influence competition for light. The model also tracks the leaf area and biomass of competing plant types, which we use to quantify changes in competitive ability and improve our understanding of potential shifts in plant type abundance.

1.7.3 Observations

Observations from the literature inform the leaf responses to carbon dioxide that we test in our modeling experiments. These observations come from manipulation experiments in which plants are treated with elevated levels of carbon dioxide in greenhouses, outdoor chambers, and ecosystem-scale Free-Air Carbon Dioxide Enrichment experiments. Manipulation experiments have been used to measure many plant responses including those of photosynthesis, transpiration, biomass, leaf area index, and leaf traits. We choose to test changes in leaf structural traits that are observed in many different plant types across ecosystems and continents, as these are likely to have large-scale impacts on ecosystems and climate.

1.8 Dissertation Structure

Here we quantify the influence of leaf trait responses to elevated carbon dioxide on large-scale climate using Earth system model experiments (Chapter 2) and on tropical forest functioning and ecological dynamics using demographic vegetation model experiments (Chapter 3). Prior to using the demographic vegetation model to test the impacts of leaf trait responses to elevated carbon dioxide, we improved its ability to simulate present-day tropical forest structure and functioning by modifying the model to include a within-canopy gradient of leaf mass per area, following observations (Chapter 4).

1.9 Future Work

This work begins to develop a hierarchy of plant trait responses that are most important to consider in projections of future ecosystems and climate. There are many other plant trait responses whose impacts should be tested and quantified. Furthermore, our findings provide additional motivation for physiological and ecological experiments that improve our understanding of plant responses to environmental drivers and the underlying mechanisms.

Chapter 2

LEAF TRAIT ACCLIMATION AMPLIFIES SIMULATED CLIMATE WARMING IN RESPONSE TO ELEVATED CARBON DIOXIDE

Marlies Kovenock[1] and Abigail L.S. Swann[2,1]

[1]Department of Biology, University of Washington, Seattle, WA; [2]Department of Atmospheric Sciences, University of Washington, Seattle, WA.

Citation: Kovenock, M., and Swann, A. L. S. (2018). Leaf trait acclimation amplifies simulated climate warming in response to elevated carbon dioxide. *Global Biogeochemical Cycles, 32,* 1437-1448. https://doi.org/10.1029/2018GB005883

Key Points:

- Acclimation of leaf traits to elevated CO_2 significantly altered global climate and carbon cycling in Earth system model experiments
- Higher carbon cost of building leaf area under elevated CO_2 offsets gains in leaf area, productivity, and evapotranspiration
- Results identify an urgent need to collect observations to constrain uncertainty in plant trait responses to a changing climate

Supporting Information referenced in this chapter can be found in Appendix A.

2.1 Abstract

Vegetation modifies Earth's climate by controlling the fluxes of energy, carbon, and water. Of critical importance is a better understanding of how vegetation responses to climate change will feedback on climate. Observations show that plant traits respond to elevated carbon dioxide concentrations. These plant trait acclimations can alter leaf area and, thus, productivity and surface energy fluxes. Yet the climate impacts of plant structural trait acclimations remain to be tested and quantified. Here we show that one leaf trait acclimation in response to elevated carbon dioxide — a one-third increase in leaf mass per area — significantly impacts climate and carbon cycling in Earth system model experiments. Global net primary productivity decreases (-5.8 PgC/year, 95% confidence interval [$CI_{95\%}$] -5.5 to -6.0), representing a decreased carbon dioxide sink of similar magnitude to current annual fossil fuel emissions (8 PgC/year). Additional anomalous terrestrial warming (+0.3 °C globally, $CI_{95\%}$ 0.2 to 0.4), especially of the northern extratropics (+0.4 °C, $CI_{95\%}$ 0.2 to 0.5), results from reduced evapotranspiration and enhanced absorption of solar radiation at the surface. Leaf trait acclimation drives declines in productivity and evapotranspiration by reducing leaf area growth in response to elevated carbon dioxide, as a one-third increase in leaf mass per area raises the cost of building leaf area and productivity fails to fully compensate. Our results suggest that plant trait acclimations, such as changing leaf mass per area, should be considered in climate projections and provide additional motivation for ecological and physiological experiments that determine plant responses to environment.

2.2 Introduction

Feedbacks between vegetation and climate change are of critical importance to future climate projections but remain highly uncertain [Friedlingstein et al., 2014, Pu and Dickinson, 2012, Arora et al., 2013, Lovenduski and Bonan, 2017]. Vegetation strongly influences the Earth's climate by controlling the fluxes of carbon, water, and energy between the land surface and the atmosphere [Bonan, 2008]. Changes in biologically mediated carbon fluxes,

such as productivity and respiration, can alter the concentration of carbon dioxide (CO_2) in the atmosphere, leading to warming of the Earth due to the radiative effects of CO_2. Given that these radiative effects are driven by biological sources of carbon, we refer to the associated temperature increase as biogeochemical warming. Since the start of the industrial era, Earth's vegetation has removed about 30% of anthropogenic CO_2 emissions from the atmosphere [Ciais et al., 2013]. Changes in vegetation can also induce warming by altering water and energy fluxes through their influence on Earth surface properties such as evapotranspiration, albedo, and roughness. We refer to increases in temperature due to alterations of the surface energy balance as biogeophysical warming. Transpiration, the biologically controlled flux of water from soil through plants into the atmosphere, makes up an estimated 60% of current terrestrial water fluxes [Wei et al., 2017], which physically cool the land surface. Rising CO_2 concentrations are expected to have profound and wide reaching effects on vegetation functioning and growth, with important implications for global carbon uptake and evapotranspirative cooling. Yet large uncertainty exists in the magnitude, and even the sign, of vegetation feedbacks on climate change [Friedlingstein et al., 2014, Pu and Dickinson, 2012, Arora et al., 2013, Lovenduski and Bonan, 2017]. This uncertainty stems in large part from the challenge of representing complex and diverse life-forms at the global scale in the Earth system models used to project future climate [Lovenduski and Bonan, 2017]. Key biological processes must be missing or poorly constrained, but we lack a clear understanding of which processes are essential for predicting climate and carbon cycling changes.

Incorporating observations of plant trait distributions and their responses to environmental drivers into Earth system models is proposed as a way to improve predictions of ecosystem functioning [Butler et al., 2017, Wright et al., 2004, Kattge and Knorr, 2007, Kattge et al., 2011, Van Bodegom et al., 2012, Verheijen et al., 2013, 2015, Reichstein et al., 2014, Fisher et al., 2015, Pavlick et al., 2013, Scheiter et al., 2013, Reich et al., 2014]. Trait databases and studies that aggregate observations across species are beginning to make it possible to characterize current plant trait distributions and their responses to environmental drivers at the global scale [e.g., Wright et al., 2004, Niinemets, 2001, Kattge and Knorr, 2007, Kattge

et al., 2011, Van Bodegom et al., 2012, Verheijen et al., 2013]. However, the biogeographic relationship between traits and climate across ecosystems, caused primarily by environmental filtering, does not tell us about short-term responses to changes in climate within an ecosystem, caused by acclimation [Van Bodegom et al., 2012, Verheijen et al., 2013]. The climate impacts of these two distinct responses, environmental filtering and acclimation, have been tested in previous work.

Studies focused on environmental filtering have shown that allowing traits to vary temporally based on observed spatial relationships between these traits and environmental drivers (i.e., space-for-time substitution) has carbon uptake and climate implications [Verheijen et al., 2013, 2015]. This approach estimates the integrated outcome of numerous biological responses to climate [e.g., adaptation, changes in species distribution, and acclimation; Van Bodegom et al., 2012, Verheijen et al., 2015]. However, it does not separate the impacts of individual biological responses (e.g., acclimation, adaptation, and species turnover) from one another and therefore cannot mechanistically explain the underlying causes of trait variation [Verheijen et al., 2013]. Further, it is uncertain if space-for-time relationships used in the environmental filtering approach will hold under future climate in part because acclimation of traits may alter these trait-environment relationships [Verheijen et al., 2015, Fisher et al., 2015]. Acclimation responses can differ in magnitude and even direction from trait responses to environmental filtering [e.g., Verheijen et al., 2013, Poorter et al., 2009].

Other studies have directly investigated the influence of some trait acclimations to temperature and elevated CO_2 (e.g., photosynthetic and stomatal conductance rates) and found profound effects on large-scale climate and carbon cycling [Sellers et al., 1996, Betts et al., 1997, Cao et al., 2010, Pu and Dickinson, 2012, Lombardozzi et al., 2015, Smith et al., 2017]. Acclimation occurs within the same individual plant and on short-time scales (e.g., a growing season), making it immediately relevant for 21st century climate. Prior studies have focused on rate traits and have not considered the potential climate feedbacks of plant structural traits. Trait responses to climate change that alter plant structure could feedback on climate and carbon cycling by modifying the surface areas (e.g., leaf area) over which the rates of

photosynthesis and stomatal conductance are summed.

Among the most widely observed plant structural trait responses to elevated CO_2 is an increase in leaf mass per area (g leaf carbon/m^2 leaf area). Leaf mass per area represents the carbon cost of building leaf area and is a quantity commonly used in Earth system models to convert from carbon available for leaf growth to leaf area. Field and greenhouse manipulation experiments show that leaf mass per area increases by as much as one third in response to elevated CO_2 in a wide range of C_3 plants, including trees, shrubs, and crops, across a variety of ecosystems on many continents [Medlyn et al., 1999, 2015, Ainsworth and Long, 2005, Poorter et al., 2009]. Acclimation to warming temperatures could potentially offset leaf mass per area increases due to elevated CO_2 but is limited to cold regions such as the boreal and arctic [Poorter et al., 2009]. Most Earth system models project increases in leaf area in response to CO_2 over the 21st century [Mahowald et al., 2016, Swann et al., 2016], which are expected to negatively feedback on climate change by promoting carbon uptake from the atmosphere and evapotranspirative cooling over land [Betts et al., 1997, Bounoua et al., 2010, Pu and Dickinson, 2012]. However, few models capture the decreased sensitivity of leaf area index to increases in leaf biomass at elevated CO_2 because they fail to represent the concomitant increase in leaf mass per area [De Kauwe et al., 2014, Medlyn et al., 2015].

Here we quantify the potential extent of climate and carbon cycling impacts of leaf mass per area acclimation to rising CO_2 using a series of Community Earth System Model coupled atmosphere-land-carbon cycle simulations (supporting information Table A.1). In the model, vegetation responds to climate by changing carbon assimilation, stomatal conductance, biomass, and leaf area. These vegetation responses can induce biogeophysical warming through feedbacks on the surface energy balance and atmosphere via changes in albedo, evapotranspiration, and surface roughness. We quantify the additional climate impacts, beyond those of elevated CO_2, of leaf mass per area acclimation to CO_2 as the difference between a leaf acclimation experiment and a climate change control simulation (CCLMA-CC). As atmospheric CO_2 concentration is held invariant over time in all simulations, biogeochemi-

cal warming is estimated from the difference in net primary productivity. The level of leaf acclimation, a one-third increase in leaf mass per area in C_3 plants, was estimated from the upper bound of acclimation to a doubling of CO_2 (355 to 710 ppm) from Poorter et al. [2009]'s meta-analysis of approximately 200 studies, which provides the most plant-type-specific CO_2 acclimation relationships for leaf mass per area currently available. The control simulation (CTRL) provides a reference for whether the effects of leaf acclimation at elevated CO_2 (CCLMA-CC) moderate (e.g., reduce the increase in leaf area) or enhance (e.g., further increase leaf area) changes due to elevated CO_2 alone (CC-CTRL). We also estimate the effects of leaf mass per area acclimation to temperature (TCCLMA-CC) and the historical influence of changing leaf mass per area (LMA-CTRL). Maximum photosynthetic rates (e.g., V_{cmax25} and J_{max25}) are the same across these simulations (CCLMA, CC, CTRL, TCCLMA, and LMA) before acclimating to temperature following Kattge and Knorr [2007]. We test the sensitivity of our results to increasing maximum photosynthetic rates concurrently with leaf mass per area (CCLMAPS).

2.3 Materials and Methods

This study used the Community Earth System Model version 1.3beta11 with interactive land and biogeochemistry [CLM4.5-BGC; Oleson et al., 2013], atmosphere [CAM5; Neale et al., 2012], mixed-layer ocean [Neale et al., 2012], and sea ice [CICE4; Hunke and Lipscomb, 2010] models. Simulations that couple the land and atmosphere, such as performed here, are required to quantify the climate impacts of changes in the land surface, as they capture the atmospheric response and land-atmosphere feedbacks. To allow for ocean heat transport and atmosphere-ocean interaction while retaining computational economy, we used a mixed-layer ocean model with prescribed lateral heat fluxes rather than a more computationally expensive full dynamical ocean model. We ran the simulations with a spatial resolution of approximately 1.9° by 2.5° gridcells. The biogeochemistry model represents a full terrestrial carbon cycle with growth, mortality, and decay — and hence leaf area and carbon storage in aboveground and belowground pools. The distribution of 15 plant functional types was

prescribed by a map of present day vegetation and held invariable; however, under unsuitable growing conditions, plants diminish to a minimum leaf area.

The climate change control simulation (CC; 2xCO_2, no leaf acclimation) represents the mean climate state when atmospheric CO_2 is fixed at 710 ppm. The CO_2 leaf acclimation experiment (CCLMA; 2xCO_2, +1/3 leaf mass per area) is identical to the climate change control simulation (CC) except that it includes a plausible extent of leaf mass per area acclimation to CO_2 in all C_3 plants [Poorter et al., 2009]. (See Supporting Text A.1.2 for details.) A second experiment (TCCLMA; 2xCO_2, no change in leaf mass per area in boreal and arctic biomes, +1/3 leaf mass per area in all other C_3 plants) tests the impact of leaf acclimation to both CO_2 and temperature [Poorter et al., 2009]. (See Supporting Text A.1.3 and A.2.1 for further details.) Leaf mass per area acclimation to CO_2 and temperature were estimated using the most plant-type-specific acclimation relationships currently available [Poorter et al., 2009]. A third experiment (CCLMAPS; 2xCO_2, +1/3 leaf mass per area, +1/3 maximum photosynthetic rates) tests the sensitivity of our results to increasing maximum photosynthetic rates and quantifies the increase in maximum photosynthetic rates required to offset the biogeophysical warming due CO_2 acclimation of leaf mass per area. All elevated CO_2 simulations (CC, CCLMA, TCCLMA, and CCLMAPS) include the effects of CO_2 radiative forcing, CO_2 fertilization, and gains in water use efficiency. A fourth experiment (LMA; 1xCO_2, +1/3 leaf mass per area) tests the sensitivity of historical climate to increased leaf mass per area. A separate control simulation (CTRL; 1xCO_2, no leaf acclimation) represents the equilibrium climate state when CO_2 concentration is fixed at 355 ppm, a common baseline for Earth system model simulations.

We held maximum photosynthetic rates (V_{cmax25}, J_{max25}, and T_{p25}) constant, so that they did not differ between the control (CC and CTRL) and CCLMA, TCCLMA, and LMA simulations prior to temperature acclimation. As the default model calculates maximum photosynthetic rates from leaf mass per area, we modified this relationship so that these rates did not differ (except CCLMAPS). In our simulations a decrease in leaf nitrogen concentration, which can also be thought of as an increase in leaf carbon-to-nitrogen ratio

(gC/gN) and a reduction in leaf nutrition, is coupled to the increase in leaf mass per area (except CCLMAPS) to maintain maximum photosynthetic rates at control (CTRL and CC) levels. (See Supporting Text A.1.2 for details.) This represents a conservative estimate of acclimation of maximum photosynthetic rates to CO_2, as evidence supports a decrease in these rates in response to elevated CO_2 [Ainsworth and Long, 2005, Leakey et al., 2012b, Smith and Dukes, 2013, Rogers et al., 2017]. The decrease in leaf nitrogen concentration with elevated CO_2 is also supported by observations [reviewed in Ainsworth and Long, 2005, Leakey et al., 2012b, Way et al., 2015]. All simulations include temperature acclimation of maximum photosynthetic rates [Kattge and Knorr, 2007, Oleson et al., 2013]. The maximum photosynthetic rate values of all simulations were within the observed range used to generate the empirical temperature acclimation function, and acclimation was not allowed outside of the range of temperature values used to generate the empirical function.

All simulations were integrated for 85 years, except the CCLMAPS experiment was integrated for 44 years. All experiment simulations were initiated by branching from the beginning of year 56 of the control run (CTRL). Temperature, leaf area index, net and gross primary productivity, evapotranspiration, and live carbon pools (leaf, live stem, live root, and fine root) reached equilibrium before year 30 in each simulation. The first 30 years of each simulation were discarded to allow for spin up. The remaining years were used in our analysis and represent many samples of the equilibrium state. Model results are available through the University of Washington Libraries ResearchWorks digital repository. The URL for the data in the ResearchWorks system is
https://digital.lib.washington.edu/researchworks/handle/1773/41856.

We use annual mean changes in biogeophysical warming and net primary productivity to quantify the upper bound of the potential climate and carbon cycling influences of leaf mass per area acclimation. We tested for differences between simulations in the annual mean at the global, latitude band, zonal mean (average for a given latitude), and gridcell scales using bootstrap methods (n = 50,000; Supporting Text A.1.4) with model years as the unit of replication. Spatial relationships between variables at the gridcell scale were tested using

simple, multiple, and stepwise linear regression methods on annual mean values. Differences and relationships were considered significant at the 95% level. (See Supporting Text A.1.4 for details.) Latitude bands were defined as southern extratropics (60°S to 20°S), tropics (20°S to 20°N), northern extratropics (20°N to 65°N), and northern high latitudes (65°N to 90°N).

Biogeochemical warming was calculated by converting the change in net primary productivity to a change in atmospheric CO_2 level (2 PgC to 1 ppm). After accounting for compensatory carbon uptake by the ocean of 60-85% [Archer et al., 2009, Broecker et al., 1979], we converted the change in atmospheric CO_2 concentration to a radiative forcing in watt per square meter following the methods of Hansen et al. [1998] and Myhre et al. [1998]. The resulting global temperature change was then estimated from the forcing using a range of climate sensitivities (temperature change due to a doubling of CO_2) from 1.5 to 4.5 °C.

2.4 Results

2.4.1 Biogeophysical Warming

Acclimation of leaf mass per area to elevated CO_2 induced significant biogeophysical warming in addition to the warming caused by the radiative effects of a doubling of CO_2 in Earth system model experiments. The change in temperature from the direct effects of a doubling of CO_2 (from 355 to 710 ppm) in our model (CC-CTRL) was 5.0 °C (95% confidence interval [$CI_{95\%}$] 5.0 to 5.1), with a higher mean warming over land of 6.1 °C ($CI_{95\%}$ 6.0 to 6.1). The influence of doubling CO_2 included plant responses such as carbon fertilization [Oleson et al., 2013] and increased water use efficiency (+27% for CC-CTRL, $CI_{95\%}$ 27 to 28) but did not account for acclimation of leaf mass per area. Consideration of leaf mass per area acclimation to CO_2 (CCLMA-CC) increased annual mean temperature over land by an additional +0.3 °C ($CI_{95\%}$ 0.2 to 0.4, Figure 2.1a and Tables 2.1 and A.2) and +0.2 °C ($CI_{95\%}$ 0.1 to 0.2) globally on top of the direct effects of CO_2. This acclimation-driven warming was especially pronounced over land in the northern extratropics (+0.4 °C, $CI_{95\%}$

0.2 to 0.5) due to above average warming over Eurasia (Figures 2.1a and 2.2a and Table 2.1). The influence of temperature acclimation of leaf mass per area (TCCLMA-CC) was limited to cold biomes and did not significantly alter the amount of additional warming over land and globally due to CO_2 acclimation (Supporting Text A.2.1; Figure A.1). The influence of leaf mass per area changes at historical CO_2 levels (LMA-CTRL) was also small (Supporting Text A.2.2).

Leaf trait acclimation enhanced biogeophysical warming over land under future CO_2 levels by offsetting the CO_2-induced increase in leaf area index (m^2 leaf area/m^2 ground). Doubling of CO_2 (CC-CTRL) increased the annual mean leaf area index by 1.2 m^2/m^2 ($CI_{95\%}$ 1.2 to 1.2) in our simulations. This magnitude of change is at the high end of Coupled Model Intercomparison Project Phase 5 model leaf area responses to RCP8.5 over the 21st century [Mahowald et al., 2016]. Inclusion of leaf mass per area acclimation strongly limited the increase in leaf area index to 0.3 m^2/m^2 ($CI_{95\%}$ 0.2 to 0.3) over the ambient CO_2 simulation (CCLMA- CTRL). This attenuation of leaf area growth occurred in almost all vegetated areas (Figures 2.1b and 2.2b and Table 2.1). However, leaf area index decreased more in response to leaf acclimation in places with high initial leaf areas, as shown by the negative spatial relationship ($r = -0.91$, $R^2 = 0.83$, Figure A.2a) between leaf area index in the control climate change case (CC) and the change in leaf area index in response to leaf acclimation (CCLMA-CC).

The reduced increase in leaf area in response to leaf trait acclimation (CCLMA-CC) induced biogeophysical warming over land by shifting the balance between surface energy budget terms. Near-surface temperature warmed in response to a moderation of the increase in evapotranspirative cooling and an increase in solar radiation absorbed at the Earth's surface (Figures 2.2 and 2.3c and Tables 2.1 and A.2). These two factors shifted additional energy to sensible heat, the term in the surface energy balance that directly drives surface temperature changes. In the tropics, warming was primarily the result of reduced evapotranspiration, followed by greater solar radiation absorbed at the surface (Figures 2.2c,d and Tables 2.1 and A.2). In the extratropics, increased absorption of solar radiation and reduced

evapotranspiration induced warming in more equal proportion (Figures 2.2b,c and Tables 2.1 and A.2). The strong influence on the surface energy budget of evapotranspiration in the tropics and the combination of evapotranspiration and solar radiation in the midlatitudes is consistent with previous studies [Bonan, 2008].

Evapotranspiration is the combination of several contributing water fluxes. Reduced transpiration (CCLMA-CC) represented the largest contribution to evapotranspiration declines in all regions, followed by lower evaporation from leaf surfaces (Tables 2.1 and A.2). However, greater soil evaporation partially offset the decline from transpiration and leaf evaporation. The reduced increase in leaf area index in response to leaf acclimation drove the reduction in evapotranspiration (Figure 2.2), aided by a slight increase in water use efficiency (CCLMA-CC; +0.5%, $CI_{95\%}$ 0.2 to 0.8). Reductions in evapotranspiration were spatially positively related to changes in leaf area (CCLMA-CC; $r = 0.57$, $R^2 = 0.32$; Figure A.2b). As leaf area provides the surface area over which transpiration and leaf evaporation occur, the acclimation-induced reduction of leaf area index diminished evapotranspiration to drive biogeophysical warming.

More solar radiation reached land when leaf mass per area acclimation was included (Figures 2.2d and 2.3c and Table 2.1) due to reduced low cloud cover over the tropics and northern extratropics (Figure A.3a). Acclimation-driven warming decreased the relative humidity of the lower atmosphere in these regions (Figure A.3b), making it less likely for water vapor to saturate the air and condense to form clouds. Relative humidity decreased because warming of the atmosphere (Figure A.3c) raised the saturation vapor pressure, outcompeting the influence of greater absolute amounts of water vapor (i.e., specific humidity) in some areas (Figure A.3d). The overall increase in solar radiation at the surface demonstrates that the effect of reduced cloud cover overwhelmed the opposing influence of a small surface albedo increase. Albedo increased because the reduced increase in leaf area index (CCLMA-CC) allowed more radiation to reach and reflect away from bare ground which is brighter than vegetation [Bonan, 2008, Oleson et al., 2013]. Albedo changes (Figure A.4) were measured by comparing the difference in solar radiation absorbed at the surface under clear-sky conditions

(a model calculation that ignores the influence of clouds).

2.4.2 Carbon Cycle and Biogeochemical Warming

In addition to biogeophysical warming, acclimation of leaf mass per area reduced carbon uptake by the biosphere (Figures 2.1c and 2.3c), which would induce further warming by increasing atmospheric CO_2 levels. Net primary productivity increased 51% (+30.1 PgC/year, $CI_{95\%}$ 29.8 to 30.4) in response to a doubling of CO_2 (CC-CTRL). Acclimation of leaf mass per area strongly moderated the positive effect of carbon fertilization on net primary productivity in response to elevated CO_2, reducing the gain in productivity by -5.8 PgC/year (CCLMA-CC; $CI_{95\%}$ -5.5 to -6.0, Tables 2.1 and A.2). This decrease in net primary productivity in response to leaf acclimation was driven by declines in the tropics, followed by the northern extratropics (Tables 2.1 and A.2).

Smaller increases in leaf area and higher temperatures in response to leaf acclimation both contributed to the reduced gains in productivity relative to the climate change control. Decreases in gross primary productivity (CCLMA-CC) were best described by a multiple regression using both changes (CCLMA-CC) in temperature and leaf area as predictors (multiple regression $R^2 = 0.32$; Figure A.2d). Changes in net primary productivity were weakly but best related to temperature change ($r = -0.49$, $R^2 = 0.24$; Figure A.2c).

From the reduced gains in carbon uptake in response to leaf mass per area acclimation we estimate a change in global mean temperature. Our simulations did not directly account for this biogeochemical warming, as atmospheric CO_2 levels within each simulation were held fixed in time. Instead, we estimate biogeochemical warming (see Materials and Methods Section) associated with the net change in carbon storage from the difference in carbon uptake by vegetation, as measured by net primary productivity, when leaf acclimation is considered (CCLMA-CC). The -5.5 to -6.0-PgC/year reduction in net primary productivity gains would increase global atmospheric CO_2 concentration by +0.4 to +1.2 ppm/year when considering the effect of oceanic buffering. We estimate that this additional atmospheric CO_2 induces biogeochemical warming of +0.1 to +1.0 °C over 100 years, the approximate

average time scale for a doubling of CO_2 from 355 to 710 ppm under the Intergovernmental Panel on Climate Change RCP8.5 and RCP6 emissions scenarios [Cubasch et al., 2013]. The sum of this biogeochemical warming and the biogeophysical warming reported above brings the total additional warming over land due to leaf mass per area acclimation (CCLMA-CC) to +0.3 to +1.4 °C greater than the warming due to a doubling of CO_2 in the control climate change simulation.

2.5 Discussion

We find that leaf trait responses could have significant large-scale climate implications. Increased leaf mass per area enhances warming beyond the direct effects of elevated CO_2 by moderating evapotranspiration and enhancing absorption of solar radiation and by lessening the rise in leaf area which lowers net primary productivity gains (Figure 2.3).

The surface temperature change in response to leaf trait acclimation is of comparable magnitude to the climate response to other important climate forcings (Figure 2.4). For example, the enhanced warming in our experiment (+0.3 to +1.4 °C) is smaller but of the same order of magnitude as the change in temperature in response to a doubling of CO_2 estimated by the Intergovernmental Panel on Climate Change (+1.5 to +4.5 °C) from observed 20th century climate change, paleoclimate, feedback analysis, and climate models [Ciais et al., 2013]. While these comparisons are not exact, as the methods and measures of uncertainty differ, they provide an order of magnitude comparison for our results. Enhanced warming in our experiment is also of greater or comparable magnitude to the temperature response to large-scale land cover change (Figure 2.4d), such as anthropogenic land cover change over the 20th century [-0.04 °C physical, +0.27 chemical, +0.22 total, over land; Pongratz et al., 2010] and theoretical global deforestation [-1.1 °C biogeophysical over land; Davin and de Noblet-Ducoudré, 2010].

Furthermore, our results show that the surface temperature change in response to leaf trait acclimation can exceed or match several well-studied plant physiological feedbacks to elevated CO_2 that are included in most climate projections (Figure 2.4c). These include

the vegetation carbon-concentration feedback [0 to -1.0 °C; estimated from the change in CO_2 implemented in this study of 355 to 710 ppm and the Coupled Model Intercomparison Project Phase 5 model range for land carbon-concentration feedback parameter from Arora et al., 2013]; stomatal conductance response to elevated CO_2 [+0.2 to +0.5 °C biogeophysical over land; Sellers et al., 1996, Betts et al., 1997, 2007, Cox et al., 1999, Boucher et al., 2009, Cao et al., 2010, Pu and Dickinson, 2012]; photosynthetic down-regulation [-0.1 to +0.3 °C biogeophysical over land; Bounoua et al., 2010, Pu and Dickinson, 2012]; and increased leaf area index (+30 to 60%) due to CO_2 fertilization and increased water use efficiency under elevated CO_2 [-0.1 to -0.4 °C biogeophysical over land; Betts et al., 1997, Bounoua et al., 2010, Pu and Dickinson, 2012].

The reduced increase in terrestrial productivity in response to leaf mass per area acclimation is on the order of other large-scale carbon cycle perturbations and moderates the effect of CO_2 fertilization on plant growth and carbon uptake from the atmosphere. The -5.8-PgC/year ($CI_{95\%}$ -5.5 to -6.0) reduction in net primary productivity in response to leaf mass per area acclimation in our simulations (CCLMA-CC) is a reduced carbon sink comparable in magnitude to current global fossil fuel emissions [8 PgC/year; Ciais et al., 2013]. It is larger than the total current terrestrial biosphere uptake of CO_2 from the atmosphere [3 PgC/year; Le Quéré et al., 2016].

Leaf mass per area acclimation to CO_2 represents a shift in the relationship between two key ecosystem properties — productivity and leaf area. As such, this acclimation will remain important for climate and carbon cycling if other trait responses further modify estimates of productivity. Notably, the magnitude of maximum photosynthetic rate (e.g., V_{cmax25} and J_{max25}) acclimation to CO_2 remains uncertain and difficult to represent at the global scale [Smith and Dukes, 2013, Rogers et al., 2017]. While most estimates suggest that maximum photosynthetic rates will decrease in response to CO_2 [Ainsworth and Long, 2005, Leakey et al., 2012b, Smith and Dukes, 2013, Rogers et al., 2017], which would amplify our results, we conservatively do not change these rates in our primary experiment (CCLMA-CC). We note that our results should be considered in relation to our treatment of maximum photosynthetic

rates, which were equivalent across experiments prior to temperature acclimation in all simulations except CCLMAPS. The CCLMAPS experiment tests the sensitivity of our results to increasing maximum photosynthetic rates. Using this experiment (CCLMAPS-CC), we estimate that maximum photosynthetic rates would need to increase (opposite direction of expected CO_2 acclimation) by one third to bolster net primary productivity enough to offset the biogeophysical warming over land due to leaf acclimation in our experiments (Supporting Text A.2.3; CCLMAPS-CC). This altered balance between productivity (biogeochemical warming) and leaf area (biogeophysical warming) demonstrates the importance of including leaf mass per area acclimation to CO_2.

In addition to leaf mass per area, other changes in coordinated leaf traits could be expected to occur under climate change and further influence biogeophysical and biogeochemical warming. Longer leaf lifespans are correlated with higher leaf mass per area across species [Wright et al., 2004] and could be expected to offset the climate influence of leaf mass per area by enhancing productivity beyond current estimates. However, this correlation observed across species does not necessarily hold for trait changes within a species, such as in response to acclimation [Lusk et al., 2008, Fisher et al., 2015, Anderegg et al., 2018]. Observations of leaf lifespan acclimation to elevated CO_2 indicate that the response is highly variable in magnitude and sign and inconsistently associated with higher leaf mass per area [e.g., Norby et al., 2003, 2010, Taylor et al., 2008, and references therein]. As the observational evidence does not support an increase in leaf lifespan in coordination with leaf mass per area acclimation to CO_2, we chose not to impose this change in our simulations. However, we do include changes in leaf area duration due to phenological responses to warming temperature and soil moisture in all simulations [Oleson et al., 2013]. Litter decomposition has also been hypothesized to slow with leaf responses to elevated CO_2 with implications for carbon cycling [Strain and Bazzaz, 1983]. However, a meta-analysis of observations found that the effect of elevated CO_2 on leaf decomposition processes was not significant, despite changes in leaf litter traits [Norby et al., 2001]. We therefore do not test changes in litter decomposition here. Lastly, changes in leaf nitrogen concentration and anatomy in response to climate

change could alter albedo through their influence on leaf reflectance and transmittance [e.g., Ollinger, 2011], a possible avenue for future research. Leaf acclimation in our simulations was allowed to influence albedo indirectly by altering leaf area index but did not alter leaf optical characteristics because the influence of individual leaf traits (e.g., leaf mass per area) on these properties remains highly uncertain especially under future conditions [Ollinger, 2011].

Several environmental drivers of leaf mass per area acclimation — CO_2, temperature, and nutrient limitation — will likely be modified by climate change. We estimate that the influence of temperature acclimation of leaf mass per area globally is secondary to CO_2 (Supporting Text A.2.1 and Figure A.1). The effect of temperature warming on leaf mass per area occurs under cold conditions; thus, the acclimation is limited to high latitude boreal regions (Figure A.5). Nutrient limitation is expected to increase with CO_2 fertilization of plant growth [Wieder et al., 2015, Norby et al., 2010] and has been found to enhance leaf mass per area in manipulation experiments [Poorter et al., 2009], which could further amplify the impacts of leaf acclimation to elevated CO_2. The magnitude of leaf mass per area acclimation in response to climate change may ultimately depend upon the combined influence, including potential interaction effects, of multiple climate drivers.

Accounting for leaf acclimation in climate projections will require the ability to represent the functional relationship between leaf mass per area and its climate drivers, especially CO_2, by biome at the global scale. This remains challenging [Medlyn et al., 2015]. Poorter et al. [2009]'s empirical relationship, used herein, shows that on average leaf mass per area increases with CO_2 in C_3 species. However, the proportion of variance in the magnitude of acclimation explained by this relationship is relatively low [Poorter et al., 2009], suggesting that other key drivers, such as plant type, still need to be incorporated. A mechanistic model of leaf mass per area acclimation also remains elusive. The leading hypothesis for why elevated CO_2 increases leaf mass per area is that the abundance of carbon causes nonstructural carbohydrates to accumulate in leaves [Poorter et al., 2009, 1997, Pritchard et al., 1999, Roumet et al., 1999]. One possible advantage for plants of increasing leaf mass

per area under elevated CO_2 is that it maintains a high level of leaf nitrogen per leaf area (gN/m^2 leaf area), an essential component of photosynthetic machinery, by counteracting a decrease in leaf nitrogen concentration (gN/g leaf) driven by larger pools of nonstructural carbohydrates [N per area = N per mass x leaf mass per area; Luo et al., 1994, Poorter et al., 1997, Peterson et al., 1999, Stitt and Krapp, 1999, Ishizaki et al., 2003]. However, this process operates differently across environments, plant species, and even genotypes [Luo et al., 1994, Körner et al., 1997, Poorter et al., 1997, 2009, Peterson et al., 1999, Stitt and Krapp, 1999, Roumet et al., 1999, Pritchard et al., 1999]. Further research into the underlying mechanism, influences of multiple environmental drivers, and differences in acclimation between plant types is needed to develop a representation of leaf mass per area acclimation suitable for use in Earth system models.

The climate implications of increased leaf mass per area reveal an urgent need for observational constraints on the magnitude and mechanism of leaf trait acclimation to future climate conditions. Other structural trait acclimations that influence leaf area may have similar climate implications that require testing. Our findings suggest that the uncertainty in vegetation-climate feedbacks, and therefore climate change projections, is even larger than previously thought.

2.6 Acknowledgements

We thank M. Laguë and E. Garcia for help with model setup. We acknowledge support from the National Science Foundation AGS-1321745 and AGS-1553715 to the University of Washington. High-performance computing support from Yellowstone (ark:/ 85065/d7wd3xhc) was provided by NCAR's Computational and Information Systems Laboratory, sponsored by the National Science Foundation. M. K. thanks the UW Program on Climate Change Graduate Fellowship for support. Model results are available through the University of Washington Libraries ResearchWorks digital repository. The URL for the data in the ResearchWorks system is https://digital.lib.washington.edu/researchworks/handle/1773/41856.

2.7 Figures and Tables

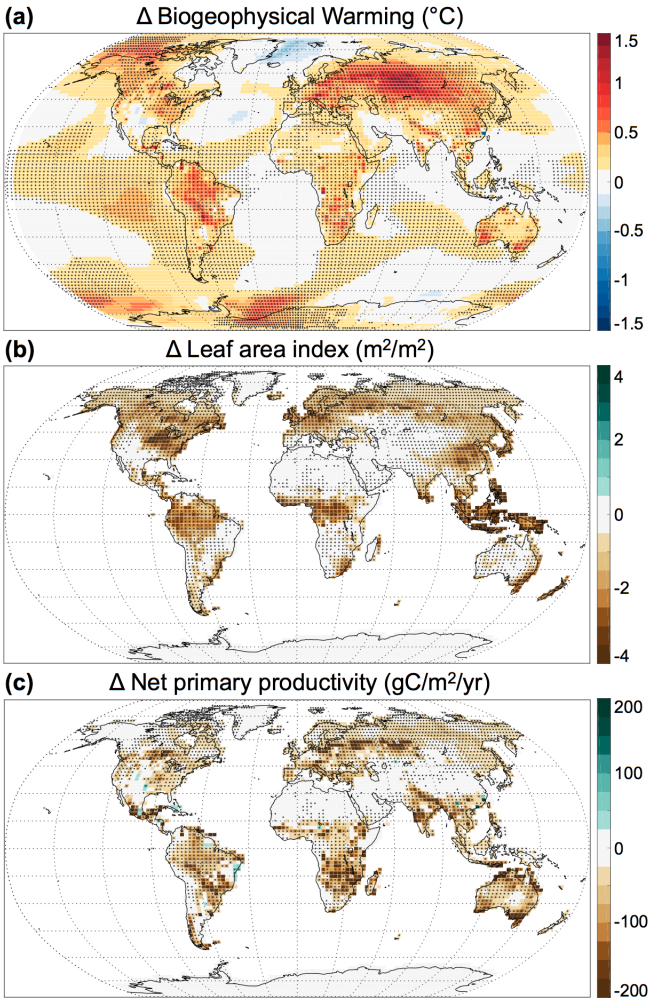

Figure 2.1: Annual mean change due to leaf acclimation to CO_2 (CCLMA-CC) of (a) biogeophysical warming (°C); (b) leaf area index (m^2/m^2); and (c) net primary productivity (gC/m^2/year). Stippling indicates significance at the 95% level.

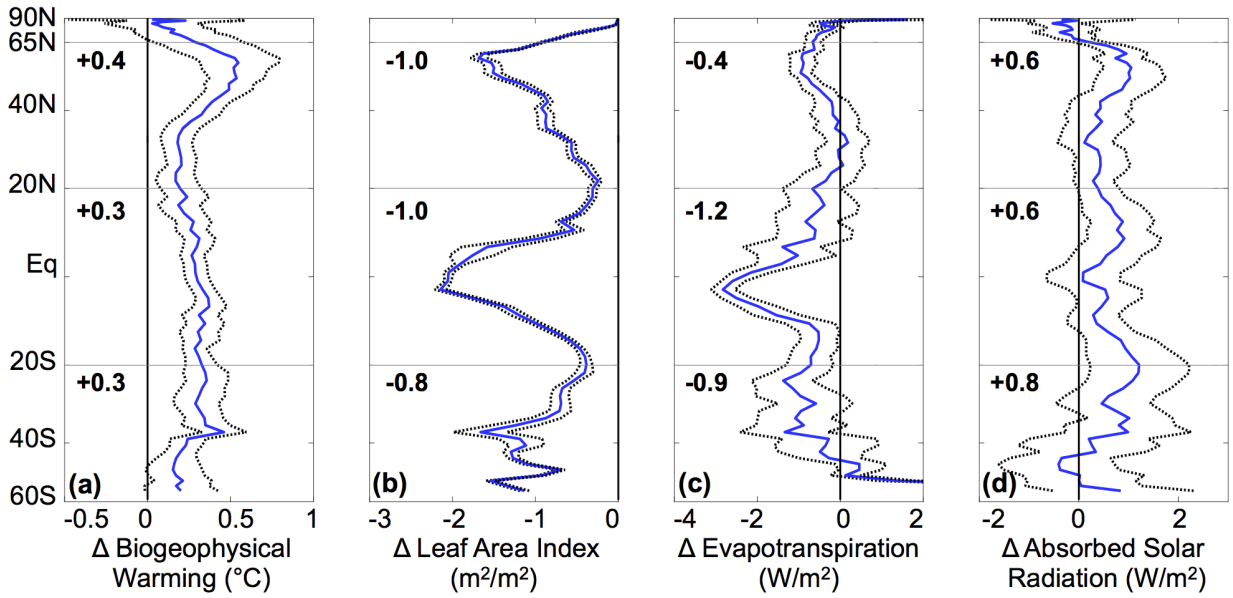

Figure 2.2: Zonal annual mean change over land due to leaf acclimation to CO_2 (CCLMA-CC) of (a) biogeophysical warming (°C); (b) leaf area index (m^2/m^2); (c) evapotranspiration (W/m^2); and (d) net solar radiation absorbed at the surface (W/m^2). The mean difference is shown in blue, along with the 95% bootstrap confidence interval (black dashed) and average zonal mean change on land (bold numbers) for each latitude band (bounded by gray lines).

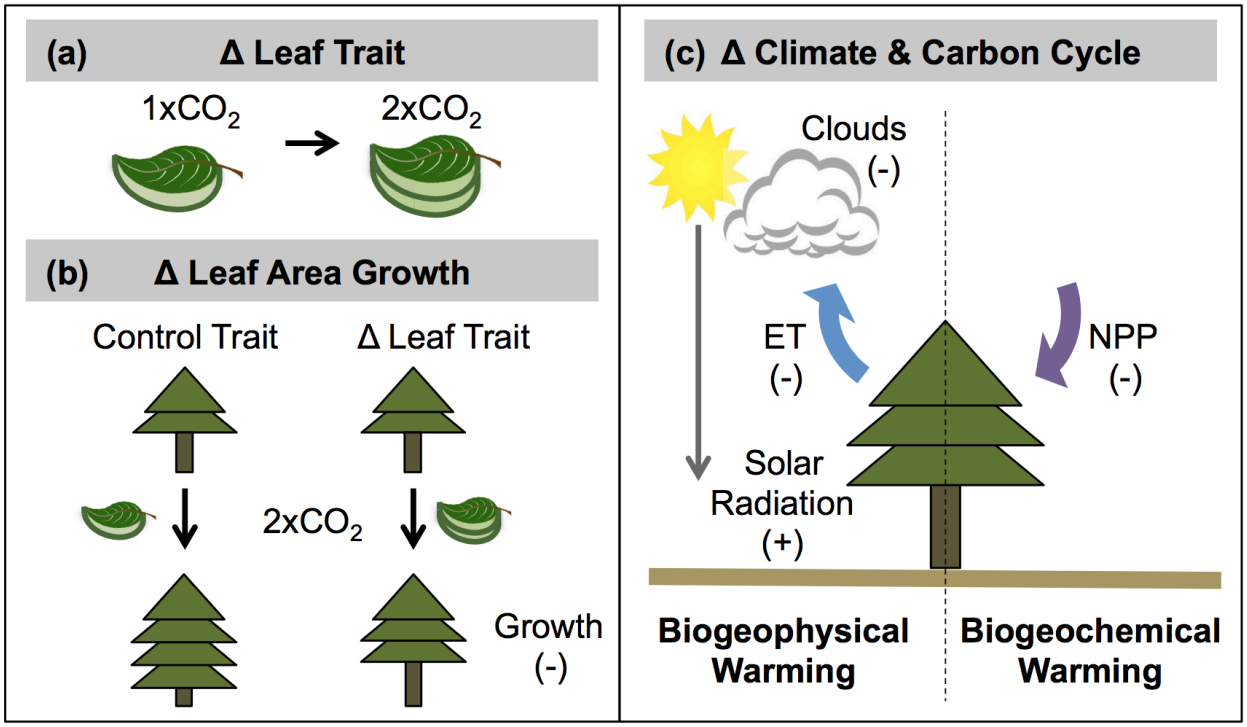

Figure 2.3: Schematic summary of changes due to leaf trait acclimation to elevated CO_2. (a) Leaf mass per area increases in response to elevated CO_2 in C_3 plants (CCLMA). Light green represents leaf mass (gC); dark green represents leaf area (m^2). (b) Leaf trait acclimation reduces leaf area growth in response to elevated CO_2 compared to the climate change control (CCLMA-CC). (c) Lower leaf area growth drives additional biogeophysical warming over land compared to the climate change control (CCLMA-CC) by diminishing evapotranspirative (ET) cooling, reducing cloud cover, and enhancing solar radiation absorbed by the surface. It also decreases net primary productivity (NPP), which can drive additional anomalous biogeochemical warming by reducing land uptake of CO_2 from the atmosphere. A positive sign (+) indicates an increase and a negative sign (-) represents a decrease in response to leaf trait acclimation (CCLMA-CC).

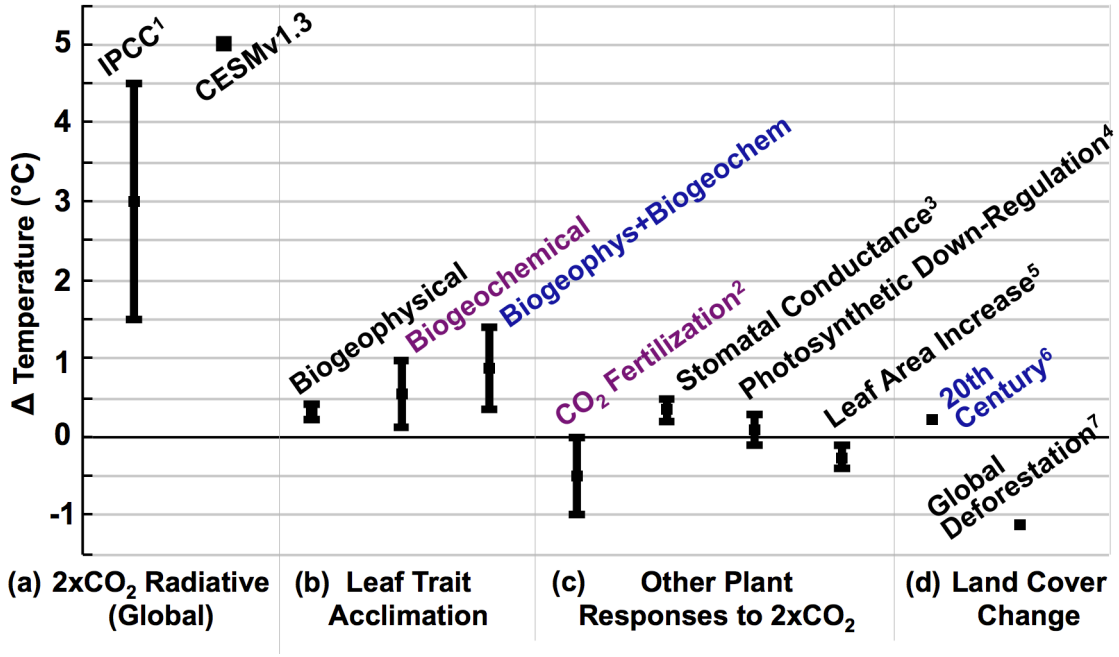

Figure 2.4: Comparison of temperature changes in response to a doubling of CO_2 (a) radiative forcing; (b) acclimation of leaf mass per area; (c) other plant responses; and (d) land cover change with color of text indicating biogeophysical warming (black text), biogeochemical warming (purple text), and combined warming (blue text). Estimates were drawn from the literature as follows: [1]Ciais et al. [2013] range based on observations of 20th century climate change, paleoclimate, Coupled Model Intercomparison Project Phase 5 climate models, and feedback analysis; [2]Estimated temperature response to radiative forcing from carbon-concentration feedback parameters for land across Coupled Model Intercomparison Project Phase 5 models [Arora et al., 2013] and CO_2 doubling in this study (355 to 710 ppm); [3]Mean responses across studies [Cao et al., 2010, Pu and Dickinson, 2012, Sellers et al., 1996]; [4]Mean responses across studies [Bounoua et al., 2010, Pu and Dickinson, 2012]; [5]Mean responses across studies [Bounoua et al., 2010, Pu and Dickinson, 2012]; [6]Pongratz et al. [2010]; and [7]Davin and de Noblet-Ducoudré [2010]. Intergovernmental Panel on Climate Change (IPCC).

Table 2.1: Annual mean change over land due to leaf trait acclimation (CCLMA-CC)

	Global		**S. extratropics**		**Tropics**		**N. extratropics**	
Biogeophysical Warming (°C)	0.3	(0.1%)	0.3	(0.1%)	0.3	(0.1%)	0.4	(0.1%)
Net primary productivity (PgC/yr)	-5.8	(-6.4%)	-0.8	(-9.1%)	-2.5	(-6.1%)	-2.1	(-6.2%)
Leaf area index (m^2/m^2)	-0.9	(-26.0%)	-0.8	(-24.0%)	-1.0	(-24.3%)	-1.0	(-27.4%)
Evapotranspiration (W/m^2)	-0.7	(-1.5%)	-0.9	(-1.6%)	-1.2	(-1.6%)	-0.4	(-1.1%)
Transpiration (W/m^2)	-1.4	(-5.8%)	-1.9	(-7.2%)	-1.7	(-4.6%)	-1.1	(-6.7%)
Leaf Evaporation (W/m^2)	-0.8	(-8.6%)	-0.7	(-8.5%)	-1.3	(-8.3%)	-0.5	(-9.0%)
Soil Evaporation (W/m^2)	1.4	(9.5%)	1.6	(7.0%)	1.9	(10.6%)	1.3	(9.9%)
Absorbed Solar Radiation (W/m^2)	0.6	(0.4%)	0.8	(0.5%)	0.6	(0.4%)	0.6	(0.4%)

Note. All changes significant at the 95% level. Percent change ((CCLMA-CC)/CC) in parentheses. Confidence intervals reported in Table A.2.

Chapter 3

LEAF TRAIT PLASTICITY ALTERS COMPETITIVE ABILITY AND FUNCTIONING OF SIMULATED TROPICAL TREES IN RESPONSE TO ELEVATED CARBON DIOXIDE

Marlies Kovenock[1], Charles D. Koven[2], Ryan G. Knox[2], Rosie A. Fisher[3], and Abigail L.S. Swann[4,1]

[1]Department of Biology, University of Washington, Seattle, WA; [2]Lawrence Berkeley National Laboratory, Berkeley, CA; [3]National Center for Atmospheric Research, Boulder, CO; [4]Department of Atmospheric Sciences, University of Washington, Seattle, WA.

Supporting Information referenced in this chapter can be found in Appendix B.

3.1 Abstract

The response of tropical ecosystems to elevated carbon dioxide (CO_2) remains a critical uncertainty in projections of future climate. Here we investigate how leaf trait plasticity in response to elevated CO_2 alters projections of tropical forest competitive dynamics and functioning. We use demographic vegetation model simulations to quantify how plasticity in leaf mass per area and the ratio of leaf carbon to nitrogen alter the responses of carbon uptake, evapotranspiration, and competitive ability to a doubling of CO_2 in a tropical forest. We find that observationally constrained leaf trait plasticity levels in response to CO_2 fertilization reduce the enhancement in tropical tree carbon uptake (up to -14.7%, 95% confidence interval [$CI_{95\%}$] -14.4 to -15.0), further diminish evapotranspiration (up to -7.0%, $CI_{95\%}$ -6.4 to -7.7), and lower competitive ability under a doubling of CO_2 in our simulations. Thus, consideration of leaf trait plasticity to elevated CO_2 lowers simulated tropical ecosystem carbon uptake and evapotranspirative cooling in the absence of changes in plant type abundance. However, given that more competitively advantageous leaf trait plasticity responses also maintain higher levels of plant productivity and evapotranspiration, including changes in plant type abundance may mitigate these decreases in ecosystem functioning. Models that explicitly represent competition between plants with alternative leaf trait plasticity in response to elevated CO_2 are needed to capture these influences on tropical forest functioning and large-scale climate.

3.2 Introduction

Tropical forests currently exert strong control over large-scale carbon, water, and energy fluxes and thus strongly influence global climate [Bonan, 2008, Davin and de Noblet-Ducoudré, 2010, Cusack et al., 2016, Cox et al., 2000]. Yet, the poorly understood response of tropical ecosystems to elevated carbon dioxide (CO_2) over the coming decades and centuries remains a key uncertainty in projections of future climate [e.g., Ciais et al., 2013, Zhang et al., 2015, Lloyd and Farquhar, 2008, Schimel et al., 2015, Brienen et al., 2015, Hickler

et al., 2008, Cernusak et al., 2013, Leakey et al., 2012a, van der Sleen et al., 2015, Cusack et al., 2016]. A number of leaf traits have been observed to respond to rising CO_2 concentrations. This leaf trait plasticity could alter tropical ecosystem functioning, with potential implications for large-scale climate. Alterations in leaf traits can modify plant photosynthesis and evapotranspiration rates. Given this, the capacity for leaf trait plasticity to alter ecosystem functioning could be direct, without changes in plant type abundance, as well as indirect, through changes in plant competitive dynamics and, thus, the relative abundance of different plant types.

Among the most commonly observed plant trait responses to experimentally elevated CO_2 are increases in leaf mass per area (LMA, g leaf carbon m^{-2} leaf area) and the ratio of carbon to nitrogen within leaves ($C:N_{leaf}$, g leaf carbon g^{-1} leaf nitrogen). Observations suggest that each of these leaf traits could increase by as much as one third in response to a doubling of CO_2 in a wide range of tropical tree species spanning successional classes [Figure 3.1; Lovelock et al., 1998, Reekie and Bazzaz, 1989, Winter et al., 2000, Winter and Lovelock, 1999] implying thicker leaves with lower per-mass nitrogen concentrations. Comparison of Earth system model simulations to observations at ecosystem-scale CO_2 enrichment experiments suggests that accurately representing these two leaf traits is critical to predicting ecosystem responses to elevated CO_2 [Zaehle et al., 2014, De Kauwe et al., 2014, Medlyn et al., 2015].

The leading hypothesis for why $C:N_{leaf}$ and LMA increase with elevated CO_2 is that CO_2 fertilization leads to nitrogen limitation of plant growth and the accumulation of nonstructural carbohydrates in leaves [Winter et al., 2001, Poorter et al., 2009, 1997, Pritchard et al., 1999, Roumet et al., 1999, Meyerholt and Zaehle, 2015]. Here we use the term "plastic" to describe these changes. While both trait changes have potential benefits (discussed below), it is possible that these changes are forced upon plants as there is not enough nitrogen to retain default leaf traits under high CO_2.

3.2.1 Direct Effects

Plasticity in C:N_{leaf} and LMA could directly influence tropical forest functioning by altering maximum area-based photosynthetic rates. C:N_{leaf} describes the amount of nitrogen present in a given unit of leaf mass, with higher C:N_{leaf} indicating a lower amount of nitrogen per unit leaf mass. LMA describes the amount of mass used to construct a unit of leaf area. Together these two traits control the amount of nitrogen per leaf area (N_{area}, g leaf N m^{-2} leaf area) as follows:

$$N_{area} = \frac{LMA}{C{:}N_{leaf}} \tag{3.1}$$

where LMA is leaf mass per area (g leaf C m^{-2} leaf area) and C:N_{leaf} is the leaf carbon to nitrogen ratio (g leaf C g^{-1} leaf N). Given that nitrogen is an essential component of photosynthetic enzymes, particularly rubisco, N_{area} is an important determinant of maximum photosynthetic rates per leaf area [Drake et al., 1997, Kattge et al., 2009, 2011, Walker et al., 2014, Norby et al., 2017]. N_{area} is therefore used in many terrestrial biosphere models to estimate photosynthetic parameters, which in turn exert strong influence over modeled carbon uptake [Verheijen et al., 2013, Bonan et al., 2011, Walker et al., 2017, Rogers et al., 2017]. Changes in maximum photosynthetic rates due to altered N_{area} can also influence rates of evapotranspirative cooling, as transpiration is coupled to photosynthesis in all commonly used stomatal conductance algorithms [Ball et al., 1987, Medlyn et al., 2011].

Experimental manipulation of CO_2 in tropical forest systems was observed to modify both traits in a wide range of tropical tree species across successional classes [Lovelock et al., 1998]. Observations suggest that co-occurring changes in LMA and C:N_{leaf} in response to a doubling of CO_2 most often cause N_{area} to decrease (Figure 3.1 below diagonal line) or, in fewer cases, to be maintained [Figure 3.1 on diagonal line; Lovelock et al., 1998]. Thus, in the absence of other changes [such as adjusted partitioning of nitrogen between different photosynthetic processes; e.g., Xu et al., 2012, Leakey et al., 2012b, Smith et al.,

2019] observed leaf trait plasticity in response to elevated CO_2 has the potential to lower projections of tropical ecosystem carbon uptake and evapotranspirative cooling by reducing photosynthetic rates and stomatal conductance.

Leaf trait plasticity could also directly influence ecosystem functioning by modifying leaf area index (m^2 leaf area m^{-2} ground), which provides the surface area over which photosynthesis and transpiration are scaled to the ecosystem level. Increasing LMA increases the carbon cost of building leaf area, as thicker leaves require more carbon to build a given unit of leaf area. For a given unit of mass carbon allocated to leaves, LMA is universally used to calculate plant leaf area. For a given C:N_{leaf}, increasing LMA also increases nitrogen requirements, while, increasing C:N_{leaf} makes leaf area less expensive in terms of nitrogen. In models, these dynamics are of course only applicable when active nitrogen cycling is represented.

The influences of leaf plasticity in C:N_{leaf} and LMA on photosynthetic rates and leaf area exhibit trade-offs under elevated CO_2. Increases in C:N_{leaf} could reduce maximum photosynthetic rates but do not alter the carbon cost of building leaf area; increases in LMA could offset reductions in maximum photosynthetic rates due to higher C:N_{leaf} but increase the cost of building leaf area. Given both the conflicting impacts of increasing C:N_{leaf} and LMA on N_{area}, and the secondary impacts on leaf area, the likely net response of ecosystems to elevated CO_2 taking into account this type of leaf trait plasticity is not immediately apparent.

3.2.2 Indirect Effects

Competition for light is recognized to be a dominant driver of community composition in tropical forests [e.g., Sterck et al., 2011]. In addition to the direct influences described above, tropical tree responses to increasing CO_2 could also indirectly change ecosystem functioning by altering plant competition for light and the relative abundance of different plant types [reviewed by Cusack et al., 2016]. The magnitude of leaf trait responses to elevated CO_2 has been observed to differ among tropical tree species [Lovelock et al., 1998, Reekie and Bazzaz,

1989, Winter et al., 2000, Winter and Lovelock, 1999]. Such variation in leaf trait plasticity across tropical tree types could lead to differential changes in the competitive ability for light in response to elevated CO_2 and thus alter the abundance of different plant types. Leaf area index and biomass can influence plant competitive ability. In general, trees which accumulate less biomass may not be able to grow as tall as their neighbors and may therefore become more heavily shaded; while trees with lower leaf area index may not be able to capture as much light or shade their neighbors in competition for light. LMA and C:N_{leaf} both can alter leaf area index and biomass through their influence on per-area photosynthetic rates as well as total leaf area. Thus changes in these traits are likely to differentially alter the competitive ability of individuals depending on their magnitude of plasticity.

3.2.3 Critical Unknowns

Due to the trade-offs associated with higher C:N_{leaf} and increases in LMA, it remains unknown how leaf trait plasticity will alter overall tropical tree functioning and competitive success under future elevated CO_2 conditions. Manipulation experiments have shown that tropical tree trait responses to CO_2 are species-specific [Lovelock et al., 1998, Reekie and Bazzaz, 1989, Winter et al., 2000, Winter and Lovelock, 1999] and suggest that differences in CO_2 responses across species could lead to changes in community structure [reviewed by Cusack et al., 2016]. Investigating the relationship between individual traits and community outcomes is challenging in empirical studies due to multiple, confounding changes in plants treated with elevated CO_2 [Lovelock et al., 1998, Reekie and Bazzaz, 1989]. Increasing C:N_{leaf} may benefit plants. McMurtrie et al. [2008] showed that a temperate monoculture was able to maximize productivity under limited nitrogen availability and elevated CO_2 by increasing C:N_{leaf} which enabled increased leaf area. Increasing LMA could also be beneficial. Previous modeling studies have used observations of LMA and C:N_{leaf} change to simulate changes in assimilation and individual plant growth and found that increasing LMA helps to offset negative effects of higher C:N_{leaf} on photosynthetic rates per leaf area under elevated CO_2 [Luo et al., 1994, Ishizaki et al., 2003]. However, none of these studies considered communities

of plants or the effects of competition between different plant types, nor did they focus on tropical tree species. Other modeling studies have found variability in plant traits, such as LMA, to have strong influences on plant competition for resources and ecosystem functioning under elevated CO_2, but did not consider the observed concomitant changes in C:N_{leaf} [Ali et al., 2015, Verheijen et al., 2015, Fisher et al., 2010]. This distinction is important because without representing the potential benefit of increasing LMA, Ali et al. [2015] found that decreasing LMA (opposite of observed change) was beneficial to competitive success under elevated CO_2. Thus, how the combination of these observed trait responses to CO_2 will influence plant competitive dynamics, the survival of responsive trees, and tropical ecosystem structure and functioning in the future remains unknown. Further, leaf trait plasticity and its influence on tropical ecosystem functioning could have implications for climate both locally, through altering evapotranspirative cooling, and globally through altering tropical ecosystem carbon uptake [Verheijen et al., 2015, Kovenock and Swann, 2018].

In this study we explore how plasticity in two key leaf traits mediates tropical ecosystem carbon uptake and evapotranspirative cooling responses to a doubling of CO_2 using an ensemble of demographic vegetation model simulations run with the Functionally Assembled Terrestrial Ecosystem Simulator [FATES, Fisher et al., 2015, 2018] at a tropical forest test site, Barro Colorado Island, Panama. We investigate how different levels of plasticity in C:N_{leaf} and LMA (gray squares in Figure 3.1) in response to a doubling of CO_2: 1) modify ecosystem level carbon uptake and evapotranspirative cooling in the absence of competition; 2) alter biomass and leaf area index, which are key determinants of competitive ability for light; and 3) alter competitive outcomes when two plant types with different leaf trait plasticity responses compete. We test leaf trait plasticity levels that decrease (-N_{area}), maintain (=N_{area}), and increase N_{area} (+N_{area}). As our simulations do not explicitly represent growth limitation by or competition for nitrogen, we are able to quantify whether the change in total canopy nitrogen (g N m^{-2} ground) required to support an ecosystem with each level of leaf trait plasticity under a doubling of CO_2 would be consistent with available soil nitrogen

resources. We find that leaf trait plasticity levels that decrease N_{area}, as are consistent with observed responses, could reduce projections of future carbon uptake and evapotranspiration in the absence of competition. However, trees that maintain or increase N_{area} under elevated CO_2 would likely have a competitive advantage and also maintain higher levels of carbon uptake and evapotranspirative cooling.

3.3 Materials and Methods

3.3.1 Model Overview

We use an ensemble of simulations of the Functionally Assembled Terrestrial Ecosystem Simulator [FATES, Fisher et al., 2015, 2018] embedded within the Community Land Model version 5 [Lawrence et al., 2018] to test the influence of leaf trait plasticity on tropical ecosystem functioning and competitive dynamics. CLM(FATES) is a cohort-based demographic vegetation model [Fisher et al., 2018] that mechanistically simulates plant ecological dynamics and ecosystem assembly via processes including plant growth, competition for light, recovery from disturbance, reproduction, mortality, and recruitment. A key feature of the model, based on the ecosystem demography concept [Moorcroft et al., 2001], is that it resolves distributions of vegetation height and time since disturbance, which allows it to simulate competition for light. In the model, disturbance, from tree mortality, fire, or logging, periodically befalls some patches of the simulated ecosystem. Plants within these "patches" are considered to share an age class, which represents their age since last disturbance. Within a patch, individual plants are grouped into "cohorts", which can differ in height. Cohorts represent individual plants of the same plant type and height as a representative average individual. The height structure of cohorts within a patch determines the light profile experienced by each cohort. The leaf area of taller cohorts in the canopy can shade cohorts deeper in the canopy, which is depicted as discrete layers using the perfect plasticity approximation [Purves et al., 2008]. Photosynthesis, respiration, turnover, and mortality, as well as the interaction of these processes with the abiotic environment, control

the amount of carbon each cohort can use for growth. Growth and size-dependent allometric equations then determine the height, biomass, and target leaf area of each cohort. Thus, carbon uptake is dynamic and influences plant growth, leaf area, and size, which in turn influence competition for light. Radiation streams for direct and diffuse light are calculated at the leaf layer level for each plant type. This incoming energy influences photosynthesis and the leaf energy budget, and thus rates of carbon uptake and transpiration. In sum, the model tracks fluxes of carbon, water, and energy throughout the ecosystem. CLM(FATES) does not yet explicitly represent growth limitation by or competition for nutrients, which allows us to implement C:N_{leaf} and LMA plasticity levels that represent the potential influences of nutrient limitation and quantify the total canopy nitrogen required to support each leaf trait plasticity level.

Baseline parameters for the model (Table B.1) were chosen from a parameter ensemble that sampled plant parameters from observations when possible. Our primary results used the parameterization that allowed the simulated ecosystem to best match present-day measurements of leaf area index, above-ground biomass, basal area, gross primary productivity, latent heat fluxes, and sensible heat fluxes at our test site, Barro Colorado Island, Panama. We also test the sensitivity of our results to the next two best performing parameter sets. (See Supporting Information Text B.1.1 and B.2.1 for details.)

3.3.2 Leaf trait plasticity estimation and implementation

In this study we impose prescribed changes in two plant traits: C:N_{leaf} and LMA. Our experiments test 13 levels of leaf plasticity in C:N_{leaf} and LMA sampled from the two-dimensional leaf trait plasticity space in Figure 3.1 (gray squares). This leaf trait plasticity space represents both observed (at or below diagonal line in Figure 3.1) and hypothetical (above diagonal line in Figure 3.1) levels of leaf trait plasticity. The observed leaf trait plasticity space is estimated from observations of leaf responses to a doubling of CO_2 in nine tropical tree species, including early, mid- and late successional classes [red circles in Figure 3.1; Lovelock et al., 1998], and supported by additional studies in tropical trees and

many other C_3 plant types [e.g., Lovelock et al., 1998, Reekie and Bazzaz, 1989, Winter et al., 2000, Winter and Lovelock, 1999, Poorter et al., 2009, Ainsworth and Long, 2005, Medlyn et al., 2015]. These observations suggest that C:N_{leaf} and LMA could increase by as much as one third in response to a doubling of CO_2 with the result that N_{area} decreases or remains constant following Equation 3.1. Thus, we define observed leaf trait plasticity levels as those that maintain N_{area} at (=N_{area}) or below (-N_{area}) control (CTRL and CC) levels. We also test leaf trait plasticity levels that increase N_{area} (+N_{area}), to determine if such a response could help tropical trees enhance their productivity and competitive ability. Given the wide diversity of tropical tree species it is possible that some tropical tree species, perhaps those with traits that enhance nutrient foraging or fixing capabilities, increase N_{area} (above diagonal line in Figure 3.1) in response to higher CO_2.

Changes in C:N_{leaf} and LMA in our simulations drive changes in N_{area}, maximum photosynthetic and respiration rates, and leaf area index. We assume that LMA decreases with canopy depth following the observations of Lloyd et al. [2010] as previously implemented in CLM(FATES) in Chapter 4. As leaf area index responds dynamically to carbon available for leaf growth, C:N_{leaf} drives changes in leaf area index through its influence on productivity. (See Supporting Information Text B.1.2 for details.)

3.3.3 Simulations

We ran simulations for a tropical forest test site, Barro Colorado Island, Panama. All simulations were forced with repeating meteorological data for this site from the years 2003-2016 [Faybishenko et al., 2018]. Vegetation in our simulations is broadly categorized by a single biogeographic plant functional type, the broadleaf evergreen tropical tree, which is characteristic of our tropical forest test site. This plant functional type represents an average of many species within the evergreen tropical tree plant type. Two control simulations represent a baseline tropical forest ecosystem without leaf trait plasticity. The first control simulates the ecosystem with CO_2 concentration fixed at 400 ppm CO_2 (CTRL; 1xCO_2). The second control is identical to the first except that the ecosystem experiences a fixed

atmospheric CO_2 concentration of 800 ppm (CC; 2xCO_2). Plants in these control simulations do not experience leaf trait plasticity in response to elevated CO_2 (gray square at origin in Figure 3.1). The difference between the control simulations (CC - CTRL) quantifies the influence of CO_2 fertilization on the baseline simulated tropical ecosystem. Temperature does not change in response to elevated CO_2 in our simulations.

We quantify the direct influence of different degrees of leaf trait plasticity, in the absence of competition, using an ensemble of simulations that are identical to the 2xCO_2 control (CC). Each ensemble member imposes a different level of leaf trait plasticity (gray squares sampled from leaf trait plasticity space in Figure 3.1) on all plants in the simulation. We call these simulations of the ecosystem "in absence of competition" between different plant types. We further group leaf trait plasticity experiments by whether they decrease (-N_{area}, below diagonal line in Figure 3.1), maintain (=N_{area}, on diagonal line in Figure 3.1), or enhance N_{area} (+N_{area}, above diagonal line in Figure 3.1). We calculate the total canopy nitrogen required for each "in absence of competition" simulation as total canopy leaf carbon (g leaf C m^{-2} ground) divided by C:N_{leaf} (g C g^{-1} N).

We test the influence of leaf trait plasticity level on competitive ability using a second ensemble of simulations, which we refer to as "pairwise competition" simulations. These simulations are identical to the 2xCO_2 control (CC) except that each experiment includes two different plant types, which are identical in all traits except in their level of leaf trait plasticity. The two plant types are allowed to compete for light within the ecosystem. We repeat these pairwise competition experiments for all combinations of two levels of leaf trait plasticity sampled from the leaf trait plasticity space (gray squares in Figure 3.1), including the control "no leaf trait plasticity" plant type (gray square at origin in Figure 3.1). In each competition simulation, one plant type (i.e., one level of leaf trait plasticity) always eventually outcompetes the other. We define one plant type as "winning" the competition when it overtakes at least two thirds of the total ecosystem biomass (see below for further details). We quantify differences in competitive ability due to leaf trait plasticity using a measure called percent wins (% wins), which is the percent of all pairwise competitions a

plant type with a given leaf trait plasticity level wins.

The 1xCO_2 control simulation (CTRL) was started from near-bare ground and integrated for 700 years. All control variables came into equilibrium within 450 years, the time required to grow a mature forest with our model set up. The 2xCO_2 control simulation (CC) and all experiments were branched from the 1xCO_2 control simulation (mature forest) at year 500 and experienced an abrupt doubling of CO_2 to a time-invariant concentration of 800 ppm CO_2. The 2xCO_2 control and experiment simulations were run until one plant type had become dominant (taken over at least 67% of ecosystem biomass and trending towards overtaking all ecosystem biomass). We analyze the last 100 years of each simulation as our equilibrium ecosystem. All simulations were run on the National Center for Atmospheric Research's Cheyenne system.

3.3.4 Statistical Analysis

We quantify the influence of leaf trait plasticity on tropical ecosystem properties using differences in annual mean ecosystem properties and relationships between leaf trait plasticity levels and annual mean ecosystem properties across simulations in the absence of competition (i.e., simulations with only one plant type). We use bootstrap methods with model years as the unit of replication (n = 50,000) to construct confidence intervals for annual mean leaf area index, biomass, net primary productivity, evapotranspiration, and total canopy nitrogen and test for differences between simulations. We use simple, multiple, and stepwise linear regression methods to test for relationships between leaf trait plasticity levels (C:N_{leaf}, LMA, N_{area}) and annual mean ecosystem properties across simulations. Correlations between percent wins and annual mean net primary productivity and evapotranspiration across simulations are quantified using Pearson's linear correlation coefficient. Differences, relationships, and correlations were considered statistically significant at the 95% level. (See Supporting Information Text B.1.4 for details.)

3.4 Results

3.4.1 Elevated CO_2 response in the control simulation

Previous observations, simulations, and theory show that elevated atmospheric CO_2 concentration enhances photosynthesis and reduces stomatal conductance, which has the potential to enhance productivity and reduce evapotranspiration at the ecosystem scale [e.g., Cernusak et al., 2013, Cusack et al., 2016, Zhu et al., 2016, Lloyd and Farquhar, 2008, Swann et al., 2016, De Kauwe et al., 2013, and references therein]. In our control simulation (no leaf trait plasticity; CC-CTRL) a doubling of atmospheric CO_2 concentration from 400 ppm to 800 ppm increases annual mean net primary productivity (+74.2%, 95% confidence interval [$CI_{95\%}$] 73.2 to 75.1), leaf area index (+7.0%, $CI_{95\%}$ 6.8 to 7.2), and biomass (+102.6%, $CI_{95\%}$ 102.1 to 103.0), and reduces evapotranspiration (-9.2%, $CI_{95\%}$ -8.6 to -9.8; Figures 3.2 and 3.4; Table 3.1). It is important to note that these results are in the absence of nutrient limitation, as this allows us to implement leaf changes in our experiments that represent potential influences of nutrient limitation and quantify the total canopy nitrogen required to support each leaf trait plasticity level.

The actual expected magnitude of tropical forest responses to elevated CO_2 is highly uncertain and little experimental data exists, particularly at the ecosystem scale [Lloyd and Farquhar, 2008, Hickler et al., 2008, Mahowald et al., 2016, Cusack et al., 2016, Norby et al., 2016]. However, our control simulation response to elevated CO_2 shows reasonable agreement with observations from temperate forest FACE experiments [De Kauwe et al., 2013, 2014] after scaling linearly for CO_2 increase. For example, a +200ppm CO_2 increase at Duke Forest enhanced net primary productivity by approximately 30% [De Kauwe et al., 2013]. If the response scales linearly with CO_2 [Cernusak et al., 2019], Duke Forest would see the equivalent of a +60% increase in net primary productivity for a +400 ppm increase in CO_2 as used herein. Similarly, these FACE experiments saw changes equivalent to approximately +6% and +30% in leaf area index at Oak Ridge and Duke, respectively; -40% in transpiration at Oak Ridge (no significant change at Duke Forest); and +100% in biomass increment at

Duke for +400 ppm CO_2. Although biomass increment and total biomass are not directly comparable measures, the increase in total biomass in our control simulation (+102%) is of similar magnitude. Thus our modeled changes are all roughly comparable with these ranges, with slightly higher modeled increases in net primary productivity in our tropical simulations compared to these observational estimates from temperate forests. Lastly, changes in each of these ecosystem properties in our control simulation also fall within the simulated ranges from 11 Earth system models at these two temperate forest FACE sites after linearly scaling for CO_2 concentration [De Kauwe et al., 2013, 2014]. While our control simulation response to elevated CO_2 is comparable to those estimated from observations in temperate forests, tropical forest responses may of course be subject to different constraints [e.g., De Graaff et al., 2006, Luo et al., 2006, Hickler et al., 2008, Zaehle et al., 2014].

3.4.2 Influence of leaf trait plasticity on canopy structure in absence of competition

We find that leaf trait plasticity alters biomass and leaf area index responses to a doubling of CO_2 in the absence of competition (Figure 3.2). Under elevated CO_2, increasing C:N_{leaf} by one third (the upper bound of the observed range we test herein) diminishes the increase in biomass (-10.6 kg C m^{-2}, $CI_{95\%}$ -10.5 to -10.7) and decreases leaf area index (-0.7 m^2 m^{-2}, $CI_{95\%}$ -0.7 to -0.8) compared to the control plant type (CN - CC). In contrast, increasing LMA by one third enhances the increases in both biomass (+7.2 kg C m^{-2}, $CI_{95\%}$ 7.1 to 7.4) and leaf area index (+1.4 m^2 m^{-2}, $CI_{95\%}$ 1.3 to 1.4) compared to the control plant type (LMA - CC). Increasing both C:N_{leaf} and LMA simultaneously by one third under a doubling of CO_2 (CNLMA) results in only a slightly reduced increase in biomass (-2.6 kg C m^{-2}, $CI_{95\%}$ -2.4 to -2.7) and no change in leaf area index (0.0, $CI_{95\%}$ 0.0 to 0.0) compared to the control plant type (CNLMA - CC).

Leaf trait plasticity levels are significant predictors of leaf area index and biomass responses to elevated CO_2. LMA and C:N_{leaf} are each significant predictors of leaf area index ($r = 0.67$ and $r = -0.71$, respectively) and biomass ($r = 0.60$, $r = -0.80$, respectively) across simulations in the absence of competition and under a doubling of CO_2. However, leaf area

index and biomass are best described using information about both leaf trait levels. Leaf area index is best predicted by N_{area} (r = 0.99), which takes into account information about both LMA and C:N_{leaf} (following Equation 3.1). Biomass is best described using both LMA and C:N_{leaf} as predictors (multiple regression adjusted R^2 = 0.996) or N_{area} (r = 0.98). Thus, for any given increase in C:N_{leaf}, simultaneously increasing LMA helps plants to maintain biomass and leaf area index that are closer to the control plant type.

The changes in biomass and leaf area index in the absence of competition we report here provide mechanistic insight into how leaf trait plasticity could alter competitive ability. The responses of biomass and leaf area index to leaf trait plasticity in the absence of competition suggest that increases in C:N_{leaf} may diminish competitive ability by reducing plant biomass and leaf area index compared to the control plant type; whereas, increasing LMA could improve competitive ability by enhancing biomass and leaf area index.

3.4.3 Influence of leaf trait plasticity on competitive ability

We find that the control plant type, with no leaf trait plasticity, is more competitively advantageous than all leaf trait plasticity levels sampled from the equal or reduced N_{area} plasticity space under a doubling of CO_2 (Figure 3.3). The control plant type (origin in Figure 3.3) wins all pairwise competitions against plant types with leaf trait plasticity levels sampled from the trait changes that maintain N_{area} (=N_{area}, along black dashed diagonal line in Figure 3.3) or reduce N_{area} (-N_{area}, below black dashed diagonal line in Figure 3.3).

Increasing C:N_{leaf} strongly diminishes competitive ability, as evidenced by the decreasing percentage of competitions a plant type wins as C:N_{leaf} increases (left to right, Figure 3.3). At a given C:N_{leaf}, increasing LMA typically enhances competitive ability.

These results from our competition experiments are consistent with our findings in the absence of competition (higher C:N_{leaf} leads to lower biomass and leaf area index and increasing LMA results in biomass and leaf area index gains; Figure 3.2). However, LMA increases sampled from leaf trait plasticity levels that maintain or decrease N_{area} do not, in this model, fully compensate for the negative influence of higher C:N_{leaf} on competitive

ability at any level. Furthermore, the competitive benefit of increasing LMA diminishes at higher C:N_{leaf}, as evidenced by the sinusoidal shape of the 50% wins shading (white) in Figure 3.3. In sum, plant types that can maintain higher N_{area} under elevated CO_2, have greater competitive ability.

Leaf trait plasticity levels that enhance N_{area} (+N_{area}, above diagonal line in Figure 3.3) enhance competitive ability compared to the control leaf type, as well as all leaf trait plasticity levels sampled from the =N_{area} and -N_{area} space (Figure 3.3). In this part of the leaf trait plasticity space, increasing LMA more than C:N_{leaf}, which enhances N_{area}, confers a competitive advantage. This is consistent with our finding that increasing LMA in isolation enhances biomass and leaf area index beyond the control in the absence of competition.

Competitive ability is related to leaf trait plasticity levels, as well as leaf area index and biomass. The percent wins of a leaf trait plasticity level is best predicted by both C:N_{leaf} and LMA levels (multiple regression adjusted R^2 = 0.985), where C:N_{leaf} is negatively related to percent wins (r = -0.92) and LMA is weakly but positively related to percent wins (r = 0.36). Percent wins is also highly related (r = 0.91) to N_{area} (i.e., LMA divided by C:N_{leaf}). As expected, percent wins is positively related to leaf area index (r = 0.90) and biomass (r = 0.96).

3.4.4 Changes in carbon uptake and evapotranspirative cooling

Ecosystem carbon uptake and evapotranspiration are linked to leaf area and photosynthetic rates, and thus have the potential to be altered by changes in LMA and C:N_{leaf}. Leaf trait plasticity levels sampled from the -N_{area} space reduce carbon uptake and evapotranspiration compared to the control response to a doubling of CO_2 (CC) in our experiments (Figure 3.4, Table 3.2). On average the observed changes in C:N_{leaf} and LMA reduce the increase in annual mean net primary productivity by -9.2% ($CI_{95\%}$ -8.9 to -9.5) and further reduce annual mean evapotranspiration by -4.4% ($CI_{95\%}$ -3.9 to -5.0) compared to the 2xCO_2 control (-N_{area} - CC). The largest reduction in net primary productivity (-14.7%, $CI_{95\%}$ -14.4 to -15.0) and evapotranspiration (-7.0%, $CI_{95\%}$ -6.4 to -7.7) results from the leaf trait

plasticity level that increases C:N_{leaf} by one third without a co-occurring increase in LMA (CN - CC).

Leaf trait plasticity levels that maintain N_{area} equal to the control (=N_{area}) also maintain carbon uptake and evapotranspiration at control levels (Figure 3.4, Table 3.2). Annual mean net primary productivity and evapotranspiration do not differ significantly between =N_{area} simulations and the control simulation under a doubling of CO_2 (=N_{area} - CC).

Leaf changes that enhance N_{area} (+N_{area}) increase carbon uptake and lessen the reduction in evapotranspiration compared to the control response to a doubling of CO_2 (Figure 3.4, Table 3.2). On average +N_{area} leaf trait plasticity levels increase annual mean net primary productivity by +8.4% ($CI_{95\%}$ 8.1 to 8.8) and lessen the reduction in evapotranspiration by +4.8% ($CI_{95\%}$ 4.2 to 5.3; +N_{area} - CC). The largest enhancement of net primary productivity (+13.4%, $CI_{95\%}$ 12.9 to 13.9) and evapotranspiration (+7.9%, $CI_{95\%}$ 7.2 to 8.6) results from the leaf trait plasticity level that increases LMA by one third but does not alter C:N_{leaf} (LMA - CC).

We find that the level of leaf N_{area}, which combines information about changes in LMA and C:N_{leaf}, best explains differences in annual mean net primary productivity (r = 0.99) and evapotranspiration (r = 1.00) among simulations. As expected, LMA is positively correlated with both net primary productivity (r = 0.71) and evapotranspiration (r = 0.70); while C:N_{leaf} is negatively correlated with net primary productivity (r = -0.71) and evapotranspiration (r = -0.71).

3.4.5 Influence of competition on carbon uptake and evapotranspirative cooling

Leaf trait plasticity levels that confer a higher competitive advantage also result in higher carbon uptake and evapotranspirative cooling (Figure 3.4). The competitive ability of a plant type with a given level of leaf trait plasticity, as measured by the percent of pairwise competitions won against plant types with other levels of plasticity (percent wins), is significantly correlated with net primary productivity (r = 0.91) and evapotranspiration (r = 0.91).

3.4.6 Total canopy nitrogen

Progressive nitrogen limitation is hypothesized to limit plant growth in response to elevated CO_2 [Luo et al., 2004] and may be a cause of C:N_{leaf} and LMA plasticity in response to elevated CO_2 [Poorter et al., 2009, 1997, Pritchard et al., 1999, Roumet et al., 1999, Meyerholt and Zaehle, 2015]. Here we report the total amounts of canopy nitrogen required for ecosystems with differing levels of leaf trait plasticity in the absence of nitrogen limitation and compare them to the 1xCO_2 control simulation (CTRL). The 1xCO_2 control (CTRL) provides a reference for the amount of nitrogen used by canopies in the simulated current-day ecosystem. Variation in total canopy nitrogen across simulations results from the leaf trait plasticity changes we imposed and changes in overall leaf carbon, which is an emergent property of each simulation.

We find that leaf trait plasticity levels that reduce leaf N_{area} (-N_{area}) are required to maintain or reduce the ecosystem's total canopy nitrogen requirement. Under 1xCO_2 conditions, our control simulation had a total canopy nitrogen requirement of 8.3 g N m^{-2} ground ($CI_{95\%}$ 8.3 to 8.3; CTRL). Doubling CO_2 increased the control ecosystem's total canopy nitrogen requirement by +0.3 g N m^{-2} ($CI_{95\%}$ 0.3 to 0.3) or +3.2% ($CI_{95\%}$ 3.1 to 3.3; CC - CTRL; Figure 3.3). Leaf trait plasticity levels that maintain N_{area} at control levels (=N_{area}) also increase the total amount of canopy nitrogen required beyond the 1xCO_2 control level but by slightly less with the mean change across =N_{area} simulations ranging from +2.1% to 3.0% (=N_{area} - CTRL; Figure 3.3). Leaf trait plasticity levels that reduce N_{area} compared to the control (-N_{area}) are needed to maintain total canopy nitrogen at or below the 1xCO_2 control level (-N_{area}; Figure 3.3). Across the observed range of leaf trait plasticity the total canopy nitrogen requirement was lowered by as much as -23.2% ($CI_{95\%}$ -23.2 to -23.3; CN - CTRL). Leaf trait plasticity levels that enhance N_{area} (+N_{area}) increased the total canopy nitrogen requirement beyond the 1xCO_2 by as much as +36.3% ($CI_{95\%}$ 36.2 to 36.5; LMA - CTRL; Figure 3.3).

3.5 Discussion

3.5.1 Large-scale climate implications

We find that observed changes in C:N_{leaf} and LMA reduce model predictions of tropical tree productivity, evapotranspiration, and competitive ability under high CO_2 and alter carbon and water fluxes, with implications for projections of future large-scale climate. We expect that reductions in evapotranspirative cooling over tropical forests would lead directly to local warming [Kovenock and Swann, 2018]. Reductions in carbon uptake leave more CO_2 in the atmosphere. If these reductions were to be widespread over tropical forests this could have global scale implications for warming through the greenhouse effect of CO_2 [Kovenock and Swann, 2018]. Tropical trees which are more able to maintain their leaf N_{area} near present-day levels have the highest competitive abilities and also show the smallest changes in carbon and water fluxes (Figure 3.4), suggesting that if changes in plant type abundance shift to reflect the most competitive members of the community this will allow maintenance of higher gas exchange rates, leaf area index, and biomass.

3.5.2 Constraints from canopy nitrogen budgets

Maintaining present-day N_{area} with a doubling of CO_2 requires an increase in canopy nitrogen for the control case (CC) as well as an increase in canopy nitrogen for all leaf trait plasticity levels which track ($=N_{area}$) or enhance ($+N_{area}$) the N_{area} of the control (Figure 3.3). Thus, if conservation of total canopy nitrogen due to ecosystem nitrogen limitation were to be imposed as a requirement of the possible trait plasticity space, the control (CC), $=N_{area}$, and $+N_{area}$ plant types (central diagonal line and upper-left triangle in Figure 3.3) would be excluded. This may partially explain why the control case is not observed in the real world [Lovelock et al., 1998]. Although phosphorus limitation is thought to be the primary nutrient constraint on plant growth in the tropics, evidence from empirical studies and manipulation experiments suggests that tree growth is also limited by nitrogen in the tropics [e.g., Winter et al., 2001, Cernusak et al., 2013]. Most of the changes observed by

Lovelock et al. [1998] show reduced N_{area}, which given our simulations suggests that total canopy nitrogen also decreased. This could be due to a change in nitrogen allocation. For example, nitrogen allocation to roots could increase or woody biomass gains could require greater total amounts of nitrogen (see discussion below).

3.5.3 Why do leaf changes occur?

Our model results suggest that observed increases in $C:N_{leaf}$ in response to elevated CO_2 do not confer a competitive advantage. We find that plant types in which $C:N_{leaf}$ increases in response to elevated CO_2 suffer in several metrics of plant fitness, including biomass, leaf area index, net primary productivity, and competitive ability. Thus our results suggest that changes in $C:N_{leaf}$ are likely forced upon plants by changes in elevated CO_2, rather than as a beneficial acclimation. This is consistent with the leading hypothesis for the mechanism underlying $C:N_{leaf}$ increases with elevated CO_2. Nitrogen limitation has been proposed as a cause for lower mass-based nitrogen concentrations in leaves [e.g., Poorter et al., 1997, Winter et al., 2001, Fyllas et al., 2009, Cusack et al., 2016]. As carbon dioxide fertilizes plant growth the demand for nutrients is likely to increase and eventually result in the depletion of nitrogen available for growth [Luo et al., 2004, Hungate et al., 2003]. The limited availability of nitrogen, as well as accumulation of nonstructural carbohydrates due to sink limitation of growth, could lower mass-based leaf nitrogen concentrations and result in higher $C:N_{leaf}$ [e.g., Poorter et al., 1997, Winter et al., 2001]. Manipulation experiments in which tropical tree seedlings are treated with elevated CO_2 provide evidence that CO_2 stimulation of growth is enhanced by the addition of soil nutrients, suggesting that nutrient limitation does indeed impact leaf trait responses [Winter et al., 2001]. Plants in which $C:N_{leaf}$ increases more in response to elevated CO_2 may be those that are unable to adjust to lower nitrogen availability or higher competition for nitrogen. Tropical trees with traits that allow them to better acquire nitrogen, for example associations with nitrogen fixing bacteria or fungi, may be better able to maintain $C:N_{leaf}$ levels under elevated CO_2 with advantages for growth and competitive success [Lovelock et al., 1998, Cusack et al., 2016,

Cernusak et al., 2013].

Further, it has been suggested that the increase in LMA with elevated CO_2 is mediated by nitrogen (or other resource limitation of plant growth) causing nonstructural carbohydrate accumulation in leaves [Poorter et al., 2009, 1997, Pritchard et al., 1999, Roumet et al., 1999]. Our results suggest a possible alternative: plants that are able to increase LMA most for a given level of C:N_{leaf} change are those that are best able to maintain high levels of functioning (including biomass, leaf area index, productivity, and competitive ability). Concurrently increasing LMA along with C:N_{leaf} leads to maintenance of equal N_{area} by counteracting decreases in mass-based nitrogen concentration [Luo et al., 1994, Ishizaki et al., 2003]. Indeed, we find that even when limited to control levels of total canopy nitrogen, plants could maintain close to equal amounts of N_{area}. As nitrogen is an essential component of photosynthetic enzymes, maintaining N_{area} can maintain area-based maximum photosynthetic rates [Kattge et al., 2009, 2011, Walker et al., 2014, Norby et al., 2017]. Lovelock et al. [1998]'s observations of tropical tree leaf trait responses to a doubling of CO_2 (Figure 3.1) suggest that increases in LMA are generally higher for larger increases in C:N_{leaf}, helping to maintain N_{area} — and thus functioning — closer to control levels (Figure 3.4).

3.5.4 Other potential leaf trait plasticity trade-offs

Other coordinated plant responses to elevated CO_2 and nutrient limitation could further influence the impacts of leaf trait plasticity on competitive ability and tropical forest functioning. Observations show that many trees, including tropical trees, enhance carbon and nitrogen allocation to root growth at the expense of leaf growth in response to elevated CO_2 [e.g., Luo et al., 2006, Körner and Arnone, 1992, Cusack et al., 2016, Cernusak et al., 2013, and references therein]. Such partitioning of nitrogen away from leaves could increase C:N_{leaf} but benefit plants if they use the nitrogen to build other structures that help alleviate resource limitation, such as roots that can access further nutrients [reviewed in Cusack et al., 2016, Cernusak et al., 2013]. However, in some cases this growth strategy has been found to be ineffective [Norby et al., 2010]. Our primary results isolate the influence of leaf trait

plasticity changes and do not include changes in the target ratio of root mass to leaf area. However, we test the sensitivity of our results to increasing target root mass in coordination with leaf trait plasticity using additional simulations (Supporting Information Text B.1.3 and B.2.1). In these additional experiments, trees increase target root mass in proportion with increases in LMA. This accounts for the additional carbon cost of growing more roots to support the additional nutrient requirements for greater leaf mass. This makes it even more costly to increase LMA, which we expect should reduce the competitive advantage of doing so. In this case, we find that the control plant type is always at a competitive advantage, and the benefit of increasing LMA that we saw in our primary results no longer consistently occurs (Figure B.3).

Other potential trade-offs for leaf trait plasticity responses could be thought to alter their influence on tropical forest ecosystem dynamics and functioning. For example, enhanced leaf lifespan is associated with greater LMA across species [Wright et al., 2004] and could be expected to further enhance productivity and competitive outcomes. However, this relationship across species does not necessarily hold for within species changes [Anderegg et al., 2018, Fisher et al., 2015, Lusk et al., 2008] and varies in response to elevated CO_2 [Norby et al., 2003, 2010, Taylor et al., 2008, Lovelock et al., 1998]. We therefore choose not to couple increases in leaf lifespan with increases in LMA in our experiments. Higher carbon to nitrogen ratios are also associated with defense against herbivory [reviewed in Cusack et al., 2016], which could increase with climate change [e.g., Deutsch et al., 2018] but are not considered in our simulations.

3.5.5 Indirect effects of plant type abundance

With limited changes in the spatial distributions of plant types, the observed plastic response of plants under high CO_2 is likely to lead to decreases in N_{area} and thus to overall decreases in carbon uptake and evapotranspirative cooling. On the other hand, if the distribution of plants in an ecosystem changes due to differences in competitive ability, plant types that can maintain higher N_{area} and have a greater competitive advantage could, in the longer

term, increase in abundance and bring carbon uptake and evapotranspirative cooling more in line with projections that assume leaf traits remain as in the control. Presumably this community-scale re-assembly would play out over longer timescales than leaf trait plasticity responses. However, leaf characteristics that maximize competitive ability, carbon uptake, and evapotranspirative cooling — namely high N_{area} achieved through higher LMA — lie outside the observed range of leaf trait plasticity in response to a doubling of CO_2 from Lovelock et al. [1998]. If some tropical tree types achieve levels of leaf trait plasticity that increase N_{area}, we find that these tree types would be more competitively advantageous and enhance both carbon uptake and evapotranspiration compared to current projections. Plant types with the ability to increase N_{area} may currently exist but remain unsampled due to high diversity and small number of samples, or could potentially occur through evolution.

3.5.6 Potential role of rising temperatures

Warming temperatures could be expected to alter the response of leaf traits to CO_2, with implications for the influence of leaf trait plasticity on ecosystem functioning and composition. For example, warmer temperatures have been found to be associated with lower leaf nitrogen content across a spatial gradient in present-day tropical forests [Cusack et al., 2016, Fyllas et al., 2009, Tully and Lawrence, 2010], plausibly via the negative impacts of plant respiration with high nitrogen content [Cernusak et al., 2013]. Such decreases in leaf nutrient concentration could amplify the leaf responses to elevated CO_2 we test here. Higher temperatures have also been associated with lower LMA in manipulation experiments [Poorter et al., 2009], as well as across an elevational gradient in present-day tropical forests [Doughty et al., 2018]. This influence could be expected to offset the LMA increase in response to CO_2 we implement herein. However, warming and CO_2 are hypothesized to influence LMA through different mechanisms (leaf expansion vs. accumulation of carbohydrates, respectively), making it difficult to predict the combined influence of these two environmental factors on LMA. The combined influence of elevated CO_2 and temperature on tropical tree traits remains poorly constrained [Cusack et al., 2016, Cernusak et al., 2013].

3.5.7 Recommendations for including leaf trait plasticity in projections of future climate

We illustrate here that a better understanding of tropical tree responses to environmental change, as well as the use of plant competition models, will be required to accurately include the effects of leaf trait plasticity in projections of future climate.

First, more observations are required to constrain tropical tree leaf responses to multiple environmental factors — including CO_2, nutrient availability, and temperature — and how these responses differ by tree type (e.g., successional class or species) and developmental stage [e.g., Cusack et al., 2016]. Our ability to characterize leaf trait plasticity in response to environmental change may ultimately require a better understanding of whole plant carbon and nutrient dynamics, as leaf carbon and nitrogen can depend on supply and demand from other plant organs [e.g., Luo et al., 1994, Pritchard et al., 1999, Norby et al., 2010, Xu et al., 2012].

Second, numerous models of the terrestrial biosphere represent the cycling of nutrients, and a subset of these represent flexibility in tissue carbon to nitrogen ratios in response to nitrogen availability [Zaehle and Friend, 2010, Zaehle et al., 2014]. Here we show that simulation of changes in $C:N_{leaf}$ in isolation of apparently coordinated changes in LMA may overestimate the impact of changing stoichiometry on future gas exchange. Complex as it is, models should thus strive to represent the temporal dynamics of important plant traits themselves under changing environmental conditions, either empirically (as here), or using predictions from optimality theory [Prentice et al., 2014, Dewar et al., 2012].

Finally, we show here that models of plant competition are necessary to include the full influence of leaf trait plasticity on climate, as changes in leaf traits can alter plant competitive dynamics and the abundance of different plant types with implications for ecosystem functioning. Biosphere models that include competition between plants for resources are included in some Earth system models used to predict future climate but remain an area of active research [e.g., Fisher et al., 2018].

3.5.8 Implications

Here we show that leaf trait plasticity in response to elevated CO_2 could alter tropical forest influences on climate directly, by altering the functioning of tropical trees, and indirectly, by modifying plant competitive dynamics and the abundance of different plant types. As such, including the effects of leaf trait plasticity could have a significant influence on projections of future climate. These results further support the need for more observations of tropical tree responses to environmental change and the use of plant competition models within Earth system models used to predict future climate change.

3.6 Acknowledgements

We thank Janneke Hille Ris Lambers and Elizabeth Van Volkenburgh for their comments on an earlier version of this manuscript. We acknowledge support from the National Science Foundation AGS-1553715 to the University of Washington. High-performance computing support from Cheyenne (doi:10.5065/D6RX99HX) was provided by NCAR's Computational and Information Systems Laboratory, sponsored by the National Science Foundation.

3.7 Figures and Tables

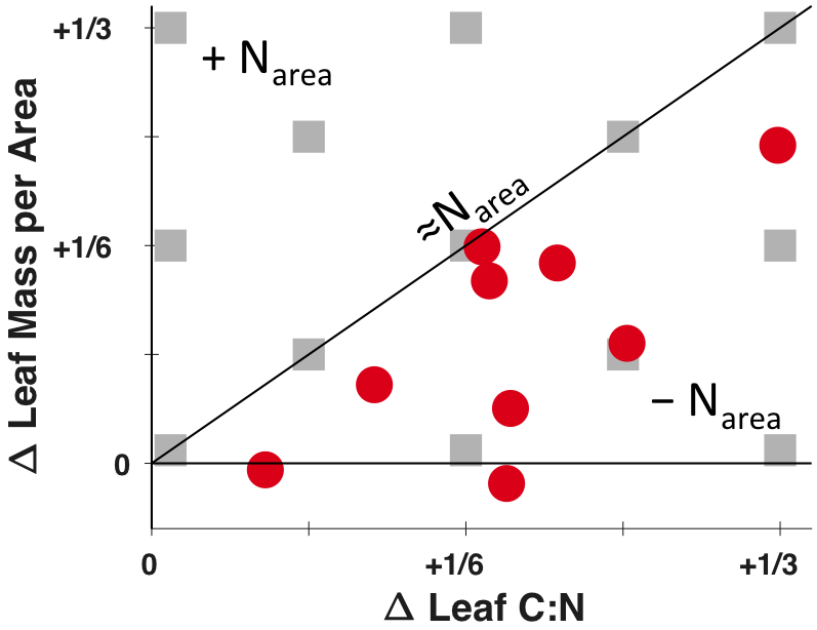

Figure 3.1: Leaf trait plasticity in response to a doubling of CO_2 in tropical trees for leaf C:N (leaf g C g^{-1} N) and leaf mass per area (g C m^{-2} leaf area). Observed changes across nine tropical tree species (red circles) from Lovelock et al. [1998]. Leaf trait plasticity levels sampled for our experiments (gray squares). Diagonal black line indicates where nitrogen per area (N_{area}, g N m^{-2} leaf area) remains at control levels. Above the diagonal line leaf nitrogen per area increases ($+N_{area}$) compared to the control; below the diagonal line it decreases ($-N_{area}$).

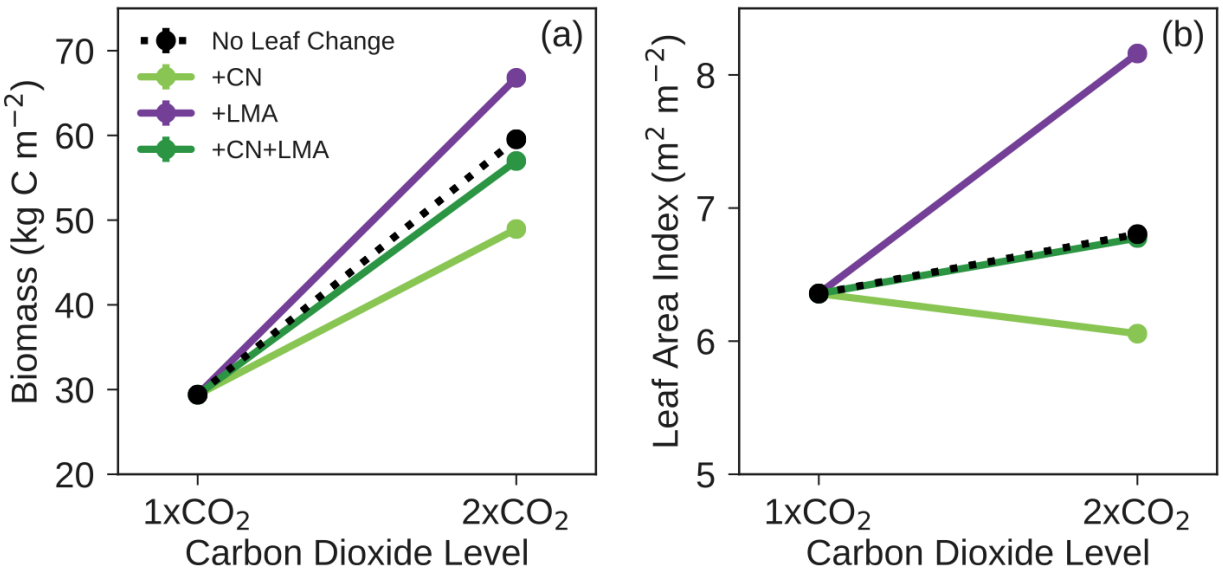

Figure 3.2: Annual mean (a) biomass (kg C m^{-2}) and (b) leaf area index (m^2 m^{-2}) for the 1xCO_2 control, 2xCO_2 control (black), and the following leaf trait plasticity levels in the absence of competition: a one-third increase in leaf C:N alone (+CN, light green), a one-third increase in leaf mass per area alone (+LMA, purple), and a one-third increase in both leaf C:N and leaf mass per area (+CN+LMA, dark green). Error bars show bootstrap 95% confidence intervals for the mean value.

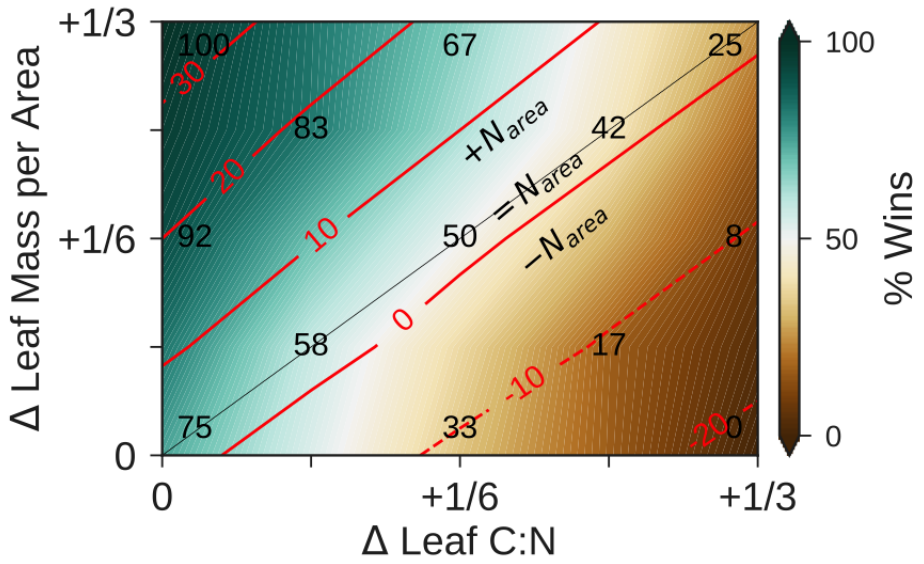

Figure 3.3: The percent of pairwise competitions won (% Wins, color shading and black numbers) and percent change in total canopy nitrogen compared to the 1xCO_2 control (red contours) for each leaf trait plasticity level of leaf C:N and leaf mass per area. Percent wins for sampled trait changes (black numbers). Diagonal line (dashed black) indicates where nitrogen per area (N_{area}, g N m^{-2} leaf area) remains at control levels (=N_{area}). Leaf trait plasticity levels below the diagonal line reduce N_{area} (-N_{area}) compared to the control plant type. Leaf trait plasticity levels above the diagonal line enhance N_{area} (+N_{area}) compared to the control plant type. Linear interpolation used to estimate percent wins and change in total canopy nitrogen between sampled trait changes.

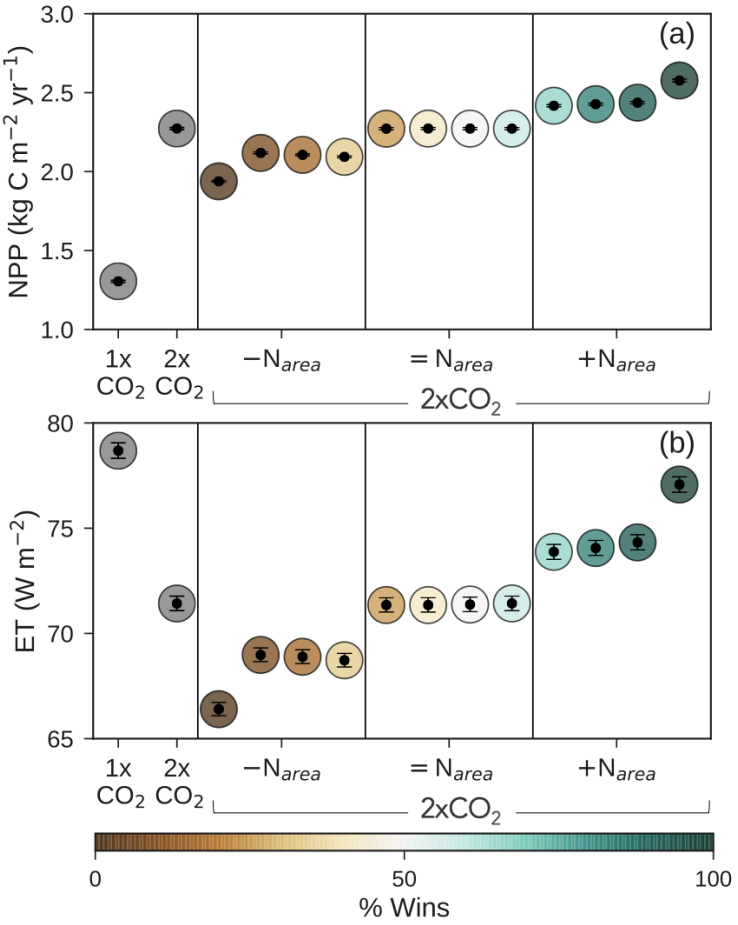

Figure 3.4: Annual mean (a) net primary productivity (NPP, kg C m^{-2} yr^{-1}) and (b) evapotranspiration (ET, W m^{-2}) for the 1xCO_2 control, 2xCO_2 control (no leaf trait plasticity), and 12 ecosystems each consisting entirely of one plant type with a different level of leaf trait plasticity sampled from the -N_{area}, =N_{area}, and +N_{area} plasticity spaces. Color indicates the percentage of all pairwise competitions won by each level of leaf trait plasticity (% Wins). Error bars show bootstrap 95% confidence intervals for the mean value.

Table 3.1: Change in tropical ecosystem properties due to a doubling of CO_2 in the control simulation (no leaf trait plasticity, CC - CTRL)

	Mean	($CI_{95\%}$)	%	($CI_{95\%}$)
Biomass (kg C m^{-2})	+30.1	(30.0, 30.2)	+102.6%	(102.1, 103.0)
LAI (m^2 m^{-2})	+0.4	(0.4, 0.5)	+7.0%	(6.8, 7.2)
NPP (kg C m^{-2} yr^{-1})	+1.0	(1.0, 1.0)	+74.2%	(73.2, 75.1)
ET (W m^{-2})	-7.3	(-6.8, -7.8)	-9.2%	(-8.6, -9.8)

Note. Leaf area index (LAI), net primary productivity (NPP), evapotranspiration (ET). Bootstrap 95% confidence intervals ($CI_{95\%}$) in parentheses. Mean and percent (%) changes calculated as (CC - CTRL) and (CC - CTRL)/CTRL, respectively, where CTRL and CC are the control simulations at 400 ppm and 800 ppm CO_2, respectively.

Table 3.2: Annual mean changes in tropical ecosystem functioning due to leaf trait plasticity under a doubling of CO_2 (Leaf Trait Plasticity Experiment - CC)

	Net primary productivity (g C m^{-2} yr^{-1})				**Evapotranspiration (W m^{-2})**			
	Mean	($CI_{95\%}$)	%	($CI_{95\%}$)	Mean	($CI_{95\%}$)	%	($CI_{95\%}$)
-N_{area}	-209	(-202, -216)	-9.2	(-8.9, -9.5)	-3.2	(-2.8, -3.6)	-4.4	(-3.9, -5.0)
= N_{area}	0	(-8, 7)	0.0	(-0.3, 0.3)	0.0	(-0.4, 0.3)	-0.1	(-0.6, 0.5)
+ N_{area}	192	(184, 200)	8.4	(8.1, 8.8)	3.4	(3.0, 3.8)	4.8	(4.2, 5.3)
CN	-334	(-326, -342)	-14.7	(-14.4, -15.0)	-5.0	(-4.6, -5.5)	-7.0	(-6.4, -7.7)
LMA	305	(294, 315)	13.4	(12.9, 13.9)	5.7	(5.1, 6.2)	7.9	(7.2, 8.6)
CNLMA	-1	(-10, 8)	0.0	(-0.4, 0.4)	-0.1	(-0.6, 0.4)	-0.1	(-0.8, 0.6)

Note. Mean and percent (%) changes calculated as (Experiment - CC) and (Experiment - CC)/CC, respectively, where CC is the control simulation under a doubling of CO_2. Bootstrap 95% confidence intervals ($CI_{95\%}$) in parentheses. -N_{area}, = N_{area}, and +N_{area} average across experiments with leaf trait plasticity levels that decrease, maintain, and enhance leaf nitrogen per area, respectively. CN experiment increases C:N_{leaf} by one third; LMA increases LMA by one third; and CNLMA, simultaneously increases C:N_{leaf} and LMA by one third.

Chapter 4

WITHIN-CANOPY GRADIENT OF SPECIFIC LEAF AREA IMPROVES SIMULATION OF TROPICAL FOREST STRUCTURE AND FUNCTIONING IN A DEMOGRAPHIC VEGETATION MODEL

Marlies Kovenock[1], Charles D. Koven[2], Ryan G. Knox[2], Rosie A. Fisher[3], and Abigail L.S. Swann[4,1]

[1]Department of Biology, University of Washington, Seattle, WA; [2]Lawrence Berkeley National Laboratory, Berkeley, CA; [3]National Center for Atmospheric Research, Boulder, CO; [4]Department of Atmospheric Sciences, University of Washington, Seattle, WA.

Supporting Information referenced in this chapter can be found in Appendix C.

4.1 Abstract

Tropical forests exert extensive control over global carbon, water, and energy fluxes and thus they play a critical role in determining future climate. Yet, their responses to climate change and the resulting vegetation feedbacks on climate remain uncertain. Explicit representation of vegetation dynamics in Earth system models has been proposed as a way to improve predictions of vegetation feedbacks on future climate, particularly in tropical ecosystems. The Functionally Assembled Terrestrial Ecosystem Simulator (FATES) model improves process-based representation of ecosystem dynamics and demography, and can be embedded within Earth system models. However, the model simulates leaf area index that is well below observations at tropical forest sites, which could have significant implications for predictions of ecosystem dynamics, structure, and functioning. Here we implement a canopy profile of specific leaf area in the FATES model, following observations, and benchmark the modified model's performance against observations at a tropical forest site, Barro Colorado Island, Panama, across 287 plausible plant trait parameterizations. We find that our more realistic representation of within-canopy leaf trait dynamics improves the simulation of leaf area index and several other measures of ecosystem structure and functioning — gross primary productivity, latent heat, and sensible heat fluxes; above-ground biomass; and basal area. We also identify three high-performing parameter sets for use in future experiments and suggest constrained parameter ranges for a selection of individual plant trait parameters that strongly influence performance in our benchmarking analysis. In sum, this work improves the simulation of tropical forest structure and functioning in the FATES vegetation demography model through a more realistic representation of within-canopy leaf dynamics, and suggests high-performing parameter sets and constrained parameter ranges for use in future experiments.

4.2 Introduction

Tropical forests exert strong control over Earth's carbon, energy, and water fluxes [Bonan, 2008]. The responses of tropical forests to climate change and the resulting feedbacks on climate and carbon cycling remain critical uncertainties in projections of future climate [e.g., Ciais et al., 2013, Zhang et al., 2015, Lloyd and Farquhar, 2008, Schimel et al., 2015, Brienen et al., 2015, Hickler et al., 2008, Fisher et al., 2010, Cernusak et al., 2013, Leakey et al., 2012a, van der Sleen et al., 2015, Cusack et al., 2016]. Better representation of terrestrial ecological dynamics in Earth system models has been proposed as a way to improve the simulation of vegetation responses and feedbacks on climate and carbon cycling [e.g., Evans, 2012, Fisher et al., 2018, Moorcroft, 2006, Purves and Pacala, 2008]. Consideration of ecological and demographic processes could be particularly important in tropical forests, as these dynamics play a dominant role in shaping tropical ecosystem structure and functioning [e.g., Fisher et al., 2010, Levine et al., 2016, Moorcroft et al., 2001]. Demographic vegetation models that include mechanistic representations of ecological and demographic processes and can be embedded within Earth system models offer a promising avenue forward. However, with additional ecological complexity comes the necessity to validate these models and their processes by benchmarking their performance against observations [e.g., Fisher et al., 2018, Moorcroft, 2006, Purves and Pacala, 2008]. A key test prior to simulating future biosphere changes is the ability to simulate the current biosphere as benchmarked against observations.

FATES is a vegetation demography model [Fisher et al., 2015, 2018] that can be embedded within Earth system models and adds more realistic representation of the biosphere by mechanistically simulating plant ecological dynamics and ecosystem assembly via processes including plant growth, competition for light and water, recovery from disturbance, reproduction, mortality, and recruitment. In present day simulations of tropical forests, FATES simulates many aspects of ecosystem structure and functioning well [Koven et al., unpublished]. However, it severely underestimates a critical ecosystem property – leaf area index. Insufficient leaf area index compared to observations could have significant implications for

simulated ecosystem functioning, as leaf area provides the surface area over which the vegetation fluxes of carbon, water, and energy are summed. Additionally, low leaf area could alter ecosystem assembly and demographic processes by altering the light environment and competition between plants for this limiting resource. At the same time, the FATES model matches observations of tropical forest productivity well, suggesting the issue lies in the conversion of carbon available for leaf growth to leaf area.

One reason for the underestimation of leaf area index could be that FATES does not include a vertical gradient in the area to mass ratio of leaves with depth in the canopy (Figure 4.1a). This quantity can be referred to as specific leaf area (m^2 leaf area/gC), or, inversely as leaf mass per area (gC/m^2 leaf area). Here we will use specific leaf area. Observations show that specific leaf area increases with overlying leaf area index in tropical forests [Lloyd et al., 2010, Poorter et al., 1995, Ishida and Toma, 1999, Carswell et al., 2000, Souza and Válio, 2003], as well as in many other plant types and ecosystems across continents [reviewed in Thornton and Zimmermann, 2007, Niinemets et al., 2015]. This increase in specific leaf area with depth in the canopy, makes leaf area at the bottom of the canopy cheaper in terms of carbon to build than leaf area at the top of the canopy. Thus, the observed specific leaf area profile decreases the average carbon cost of building leaf area and therefore increases leaf area index for a give carbon investment in leaves (Figure 4.1b). Models that do not represent this profile, including FATES, could therefore incorrectly simulate the trade-off between productivity and leaf area, with consequences for simulated leaf area; carbon, water, and energy fluxes; and ecological dynamics.

The specific leaf area profile is related to the widely observed within-canopy gradients of leaf nitrogen per area and maximum photosynthetic rates, which are often represented in models of the terrestrial biosphere. In fact, the specific leaf area profile is thought to cause the vertical gradients in leaf nitrogen per area and maximum photosynthetic rates. As mass-based leaf nitrogen concentrations remain constant through the canopy, increasing specific leaf area with canopy depth drives declines in nitrogen per area (N per area = N per mass / specific leaf area) and per-area photosynthetic enzyme concentrations [e.g.,

Lloyd et al., 2010, Reich et al., 1998, Ellsworth and Reich, 1993, Evans and Poorter, 2001]. The gradients in these leaf traits are thought to maximize photosynthetic carbon gain given the gradient of light within canopies [Lloyd et al., 2010, Bonan et al., 2011, and references therein]. The profiles of nitrogen per area and photosynthetic rates through the canopy have been found to significantly influence simulations of the terrestrial biosphere and have therefore been included in a wide range of canopy, demographic vegetation, and land surface models [reviewed in Thornton and Zimmermann, 2007, Bonan et al., 2012], including FATES [Fisher et al., 2015].

Yet few biosphere models represent the corresponding profile of specific leaf area, despite its influence on the relationship between productivity and leaf area and potential to alter competition for light. In their analysis of 11 ecosystem models, De Kauwe et al. [2014] found that only one model includes the specific leaf area profile, the Community Land Model [for implementation see Thornton and Zimmermann, 2007, Bonan et al., 2011]. Sensitivity tests with this land surface model show that the specific leaf area profile can significantly influence the simulation of leaf area index and productivity [Thornton and Zimmermann, 2007]. Models missing this profile could be misrepresenting the relationship between carbon available for growth and leaf area, with significant implications for ecosystem dynamics, structure, and functioning.

Here we implement a specific leaf area profile in the FATES model; benchmark the modified model's performance against observations at a tropical forest test site; and select high-performing parameter sets that can be used as a baseline for future FATES experiments. We modify the FATES model structure to include the specific leaf area profile, following observations from Lloyd et al. [2010]. We then test the influence of the specific leaf area profile on ecosystem structure and functioning at a tropical forest site, Barro Colorado Island, Panama. To test the influence of the specific leaf area profile across plausible model parameterizations and identify parameters that strongly influence model performance, we repeat the control and specific leaf area simulations for 287 model parameter sets. Each parameter set samples the observed trait space for six plant trait values (maximum carboxylation rate,

specific leaf area, wood density, leaf carbon to nitrogen ratio, leaf longevity, and background mortality rate) and plausible trait space for an additional six plant trait values for which observational constraints are lacking (slope of stomatal conductance equation and parameters used in allometric equations). We benchmark the performance of each ensemble member against six observed variables at our test site: leaf area index, above-ground biomass, basal area, gross primary productivity, latent heat fluxes, and sensible heat fluxes. Lastly, we use our benchmarking analysis to identify individual parameters that strongly influence model performance and suggest constraints on their plausible ranges.

4.3 Materials and Methods

4.3.1 FATES Model Description

We test the influence of varying specific leaf area with depth in the canopy on ecosystem composition and functioning using the Functionally Assembled Terrestrial Ecosystem Simulator [FATES; Fisher et al., 2015, 2018]. FATES is a demographic vegetation model which can be embedded within the Community Land Model [CLM; Lawrence et al., 2018] of the Community Earth System Model. The CLM(FATES) model mechanistically simulates plant ecological dynamics and ecosystem assembly via processes including plant growth, competition for light and water, recovery from disturbance, reproduction, mortality, and recruitment. Plants are represented by a user-defined number of plant functional types, which can differ in numerous traits including but not limited to maximum photosynthetic rates, wood density, and mortality rates. FATES tracks carbon cycling through several plant biomass and litter pools. It also accounts for hydrology, surface energy fluxes, and soil carbon in coordination with its host land model.

A key feature of FATES is that the model tracks vegetation type, height, and time since disturbance. Disturbance periodically and mechanistically befalls some patches of the simulated ecosystem. Plants within these "patches" are considered to share an age class, which represents their age since last disturbance. Within a patch, individual plants are

grouped into "cohorts", which can differ in height. Cohorts represent individual plants of the same plant type and height as a representative average individual. The height structure of cohorts within a patch determines the light profile experienced by each cohort. The leaf area of taller cohorts in the canopy can shade cohorts deeper in the canopy. Photosynthesis, respiration, turnover, and mortality, as well as the interaction of these processes with the abiotic environment, control the amount of carbon each cohort can use for growth. Growth and size-dependent allometric equations then determine the height and leaf area of each cohort. Radiation streams for direct and diffuse light are calculated at the leaf layer level for each plant type. This incoming energy is required for photosynthesis and influences the leaf energy budget. In addition to competition for light, FATES represents competition for water by allowing differences in rooting depth profile between plant functional types to influence access to a shared soil moisture profile.

4.3.2 Specific Leaf Area Profile Implementation

Here we implement a specific leaf area profile in FATES that increases specific leaf area exponentially with depth in the canopy (Figure 4.1a). Previously FATES represented specific leaf area as a constant value for each plant functional type that did not change with depth in the canopy (Figure 4.1a, static SLA). Observations in tropical forests [Lloyd et al., 2010, Poorter et al., 1995, Ishida and Toma, 1999, Carswell et al., 2000, Souza and Válio, 2003], as well as in many other plant types and ecosystems across continents [reviewed in Thornton and Zimmermann, 2007, Niinemets et al., 2015], show that specific leaf area varies with depth in the canopy. We implement a new specific leaf area profile which causes the carbon cost of building leaf area — represented by the inverse of specific leaf area — to follow the same profile through the canopy as that of nitrogen per leaf area and maximum photosynthetic rates (i.e., V_{cmax25}, J_{max25}, T_{pu25}) and respiration rates, as supported by observations [e.g., Lloyd et al., 2010, Thornton and Zimmermann, 2007]. Canopy depth-varying profiles of nitrogen per area, photosynthetic rates, and respiration rates were already included in the baseline FATES model. The scaling factor for these profiles is calculated as follows:

$$nscaler(x) = exp(-kn \cdot x) \tag{4.1}$$

where x is the canopy depth in terms of overlying leaf area index (m^2 leaf area/m^2 ground) and kn is the coefficient that describes nitrogen per area decay with depth in the canopy. The exponential rate of change through the canopy of these leaf traits (specific leaf area, nitrogen per area, and maximum photosynthetic rates), often referred to as kn, differs by plant type and has been empirically related to the magnitude of maximum photosynthetic rates at the top of the canopy [Lloyd et al., 2010]. Plant types with low maximum photosynthetic rates at the top of the canopy have shallower gradients in these leaf traits, including specific leaf area; whereas, plant types with high maximum photosynthetic rates have steeper gradients. The model relates the nitrogen decay coefficient (kn) to the maximum rate of carboxylation at top of the canopy ($V_{cmax25top}$) following the empirical relationship from Lloyd et al. [2010]:

$$kn = exp(0.00963 \cdot V_{cmax25top} - 2.43) \tag{4.2}$$

Here we additionally vary the value of specific leaf area with depth in the canopy as follows:

$$SLA(x) = \frac{SLA_{top}}{nscaler(x)} \tag{4.3}$$

where SLA(x) is the specific leaf area (m^2 leaf area/gC) when overlying leaf area index equals x and SLA_{top} is the specific leaf area at the top of the canopy (m^2 leaf area/gC). Specific leaf area is allowed to increase with canopy depth until it reaches an observationally constrained maximum value [the upper 95% confidence interval for all observations in the TRY database; Kattge et al., 2011], at which point it remains at the maximum value even if overlying leaf area continues to increase. That is, leaves are allowed to become thinner relative to their mass

at lower depths in the canopy where there is less light, and this relationship is exponential to depth up to the observed maximum of specific leaf area.

FATES uses specific leaf area to calculate the carbon cost of building leaf area. The specific leaf area profile implemented herein changes the relationship between carbon allocated to leaves and leaf area from a linear to an exponential relationship (Figure 4.1b). Previously, the static specific leaf area value caused leaf area index of a tree to increase linearly with carbon allocated to leaves (Figure 4.1b) as follows:

$$LAI_{tree} = C_{leaf} \cdot SLA \tag{4.4}$$

where LAI_{tree} is leaf area index (m^2 leaf area/m^2 ground) for a representative average individual tree of a cohort (group of plants of the same plant type and height); C_{leaf} is the amount of carbon available within this tree to build leaves per area ground (gC/m^2 ground); and SLA is a constant value of specific leaf area (m^2 leaf area/gC).

With the specific leaf area profile, leaf area index increases exponentially with leaf carbon (Figure 4.1b). This occurs because specific leaf area, which represents the amount of leaf area built per unit of carbon, increases exponentially with increasing overlying leaf area index. When using the specific leaf area profile, we calculate leaf area index as a function of a dynamic specific leaf area value that increases with overlying leaf area index. We derive the relationship between leaf area index and leaf carbon in two steps. First, we set the total amount of carbon available for building leaves equal to the integrated value of one over specific leaf area, which represents the carbon cost of building one unit of leaf area, at each canopy depth x expressed in overly lying leaf area index:

$$C_{leaf} = \int_0^{LAI_{tree}} \frac{nscaler(x + LAI_{above})}{SLA_{top}}\, dx \tag{4.5}$$

where C_{leaf} is the total amount of carbon available for building leaves in this tree; LAI_{tree} is

the leaf area index of an individual tree, which we wish to calculate; SLA_{top} is the specific leaf area at the top of the canopy; nscaler is the scaling factor for the decay of nitrogen with canopy depth (as defined in equation 4.1); and LAI_{above} is the cumulative overlying leaf area index above this tree. Equation 4.5 can then be rearranged to solve for the leaf area index of a tree given the amount of carbon allocated to leaves as follows:

$$LAI_{tree} = \frac{\ln\left(e^{(-kn \cdot LAI_{above})} - kn \cdot SLA_{top} \cdot C_{leaf}\right) + kn \cdot LAI_{above}}{-kn} \tag{4.6}$$

This exponential growth equation is used to calculate leaf area index until specific leaf area reaches the observational constraint we set for maximum specific leaf area. If specific leaf area reaches this maximum value, leaf area index beyond this point increases linearly with additional leaf carbon (Figure 4.1a), as in Equation 4.4.

FATES also uses specific leaf area to determine whether a leaf layer is in positive carbon balance. If a leaf layer costs more to build in terms of carbon than it brings in through net primary productivity, the model reduces the amount of carbon allocated to leaf growth until all leaf layers are in positive annual carbon balance. Previously, FATES calculated the carbon cost of a leaf layer using a static value for specific leaf area as follows:

$$Cost_{leaf} = \frac{1 + GR_{perc}}{SLA \cdot LL} \tag{4.7}$$

where Cost_{leaf} ($\mathrm{gC/m^2}$ leaf area/yr) is the carbon mass required to build a leaf layer; SLA is the specific leaf area ($\mathrm{gC/m^2}$ leaf area); LL is the leaf longevity (years); and GR_{perc} is a fraction that accounts for the growth respiration cost. The specific leaf area profile we implement herein uses the same equation to calculate leaf cost, except that the specific leaf area value is calculated for each leaf layer following Equation 4.3. This modification reduces the cost of leaves with depth in the canopy as specific leaf area increases with overlying leaf area.

Appendix C contains the FATES code changes associated with the specific leaf area profile implemented herein.

4.3.3 Testing the Influences on Ecosystem Structure and Functioning

We tested the influence of the specific leaf area profile on tropical forest structure and functioning through an ensemble of FATES simulations at Barro Colorado Island, Panama. We compare simulations run with two model structures – a control and a specific leaf area profile structure. Simulations run with the control model structure (CTRL) represent specific leaf area as a constant value regardless of depth in the canopy. Experiment simulations (SLA) are set up identically to the control simulations except that specific leaf area varies with depth in the canopy.

To account for model parameter uncertainty, we run both the control and specific leaf area profile simulations under 287 different plant trait parameterizations. These parameterizations are drawn from samples of the tropical tree trait space for 12 parameters, following [Koven et al., unpublished]. In the sampling process, values for six of these parameters — specific leaf area at the top of the canopy, maximum rate of carboxylation at the top of the canopy ($V_{cmax25top}$), wood density, leaf carbon to nitrogen ratio, leaf longevity, and background mortality rate — were sampled from the observed trait space for tropical trees at our study location and two nearby sites, Parque Natural Metropolitano and Bosque Protector San Lorenzo, Panama. Values for the remaining six parameters were sampled from plausible distributions as observational constraints are lacking. These parameters include the slope parameter in the Ball-Berry stomatal conductance model and several allometric parameters: parameters that control the intercepts in the relationships between diameter at breast height and plant crown area, as well as diameter at breast height and target allometric leaf biomass; a parameter that controls the exponential in the relationships between diameter at breast height and both plant crown area and target allometric leaf biomass; the ratio of target leaf biomass to target fine root biomass; and the intercept of the relationship between sapwood area to leaf area. The parameter sampling maintained observed covariance between traits.

CTRL and SLA simulations used the same 287 parameter combinations.

All simulations were forced with observed meteorological data for years 2003-2016 from Barro Colorado Island [Faybishenko et al., 2018]. All vegetation patches experienced the same meteorological forcing within a single grid cell. Plants in all simulations are represented by a single plant functional type that is characteristic of this site, the broadleaf evergreen tropical tree. Simulations started from near-bare ground and ran for 300 years, the time required to grow a mature forest in the model with our setup. We tested all control and experiment simulations at two, time-invariant atmospheric carbon dioxide concentrations, 367ppm and 400ppm. These carbon dioxide concentrations bookend the change in carbon dioxide concentration between 2000-2015 [NOAA Earth System Research Laboratory, 2018], the approximate time period over which the observations to which we benchmark model performance (see Section 4.3.4) were made. All variables used in analysis came to equilibrium before 250 years. We used the last 50 years of each simulation in our analysis.

4.3.4 Evaluation of Simulations Against Observations

We benchmark each SLA simulation against observations from the Barro Colorado Island site and use this evaluation to select model parameterizations that result in the highest model skill. Barro Colorado Island is home to a 50-hectare long-term tropical forest monitoring plot with observations dating back to 1980, and is one of the best sampled sites in a tropical forest. It is a Smithsonian Tropical Research Institute site and ForestGEO site. We compare model annual mean output to reported observations of annual mean leaf area index and gross primary productivity, latent heat, and sensible heat fluxes; and annual values of above-ground biomass and basal area. Leaf area index observations come from Detto et al. [2018] and were made using hemispherical photographs approximately monthly from January 2015 to August 2017 at 188 locations at Barro Colorado Island. We use basal area observations that were collected during census surveys of a 50-hectare plot on Barro Colorado Island in 1992, 1996, 2001, 2006, and 2011 [Condit et al., 2017, 2012, Condit, 1998, Hubbell et al., 1999]. Above-ground carbon biomass estimates for Barro Colorado Island were calculated from the

1995 census survey data by Meakem et al. [2018]. They estimated above-ground biomass from two different allometric formulations, which we use to represent uncertainty in this measure. We also tested the sensitivity of our results to representing the uncertainty in above-ground biomass estimates across time, using estimates by Feeley et al. [2007] and Baraloto et al. [2013] derived from 5 year census data at Barro Colorado Island between 1985-2005. We converted their estimates of above-ground biomass (g biomass) to above-ground carbon biomass (gC) using a conversion factor of 0.47 gC/g biomass, following Meakem et al. [2018]. Our results and conclusions were not sensitive to this alternative measure of uncertainty (time variation vs. allometric formulation). Results reported herein represent uncertainty across allometric formulations. We use observations of gross primary productivity, latent heat, and sensible heat fluxes from flux tower eddy covariance measurements at Barro Colorado Island from July 2012 to August 2017 [Koven et al., unpublished].

We evaluate each SLA simulation against observations using two scoring metrics. The first metric, which we refer to as the range score (Rscore) measures the percentage of each simulation's annual mean values that fall within the observed range. The second metric measures the distance of each simulation's annual mean values from the observed mean. We refer to this second metric as the distance score (Dscore). We calculate both scores for each variable (leaf area index, gross primary productivity, etc). We then calculate a weighted average across all variables for each metric. Finally, we rank the simulations by the weighted average metrics and use these rankings to select the highest performing model parameterizations.

The Rscore measures the reliability with which the modeled values for each variable fall within the observed range. We calculate this metric for each observed variable in each SLA simulation as the proportion of years in which the model output falls within the observed range. Rscore values range from 0 to 100, where 100 indicates the model output falls within the observed range during all years analyzed. To account for relatively small sample sizes and potential measurement error within the observations we extend the observational range by 10% in either direction in this calculation. We also test the sensitivity of our results

to extending the range by 20%. A similar approach to extending the observed limits was taken by Fisher et al. [2010] when selecting parameterizations of the Ecosystem Demography model [Moorcroft et al., 2001] using observed limits of ecosystem properties.

The Dscore measures the spread, or distance, of each simulation's modeled annual mean values about the average observed value. We calculate the Dscore for each simulation and variable as the normalized root mean square error between the observed and model values. To account for the spread in the observed values when considering this distance, we normalize the root mean square error by the range in observed values. Thus the Dscore is calculated as follows:

$$Dscore = \frac{\sqrt{\sum_{k=1}^{n} \frac{(\bar{X}_{obs} - x_{model,k})^2}{n}}}{x_{obs,max} - x_{obs,min}} \tag{4.8}$$

where $\bar{X}_{obs}$ is the mean observed value, $x_{model,k}$ is the k^{th} model annual mean of n number of years of model output, and $x_{obs,max}$ and $x_{obs,min}$ are the maximum and minimum observed values, respectively. Dscore values near zero indicate that model output for the given simulation and variable is close in value to the observed mean. We also calculate the Dscore using an alternative formulation, the normalized mean absolute error. This alternative formulation normalizes the mean absolute difference between each model annual mean and the overall observed annual mean by the range in observations. This alternative formulation yields similar results and conclusions as the formulation reported above.

To measure the aggregate performance across all observed variables we calculate weighted average Rscores and Dscores for each SLA simulation. The weighted average for Rscores is calculated as follows:

$$Rscore_{avg} = \sum_{i=1}^{m} (\omega_i \cdot Rscore_i) \tag{4.9}$$

where m is the number of variables we consider (e.g., leaf area index, basal area, etc); $Rscore_i$

is the range score for each variable; and ω_i is the weighting for each variable. For the weighted average distance score ($Dscore_{avg}$), we use the Euclidean Distance to calculate the distance from the mean observation across all variables as follows:

$$Dscore_{avg} = \sqrt{\sum_{i=1}^{m} (\omega_i \cdot Dscore_i)^2} \tag{4.10}$$

where m is the number of variables we consider; $Dscore_i$ is the distance score for each variable; and ω_i is the weighting for each variable.

To identify the parameter sets that robustly performed well regardless of how variables were weighted, we tested several weighting schemes in our average score calculations. First, an even weighting scheme applied the same weighting to all variables ($\omega = 1/6$). A second weighting scheme favored structural ecosystem properties – leaf area index, above-ground biomass, and basal area. This weighting scheme reflects the likelihood that structural property measurements at Barro Colorado Island include less uncertainty than the flux measurements. The flux measurements include valuable additional information but may be challenging to accurately collect due to the island geography of this test site, as well as the challenges of maintaining an eddy covariance tower in a tropical forest. This weighting scheme assigned an $\omega = 0.3$ to each structural property and the remaining weighting evenly to the flux properties — gross primary productivity, latent heat flux, and sensible heat flux. Lastly, we tested a weighting scheme that favors leaf area index ($\omega = 0.4$), followed by above-ground biomass and basal area (each with $\omega = 0.25$), and the remaining weighting evenly distributed among the flux properties. This last weighting scheme was informed by correlations between individual variable scores. Scores for flux variables were correlated with leaf area index and with one another. As leaf area index observations likely include smaller measurement uncertainty, we chose to weight leaf area index more highly at the expense of flux measurements. We also reduced the weightings of basal area and above-ground biomass to account for their correlation with one another.

When observations had years that were not full (e.g., 28 months) we calculated annual

means starting from the beginning of the time series (e.g., months 1-24) and the end of the time series (e.g., months 5-28). For the Rscore, we allowed the observed minimum and maximum to be selected from the values in both sets of annual means. For the Dscore, we calculated the model distance from each set of annual means and selected the score with the best fit for use in the weighted averaging. Different start dates were used for observed leaf area index (January and September start dates) and for flux measurements (July and September start dates).

4.3.5 Selection of High-Performing Parameter Sets

We chose three high-performing parameter sets by ranking all simulations in order of their ability to match observations as measured by their weighted average Rscores and Dscores. Our aim was to select parameter sets that consistently perform well and whose performance is not dependent on a single formulation of model skill. We therefore test the sensitivity of each simulation's performance score to twelve different ranking methods. These ranking methods test all combinations of three weighting schemes (structure, correlation, and even; same weighting applied to each Dscore and Rscore pairing); two carbon dioxide concentrations (367ppm and 400ppm, which approximately bookend the carbon dioxide change over the observational period); and two formulations of the Rscore, in which the observed limits are extended by 10% and then by 20% to account for measurement error and sample size limitations in the observations. For all twelve combinations of weighting scheme, carbon dioxide concentration, and observed limit relaxation, we rank parameter sets by both their Dscores and Rscores. We then sum the rankings across the Dscore and Rscore pairing for each parameter. Finally, we calculate the average performance rank for each simulation across the ranking methods and use this overall average ranking to identify the parameter sets with the best performance.

4.3.6 Comparison to Additional Observations

We also compare all SLA ensemble members and high-performing members to observations of three variables that were not used in the benchmarking evaluation and selection of high-performing parameter sets: leaf height distribution, tree size distribution, and mortality rates. We use estimates of leaf area density (m^2 leaf area/m^3) made by Detto et al. [2015] using airborne waveform light detection and ranging (lidar) measurements from 2012 for our test site, Barro Colorado Island. Tree size abundance and mortality rate observations come from census surveys of a 50-hectare plot on Barro Colorado Island in 1992, 1996, 2001, 2006, and 2011 [Condit et al., 2017, 2012, Condit, 1998, Hubbell et al., 1999].

4.4 Results

The specific leaf area profile increases leaf area index in our FATES simulations. Across parameter sets, the distribution of average annual mean leaf area index shifts higher when simulations include the specific leaf area profile (SLA) compared to the control (CTRL) simulations (Figure 4.2a). This was expected given that increasing specific leaf area with canopy depth decreases the carbon cost of building leaf area lower in the canopy. The higher values of leaf area index in the SLA simulations are more aligned with observed limits and mean values (arrows and triangles in Figure 4.2). Thus, the specific leaf area profile enhances the model's ability to represent this key ecosystem property. Including the profile also increases the number of parameter combinations that match the observational means and limits for leaf area index.

The shift to higher leaf area in response to implementing the specific leaf area profile drives smaller changes in other ecosystem properties. The distribution of average annual mean gross primary productivity shifts slightly higher in the SLA simulations (Figure 4.2d). Increases in leaf area index in response to the specific leaf area profile cause gross primary productivity to rise because leaf area index provides the surface area over which photosynthesis occurs. The change in gross primary productivity is smaller than that of leaf area index because the

response of productivity to leaf area index saturates. As leaves are added to the bottom of the canopy their maximum photosynthetic rates decrease following the exponential decay of light and leaf nitrogen per area through the canopy. Thus, as leaf area increases, gross primary productivity increases but at a diminishing rate. Overall, gross primary productivity across model parameterizations continues to match observations well when the specific leaf area profile is included.

The distributions of above-ground biomass and basal area across parameterizations also shift slightly higher when the specific leaf area profile is included (Figure 4.2b,c). Increased biomass and tree size are consistent with higher gross primary productivity in the SLA simulations. As the specific leaf area profile shifts the ecosystem to a more productive state, trees have more carbon for structural growth. These shifts bring the SLA simulations in closer alignment with observations, although most parameterizations still produce above-ground biomass and basal area values that are low compared to observations.

The specific leaf area profile also drives a slight increase in the distribution of latent heat fluxes and slight decrease in sensible heat fluxes across parameterizations (Figure 4.2e,d). Latent heat flux is comprised of three components: transpiration, evaporation from leaf surfaces, and evaporation from soil. Higher leaf areas resulting from the specific leaf area profile provide more surface area for two of these components — transpiration and evaporation from leaf surfaces. Furthermore, transpiration is coupled to gross primary productivity as water exits leaves through stomatal pores when they open to take up carbon dioxide for photosynthesis. As gross primary productivity increases in response to the specific leaf area profile, so does transpiration. The response of transpiration is smaller than that of leaf area index because of the saturating response of gross primary productivity to leaf area. Additionally, solar radiation provides energy to evaporate water and increasingly diminishes with depth in the canopy at higher leaf areas. Sensible heat fluxes shift to lower values (Figure 4.2f) to balance the increase in latent heat fluxes. Overall, the specific leaf area profile brings the distribution of latent and sensible heat fluxes more in line with mean observations.

Figure 4.2 shows these changes for simulations run at 400ppm of carbon dioxide. Results

are similar for simulations run at 367ppm and are shown in Figure 4.3.

4.4.1 Benchmarking to Observations

We benchmark each SLA simulation against observations at our test site to select the highest performing parameter sets for use in future simulations. We use two measures of model skill to evaluate each simulation for each observed variable (leaf area index, aboveground biomass, basal area, gross primary productivity, latent heat flux, and sensible heat flux). The first metric, the Dscore, measures the distance of each simulation's annual mean values from the observed mean for each variable. Dscore values close to zero (yellow in Figures 4.4a and 4.5a) indicate that model values are close to the observed mean relative to the observed range for that variable. The second metric, the Rscore, measures the percent of model annual means that fall within the observed limits for each variable. Rscore values close to 100 (yellow in Figures 4.4b,c and 4.5b,c) indicate that a high proportion of model annual means fall within the observed limits. To account for measurement and sampling error in the observations, we extend the observed limits by both 10% and 20%. We measure the overall performance across all variables for each metric, Dscore and Rsore, using a weighted average of the individual variable scores. Our weighted average Dscores and Rscores test three weighting schemes: a weighting that favors structural properties (leaf area index, aboveground biomass, and basal area); a weighting that takes into account correlation between scores for individual variables, which favors leaf area index; and an even weighting across all variables. (See Section 4.3.4 for details.)

Many parameter sets perform well in several of the observed variables; however, very few parameter sets score well in all of the observed variables (Figures 4.4 and 4.5). Leaf area index is captured by a high proportion of parameter sets, as indicated by both Dscores and Rscores (Figures 4.4 and 4.5). The high proportion of parameter sets that match observations for leaf area index is also seen in the distributions of annual mean leaf area index across parameter sets (Figures 4.2a and 4.3a) as the mode of the model distribution aligns well with the observed mean and range.

Fewer parameter sets perform well against observations of basal area and above-ground biomass (Figures 4.4 and 4.5). Most parameter sets result in annual mean basal area and above-ground biomass values that are low compared to observations, a result that is slightly mediated by the new model structure that includes the specific leaf area profile (Figures 4.2b,c and 4.3b,c). Additionally, performance metrics for above-ground biomass and basal area are particularly polarizing — parameter sets generally score very well or very poorly with few mid-level values. This happens because these variables have low interannual variability (Figure 4.6b,c), resulting in model values with narrow ranges that are either all within or all outside of the observed range. Furthermore, the small observational range for basal area contributes to poor Dscores across parameter sets, as the distance between observations and model values is evaluated relative to the range in observed values. Even small differences between modeled and observed values will produce poor Dscore values when they are normalized by a small observed range. Overall, the polarizing performance metrics for above-ground biomass and basal area help to distinguish the highest performing parameter sets.

Modeled fluxes — gross primary productivity, latent heat, and sensible heat fluxes — align with observations particularly well across parameter sets. Latent heat flux and gross primary productivity scores indicate that many parameter sets match observations for this variable well, both in terms of distance from the observed mean (Dscores) and remaining within the observed limits (Rscores). The good correspondence between many parameter sets and the observed gross primary productivity and latent heat fluxes can also be seen in Figures 4.2 and 4.3, where the modes of the distributions of model means across parameter sets aligns with the observed means and ranges. For sensible heat fluxes, on the other hand, many parameter sets perform well in terms of distance from the observed mean (Dscores) but, fewer parameter sets consistently fall within the observed limits (Rscores). This difference in Dscore and Rscore performance for sensible heat fluxes occurs in part because the observed mean value lies towards the higher end of the observed range (Figures 4.2f and 4.3f). Thus many model annual means fall outside of the observed range while still remaining close in

value to the observed mean (Figures 4.2 and 4.3). Furthermore, higher variability in sensible heat fluxes in the model compared to the observations allows model values to agree well with the observed mean but extend past the observed range (Figure 4.6f).

4.4.2 High-Performing Parameter Sets

Three parameter sets performed particularly well when benchmarked against observations at our test site — parameter set numbers 86, 260, and 151 (ordered by skill). We recommend these parameters sets for use in future experiments and refer to them as our "high-performing" parameter sets. They are publicly available through the University of Washington Libraries ResearchWorks digital repository at http://hdl.handle.net/1773/43779. These parameter sets had the highest average performance rankings across the 12 combinations of ranking methods we tested. (See Materials and Methods for details.) They also consistently ranked in the seven highest performing parameter sets out of the 287 parameter sets we tested (parameter set 86 consistently ranked in the highest four), showing little sensitivity to the weighting scheme applied to average skill scores, the level of observed range extension in calculating Rscores, and carbon dioxide concentration. No other parameter sets consistently ranked in the top ten across ranking methods and the next best performing parameter set had an average ranking approximately twice as high as these three highest performing parameter sets. We report Dscores and Rscores for the three high-performing parameter sets, as well as the next seven highest performing parameter sets by average ranking, in Figures 4.4 and 4.5. The three high-performing parameter sets resulted in slightly different ecosystem properties, which we discuss in the following paragraphs.

Parameter set number 86 resulted in the best overall performance skill score for our test site and benchmarking variables. It scored well in all observed variables at both carbon dioxide concentrations, with slight exceptions for above-ground biomass and basal area (Figure 4.6). Annual mean leaf area index matched observations well at both carbon dioxide concentrations and was higher than for the other two high-performing parameter sets. Gross primary productivity, latent heat fluxes, and sensible heat fluxes matched observed

values well at both carbon dioxide concentrations. As discussed above, good performance in above-ground biomass and basal area is challenging across parameter sets. This parameterization performs relatively well in both of these variables. When run with a carbon dioxide concentration of 400ppm, parameter set 86 results in basal area that is close to the observed mean (Figures 4.4 and 4.6) and above-ground biomass that is slightly high (Figure 4.6) but relatively close to observations compared to other parameter sets (Dscore in Figure 4.4a). This high above-ground biomass could be in part due to higher wood density in this parameter set, relative to other high-performing parameter sets (Figure 4.9). At a carbon dioxide concentration of 367 ppm, this parameter set produces above-ground biomass that matches observations well. Although its basal area value is slightly low at a carbon dioxide concentration of 367ppm (Dscore in Figure 4.5a) it still falls within the observed range when extended by 10% (Rscore in Figure 4.5b). Overall, this parameter set matched benchmarking observations well at our tropical forest test site.

We also compare results from each parameter set to three observations at our test site that were not included in the benchmarking evaluation: leaf height distribution, tree size distribution, and tree mortality rates (Figures 4.7 and 4.8). While matching observations relatively well compared to many other parameter sets, the leaf height distribution in parameter set 86 results in higher than observed leaf area index midway through the canopy (20-30m in height) and lower than observed leaf area deeper in the canopy (below $\sim$15m in height). This parameter set also results in a tree size distribution that matches observations relatively well for trees with large diameters but has fewer small trees than observed. Consistent with these findings, parameter set 86 results in mortality rates for large trees that match observations but has higher than observed mortality rates for small trees. Overall, these results indicate that parameter set 86 favors large trees.

Parameter set number 260 had the second highest performance ranking in our benchmarking analysis. Like parameter set number 86, it results in leaf area index, gross primary productivity, latent heat fluxes, and sensible heat fluxes that match observations well (Figures 4.4, 4.5, and 4.6). It results in slightly lower leaf area index than observations and

parameter set 86, but still corresponds well with observations. This parameter set also results in gross primary productivity that closely matches observations and performs well in above-ground biomass across carbon dioxide concentrations. Basal area results agree well with observations at 367ppm carbon dioxide but are slightly high at 400ppm. Slightly higher latent heat fluxes than the other two high-performing parameter sets could be explained in part by this parameter set's high value for the slope parameter in the Ball-Berry stomatal conductance model (BB_slope in Figure 4.10). In comparison to observations not used in our benchmarking analysis, this parameter set's leaf height distribution matched observations relatively well (Figures 4.7 and 4.8). It resulted in leaf area index in the upper canopy that matched observations well but, like parameter set 86, leaf area in the lower canopy (below 15m in height) was slightly lower than observations. Also similar to parameter set 86, this parameter set resulted in a lower than observed number of trees with diameters below 10cm, and higher than observed mortality rates for these smaller sized trees.

The third high-performing parameter set, number 151, results in a different combination of ecosystem properties than parameter sets 86 and 260, making it an interesting parameter set for sensitivity testing. It performs well in both above-ground biomass and basal area measures at both carbon dioxide levels (Figures 4.4, 4.5, and 4.6). Latent heat fluxes and sensible heat fluxes are also in line with observations at both carbon dioxide concentrations. However, compared to observations and the other two high-performing parameter sets, it results in low leaf area index and high gross primary productivity (Figure 4.6a,d). Gross primary productivity is likely high despite low leaf area because this parameter set has a high V_{cmax25} value (Figure 4.9). Low leaf area index despite high productivity could be explained in part by this parameter set's relatively low value for specific leaf area at the top of the canopy (Figure 4.9), which represents a high carbon cost of building leaf area. Despite its poor performance in overall leaf area index and gross primary productivity, this parameter set better matches observations of leaf height distribution, tree size distribution, and mortality rates than the other two high-performing parameter sets.

4.4.3 Parameter Constraints from Benchmarking Analysis

We can use the skill rankings across the parameter ensemble simulations to constrain the range in trait parameter values that confer the best model skill for our tropical forest test site, Barro Colorado Island. Figures 4.9 and 4.10 show the performance ranking of each parameter ensemble simulation mapped onto their respective parameter trait values. For some traits, high-performing parameter sets (low average ranks, pink and dark blue color indicate 10 highest performing parameter sets in Figures 4.9 and 4.10) cluster around a narrow range of values. This indicates that these traits and values are likely to be important to simulating ecosystem structure and functioning and constrains the parameter space for this site.

In our simulations, high-performing parameter sets had values that clustered around narrow ranges for several trait parameters. Parameter sets that resulted in the best model skill had medium to high values of maximum carboxylation rates (V_{cmax25}) compared to the tropical tree trait space from which they were sampled. They also had low to medium values for specific leaf area and wood density. Additionally, high-performing ensemble members tended to have low to intermediate mortality rates. Constrained and original ranges for these trait parameters based on the ten highest performing parameter sets are reported in Table 4.1.

Several parameters used in allometric relationships within the model also stand out as having narrow ranges across high-performing parameter sets. High-performing parameter sets tended to have mid-level values for the parameter that controls the exponent in both the relationships between diameter at breast height and crown area and in the relationship between diameter at breast height and target leaf biomass (crown_dbh_exp). High-performing parameter sets also had intermediate values of the parameter that controls the intercept in the allometric relationship between diameter at breast height and the target allometric leaf biomass (bleaf_dbh). Additionally, high-performing parameter sets generally had low values for the intercept in the relationship between leaf area and sapwood area (la_to_sa, cm^2

sapwood/m^2 leaf area). Constrained and original ranges for these trait parameters are also reported in Table 4.1.

4.5 Discussion

We find that including a profile of specific leaf area with canopy depth improves model skill in matching observations at a tropical forest test site. The specific leaf area profile increases leaf area index across parameterizations in the FATES demographic vegetation model as expected, bringing model values more in line with observations. The profile also improves modeled above-ground biomass, basal area, latent heat fluxes, and sensible heat fluxes by shifting the distribution of these variables across parameterizations closer to observed values, while maintaining good agreement between simulated and observed gross primary productivity.

By benchmarking many parameterizations of a single model structure against several observed variables we were able to identify ecosystem properties that this model structure successfully captures across many parameterizations (easily attained via parameterization), as well as ecosystem properties that remain challenging to simulate across parameterizations (potential areas for model structure improvement or parameter selection). In general, the model structure with specific leaf area profile captures the observed structural ecosystem property leaf area index and ecosystem functioning properties gross primary productivity, latent heat fluxes, and sensible heat fluxes with high skill across many parameterizations. The specific leaf area profile improved simulated leaf area index, which provides the surface area over which gross primary productivity and latent heat fluxes are summed. Thus by improving modeled leaf area index we also made improvements to these fluxes.

Despite good correspondence in leaf area index and ecosystem functioning, the model matches observed above-ground biomass and basal area in far fewer parameterizations. In general, it underestimates these structural properties across the parameter sets we tested. These two variables are both measures of tree size. Basal area measures the combined cross-sectional area of tree stems for a given area of ground (m^2 tree cross-sectional area/ha

ground), while above-ground biomass is a measure carbon mass across trees for a given area of ground (kgC/m^2 ground). Basal area is more representative of all tree size classes, while above-ground biomass is more heavily weighted toward larger trees. Although both variables challenge the model's skill, basal area is the most challenging to capture across ensemble members (Figures 4.4 and 4.5). This suggests that capturing smaller size trees is exceptionally challenging for all but a few parameterizations. Low skill scores for above-ground biomass and basal area could result in part from low interannual variability of these properties, particularly in basal area observations, which allows for less overlap between observed and modeled distributions. Yet, this finding is unlikely to be merely an artifact of how we calculate skill scores. Figure 4.7 shows that the model simulates too few small trees and higher than observed mortality rates for small trees across parameter sets. We even see this behavior in our high-performing parameter sets, with the exception that parameter set 151 underestimates small tree mortality rates (Figure 4.7). Overall, the small number of parameter sets with high skill in simulating above-ground biomass and basal area indicates that improvements to model structure could be required to improve performance in these metrics and that, for this model structure, these are critical benchmarking properties for parameter selection.

We identify three parameter sets that performed particularly well when benchmarked against observations at our test site — parameter set numbers 86, 260, and 151 (ordered by skill). We recommend these high-performing parameter sets for use in future experiments and have made them available for public use (see Results Section). The two highest performing parameterizations, parameter sets 86 and 260, show high skill in all variables across benchmarking metrics and carbon dioxide concentrations we tested. They result in similar ecosystem properties but differ slightly. Parameter set 86 simulates leaf area index, gross primary productivity, and above-ground biomass that are on the high end of observations. Parameter set 260 results in slightly lower leaf area index and above-ground biomass, while aligning with observed gross primary productivity fluxes very well. Both parameterizations simulate above-ground biomass and basal area that match observations relatively well but

show slight weaknesses.

The third best performing parameterization, parameter set 151, results in ecosystem properties that differ from parameter sets 86 and 260. It shows high skill in simulating basal area and above-ground biomass but results in gross primary productivity that is high and leaf area index that is low compared to the benchmarking observations we used. Notably, this parameterization matched observations of leaf height distribution and tree size distribution, observations not used in our benchmarking evaluation, better than the two highest performing parameter sets by simulating higher understory leaf area index and a higher number of small sized trees. Overall, this parameter set provides a useful alternative parameterization and ecosystem characterization for sensitivity tests in future simulations.

In addition to identifying entire parameter sets for future use, our analysis constrains the range of viable parameter values for key individual plant traits. We evaluate the range in parameter values using the overall performance scores for each parameter set in our benchmarking analysis (Figures 4.9 and 4.10). Several parameters stand out as having narrower ranges among the highest performing parameter sets than the plausible trait space from which all parameter sets were sampled. This clustering of high-performing parameter sets around narrow trait values indicates that model skill is highly sensitive to the magnitude of these parameters. It also reveals that values for these parameters must fall in narrower ranges than those we sampled from to match observations at our test site well with this model structure. We sampled an observed trait space across tropical forest sites for parameters in Figure 4.9 and a plausible trait space for parameters in Figure 4.10 for which observational constraints are lacking. (See Materials and Methods for details.) High-performing parameter values clustered around narrower ranges for the following observed traits: maximum carboxylation rate (V_{cmax25}), specific leaf area, wood density, and mortality rate. Covariance between maximum carboxylation rate, specific leaf area, and wood density in the trait space from which our parameter sets were sampled [Koven et al., unpublished] could explain why they are all identified as strongly influencing model performance. It is possible that sensitivity to one trait drives the narrow ranges for all of the traits. For example V_{cmax25} has

been shown to be a highly influential parameter in terrestrial biosphere models and differs greatly across vegetation models in part because it provides a strong parametric control over productivity that can balance model structural errors [Bonan et al., 2011, 2012]. We also saw narrower ranges for three allometric relationship parameters — the crown area to diameter at breast height exponent (crown_dbh_exp), the target leaf biomass to diameter at breast height intercept (bleaf_dbh), and the intercept for calculating sapwood area from leaf area (la_to_sa). We report constrained ranges for these key parameters in Table 4.1, which can be used in future parameter selection and testing. Future studies could use this approach to better understand each trait parameter's influence on model results and performance for individual variables. Such analysis could help to determine which traits most strongly influence ecosystem properties that remain challenging for the model to capture, such as basal area and above-ground biomass.

4.6 Conclusions

Inclusion of the observed within-canopy gradient of leaf area to mass ratio, also called specific leaf area, drastically improves the relationship between leaf area index and productivity, as well as related ecosystem structure and functioning properties, in our demographic vegetation model simulations. With few exceptions, this structural leaf trait profile is not considered in most terrestrial biosphere models, although many consider the associated profiles of per-area leaf nitrogen and photosynthetic rates. Thus many terrestrial biosphere models could be misrepresenting the relationship between productivity and leaf area index, with severe consequences for vegetation structure, functioning, ecological dynamics, and vegetation impacts on large-scale climate. The effect of the specific leaf area profile is likely greatest in ecosystems with high leaf area index and high maximum rates of photosynthesis, such as tropical forests, as cumulative overlying leaf area index drives the change in specific leaf area with depth in the canopy and high maximum rates of photosynthesis are empirically related to steeper rates of change in specific leaf area. Highly productive and leafy ecosystems also tend to exert strong control over the Earth's carbon cycle and climate. As such,

the inclusion of the specific leaf area profile in land surface models could have large-scale impacts on simulations of Earth's current and future climate and carbon cycling.

This work improves the simulation of ecosystem structure and functioning in the FATES vegetation demography model through a more realistic representation of the within-canopy profile of the leaf area to mass ratio (specific leaf area), and suggests high-performing parameter sets and constrained parameter ranges for use in future tropical forest FATES experiments. In addition to providing an improved FATES model, our implementation of the specific leaf area profile provides a blueprint for including this important within-canopy gradient in other models of the terrestrial biosphere.

4.7 Acknowledgements

We acknowledge support from the National Science Foundation AGS-1553715 to the University of Washington. High-performance computing support from Cheyenne (doi:10.5065/D6RX99HX) was provided by NCAR's Computational and Information Systems Laboratory, sponsored by the National Science Foundation.

4.8 Figures and Tables

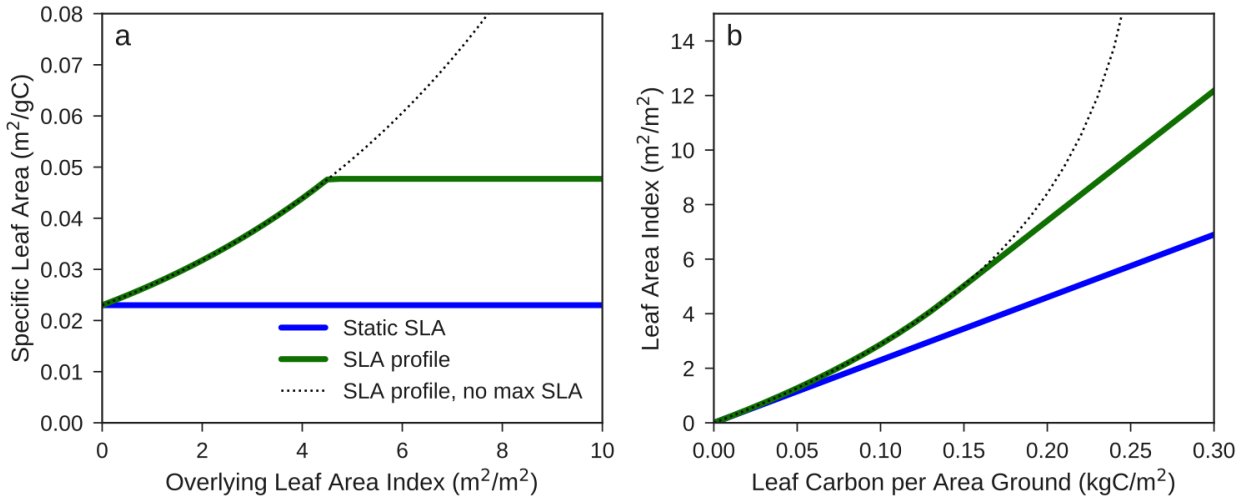

Figure 4.1: Dependence of (a) specific leaf area (m^2 leaf area/gC) on overlying leaf area index (m^2 leaf area/m^2 ground area); and (b) leaf area index (m^2 leaf area/m^2 ground area) on leaf carbon per area ground (kgC/m^2 ground) in the control model structure (blue lines) and the experiment model structure that includes the profile of specific leaf area through the canopy and an observational constraint on maximum specific leaf area (green lines), and the experiment model if it did not include a maximum specific leaf area constraint (black dashed lines).

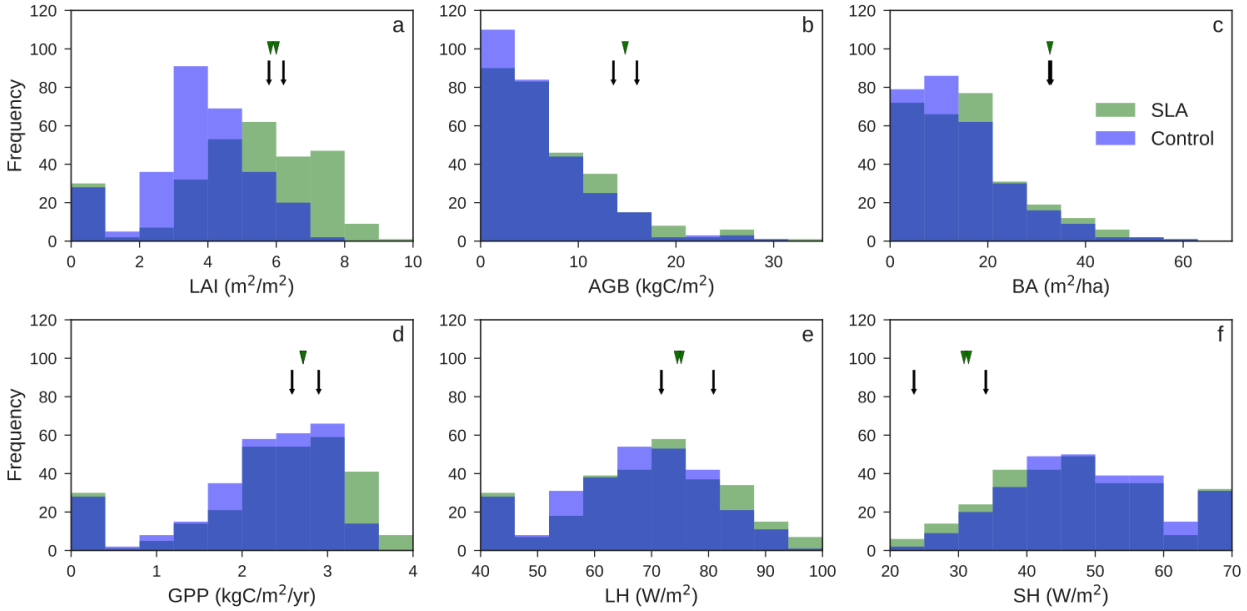

Figure 4.2: Histograms of modeled annual mean (a) leaf area index (LAI, m^2/m^2); (b) above-ground biomass (AGB, kgC/m^2); (c) basal area (BA, m^2/ha); (d) gross primary productivity (GPP, $kgC/m^2/year$); (e) latent heat flux (LH, W/m^2); and (f) sensible heat flux (SH, W/m^2) comparing each parameter ensemble member run with the control (CTRL, blue) and specific leaf area (SLA, green) model structures at 400ppm carbon dioxide. Observed means (green triangles) and limits (black arrows) are included for each variable as a reference. Observations of leaf area index come from Detto et al. [2018]; basal area from Condit et al. [2017, 2012], Condit [1998], and Hubbell et al. [1999]; above-ground biomass from Meakem et al. [2018]; and gross primary productivity, latent heat flux, and sensible heat flux from [Koven et al., unpublished]. When observations span partial years we report two annual means, one spanning the beginning of the time series and the other the end of the time series.

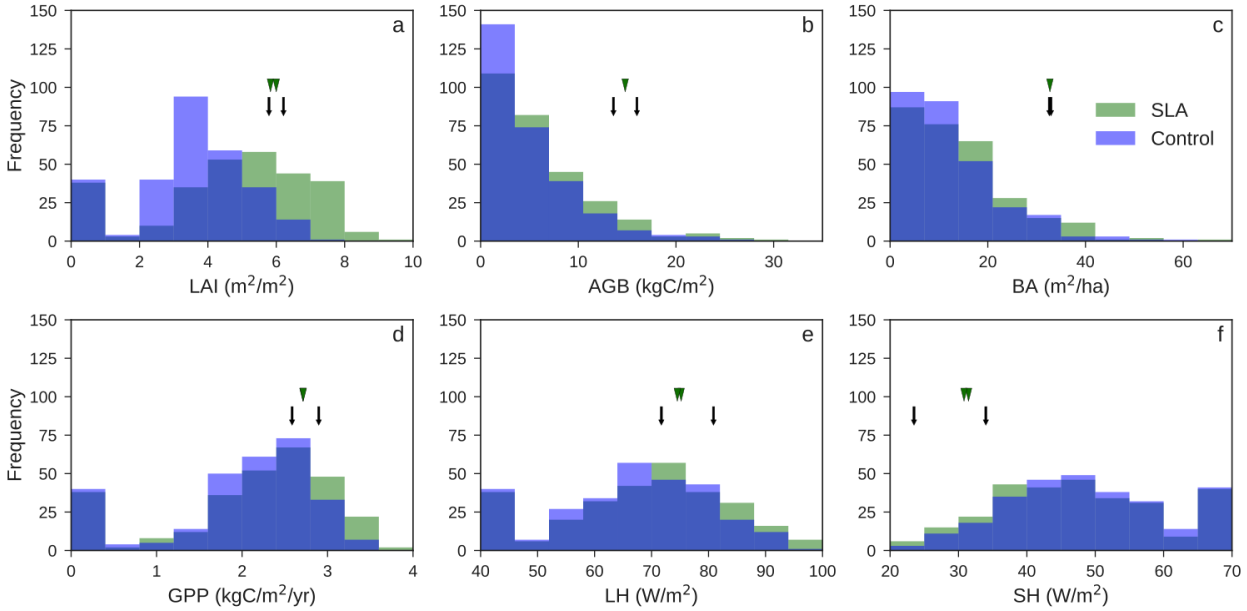

Figure 4.3: Histograms of modeled annual mean (a) leaf area index (LAI, m^2/m^2); (b) above-ground biomass (AGB, kgC/m^2); (c) basal area (BA, m^2/ha); (d) gross primary productivity (GPP, $kgC/m^2/year$); (e) latent heat flux (LH, W/m^2); and (f) sensible heat flux (SH, W/m^2) comparing each parameter ensemble member run with the control (CTRL, blue) and specific leaf area (SLA, green) model structures at 367ppm carbon dioxide. Observed means (green triangles) and limits (black arrows) are included for each variable as a reference. Observations of leaf area index come from Detto et al. [2018]; basal area from Condit et al. [2017, 2012], Condit [1998], and Hubbell et al. [1999]; above-ground biomass from Meakem et al. [2018]; and gross primary productivity, latent heat flux, and sensible heat flux from [Koven et al., unpublished]. When observations span partial years we report two annual means, one spanning the beginning of the time series and the other the end of the time series.

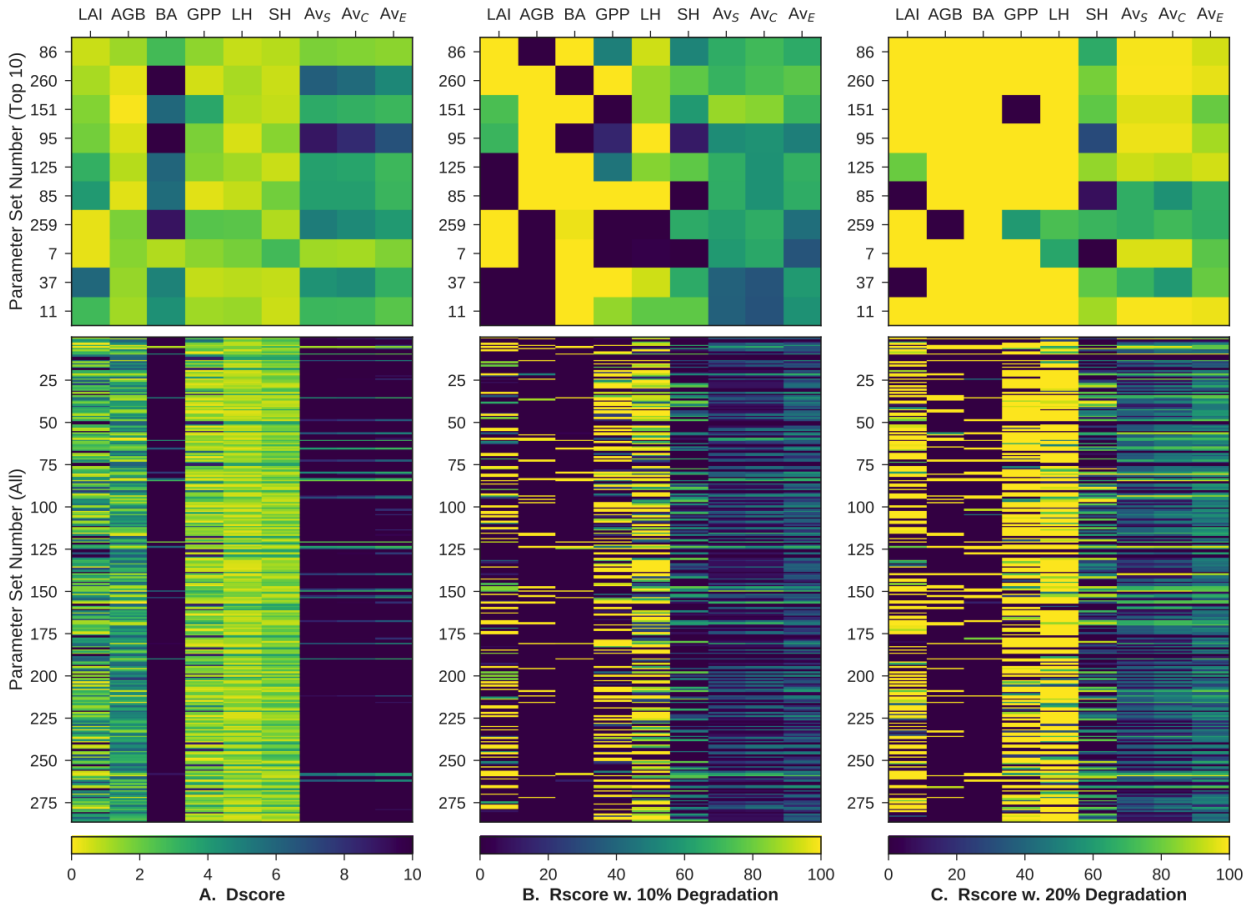

Figure 4.4: Model skill scores for ten high-performing and, for comparison, all parameter sets as measured by (a) distance between model annual mean values and observed mean (Dscore), (b) percentage of model annual means that fall within observed range when it is extended by 10% (Rscore w. 10% Degradation), and (c) percentage of model annual means that fall within observed range when it is extended by 20% (Rscore w. 20% Degradation). Each metric is reported for leaf area index (LAI), above-ground biomass (AGB), basal area (BA), gross primary productivity (GPP), latent heat flux (LH), sensible heat flux (SH), and weighted averages across variables using different weighting schemes: favoring structural properties (Av_S), based on correlations between individual variable scores and favoring leaf area index (Av_C), and evenly weighted across variables (Av_E). Good model agreement with observations (yellow), poor agreement (dark blue). Model results for simulations run at 400ppm carbon dioxide.

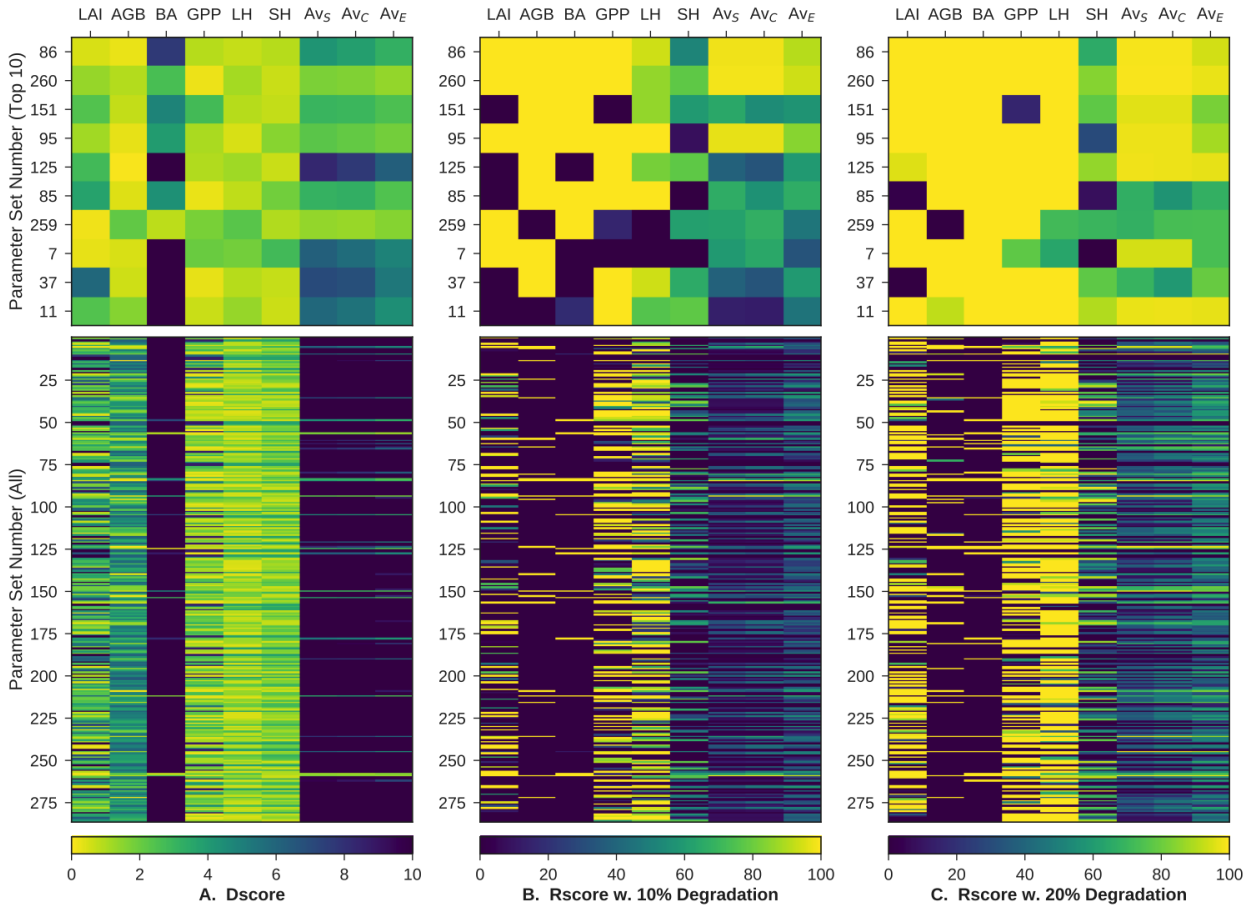

Figure 4.5: Model skill scores for ten high-performing and, for comparison, all parameter sets as measured by (a) distance between model annual mean values and observed mean (Dscore), (b) percentage of model annual means that fall within observed range when it is extended by 10% (Rscore w. 10% Degradation), and (c) percentage of model annual means that fall within observed range when it is extended by 20% (Rscore w. 20% Degradation). Each metric is reported for leaf area index (LAI), above-ground biomass (AGB), basal area (BA), gross primary productivity (GPP), latent heat flux (LH), sensible heat flux (SH), and weighted averages across variables using different weighting schemes: favoring structural properties (Av$_S$), based on correlations between individual variable scores and favoring leaf area index (Av$_C$), and evenly weighted across variables (Av$_E$). Good model agreement with observations (yellow), poor agreement (dark blue). Model results for simulations run at 367ppm carbon dioxide.

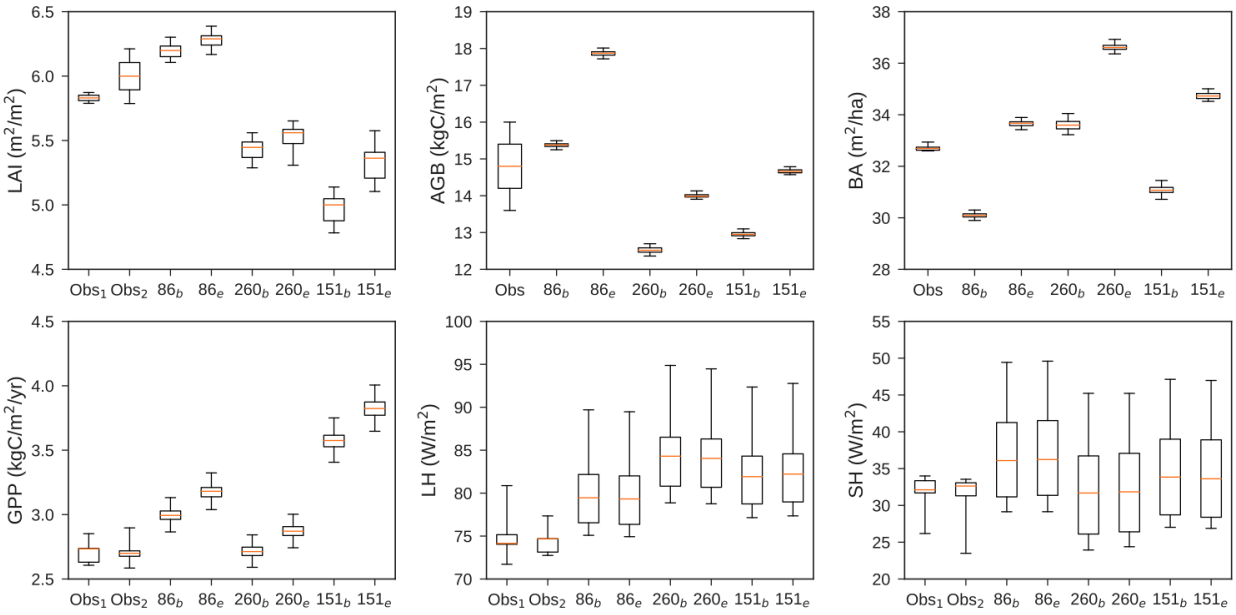

Figure 4.6: Boxplots of observed and high-performing parameter set modeled annual mean (a) leaf area index (LAI, m^2/m^2); (b) above-ground biomass (AGB, kgC/m^2); (c) basal area (BA, m^2/ha); (d) gross primary productivity (GPP, $kgC/m^2/year$); (e) latent heat flux (LH, W/m^2); and (f) sensible heat flux (SH, W/m^2). Median (orange line), interquartile range (box), range (whiskers). Parameter set indicated by number (86, 260, and 151). Subscript letters indicate carbon dioxide concentration at approximately beginning (b = 367ppm) and end of observational period (e = 400ppm). Observations of leaf area index come from Detto et al. [2018]; basal area from Condit et al. [2017, 2012], Condit [1998], and Hubbell et al. [1999]; above-ground biomass from Meakem et al. [2018]; and gross primary productivity, latent heat flux, and sensible heat flux from [Koven et al., unpublished]. Two sets of observations are reported for variables when the time period spanned incomplete years. The first observation (Obs_1) reports results for annual means starting from the beginning of the time period. The second observation (Obs_2) reports annual means that include the end of the time period.

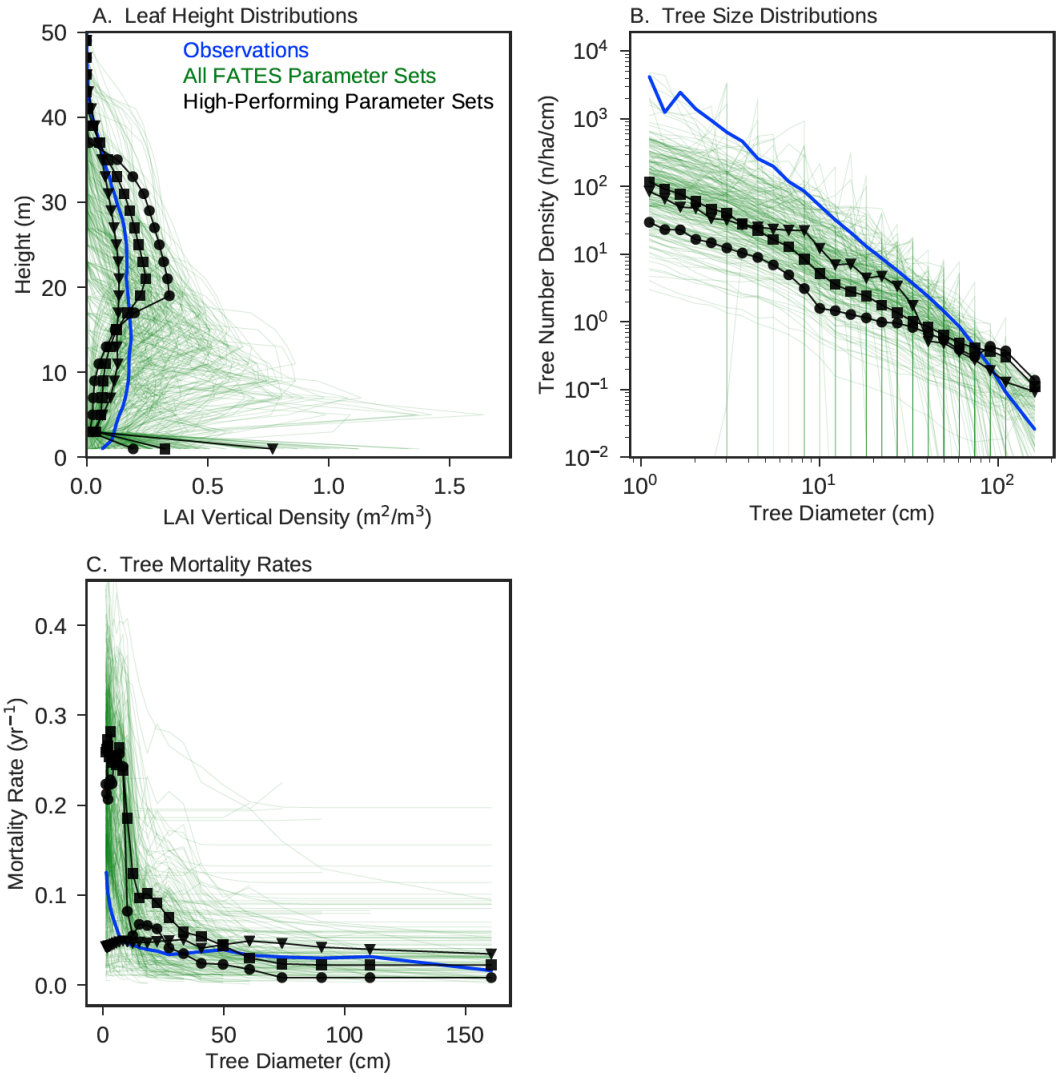

Figure 4.7: Comparison of modeled and observed (a) leaf height distribution, estimated as leaf area index vertical density (LAI Vertical Density; m^2 leaf area/m^3); (b) tree size distribution, measured by the tree number density (number of plants/ha/cm) for each tree diameter size class (cm); and (c) tree mortality rates (yr^{-1}) by tree diameter size class (cm). Mean estimates from observations at Barro Colorado Island (blue lines), mean values for all parameter sets (green lines); and mean values for three high-performing parameter sets: number 86 (black circles), number 260 (black squares), and number 151 (black triangles). All simulations run at carbon dioxide concentration of 400ppm. Estimates of leaf area index vertical density at our test site from Detto et al. [2015]. Tree size and mortality rate observations from census surveys at our test site [Condit et al., 2017, 2012, Condit, 1998, Hubbell et al., 1999].

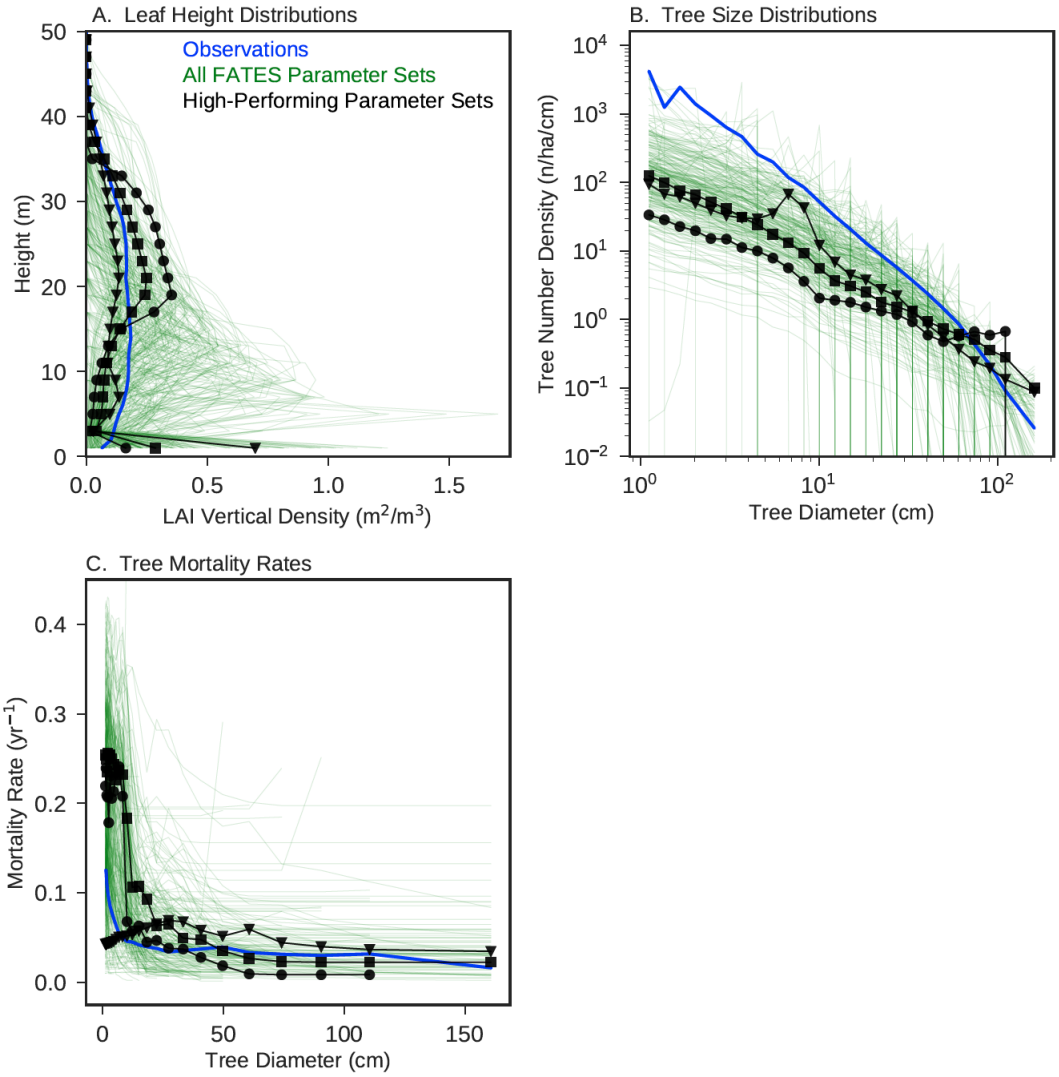

Figure 4.8: Comparison of modeled and observed (a) leaf height distribution, estimated as leaf area index vertical density (LAI Vertical Density; m^2 leaf area/m^3); (b) tree size distribution, measured by the tree number density (number of plants/ha/cm) for each tree diameter size class (cm); and (c) tree mortality rates (yr^{-1}) by tree diameter size class (cm). Mean estimates from observations at Barro Colorado Island (blue lines), mean values for all parameter sets (green lines); and mean values for three high-performing parameter sets: number 86 (black circles), number 260 (black squares), and number 151 (black triangles). All simulations run at carbon dioxide concentration of 367ppm. Estimates of leaf area index vertical density at our test site from Detto et al. [2015]. Tree size and mortality rate observations from census surveys at our test site [Condit et al., 2017, 2012, Condit, 1998, Hubbell et al., 1999].

Figure 4.9: Trait covariance across parameter sets for all trait values sampled from observed trait space. Diagonal plots show the sampled distribution for each trait. Color indicates the overall average performance ranking for each parameter set. The three highest performing parameter sets (PS 86, 260, and 151) are indicated in shades of pink; the next seven highest performing parameter sets (with average rankings of 10+ and below 25) are shown in blue. Parameters: maximum rate of carboxylation at the top of the canopy (Vcmax25, μmol $CO_2/m^2/s$), wood density (g/cm^3), specific leaf area at the top of the canopy (SLA, m^2 leaf area/gC), leaf nitrogen per area (Narea, gN/m^2 leaf area), leaf lifespan (Lifespan, days), and background mortality rate (Mortality, 1/100yrs).

Figure 4.10: Trait covariance across parameter sets for all trait values sampled from plausible trait space. Diagonal plots show the sampled distribution for each trait. Color legend as in Figure 4.9. Parameters: intercept in the relationship between diameter at breast height and plant crown area (crown_dbh_coef), exponent in both the relationship between diameter at breast height and crown area and in the relationship between diameter at breast height and target leaf biomass (crown_dbh_exp), intercept in the allometric relationship between diameter at breast height and the target allometric leaf biomass (bleaf_dbh), ratio of fine root carbon to leaf carbon (fineroot_leaf, gC fine root/gC leaf), Ball-Berry stomatal conductance equation slope (BB_slope, unitless), and intercept of leaf area to sapwood area conversion (latosa, cm^2 sapwood/m^2 leaf area).

Table 4.1: Parameter constraints from ten highest performing parameter sets.

Trait Parameter	**Constrained**		**Original**	
	Mean	Range	Mean	Range
V_{cmax25} (μmol CO_2/m^2/s)	63.9	(36.7, 106.6)	51.1	(0.4, 121.8)
Specific leaf area (m^2/gC)	0.029	(0.014, 0.060)	0.028	(0.008, 0.084)
Wood density (g/cm^3)	0.41	(0.26, 0.61)	0.54	(0.12, 0.97)
Mortality (1/100yrs)	2.49	(0.46, 5.12)	3.57	(0.12, 22.98)
Crown to dbh exponent	1.29	(1.22, 1.35)	1.30	(1.15, 1.47)
Leaf biomass to dbh	0.18	(0.09, 0.26)	0.20	(0.07, 0.34)
Sapwood area to leaf area (cm^2/m^2)	0.13	(0.051,0.25)	0.32	(0.0011, 0.85)

Notes. Maximum rate of carboxylation (V_{cmax25}), diameter at breast height (dbh).

BIBLIOGRAPHY

E. A. Ainsworth and S. P. Long. What have we learned from 15 years of free-air CO_2 enrichment (FACE)? A meta-analytic review of the responses of photosynthesis, canopy properties and plant production to rising CO_2. *New Phytologist*, 165(2):351–371, 2005.

E. A. Ainsworth and A. Rogers. The response of photosynthesis and stomatal conductance to rising [CO_2]: mechanisms and environmental interactions. *Plant, Cell and Environment*, 30(3):258–270, 2007.

A. A. Ali, B. E. Medlyn, T. G. Aubier, K. Y. Crous, and P. B. Reich. Elevated carbon dioxide is predicted to promote coexistence among competing species in a trait-based model. *Ecology and Evolution*, 5(20):4717–4733, 2015.

L. D. Anderegg, L. T. Berner, G. Badgley, M. L. Sethi, B. E. Law, and J. HilleRisLambers. Within-species patterns challenge our understanding of the leaf economics spectrum. *Ecology Letters*, 21(5):734–744, 2018.

D. Archer, M. Eby, V. Brovkin, A. Ridgwell, L. Cao, U. Mikolajewicz, K. Caldeira, K. Matsumoto, G. Munhoven, A. Montenegro, and K. Tokos. Atmospheric Lifetime of Fossil Fuel Carbon Dioxide. *Annual Review of Earth and Planetary Sciences*, 37(1):117–134, 2009.

V. K. Arora, G. J. Boer, P. Friedlingstein, and M. Eby. Carbon–concentration and carbon–climate feedbacks in CMIP5 Earth system models. *Journal of Climate*, 26(15):5289–5314, 2013.

J. T. Ball, I. E. Woodrow, and J. A. Berry. A model predicting stomatal conductance and its contribution to the control of photosynthesis under different environmental conditions. *Progress in Photosynthesis Research*, 4:221–224, 1987.

C. Baraloto, Q. Molto, S. Rabaud, B. Hérault, R. Valencia, L. Blanc, P. V. Fine, and J. Thompson. Rapid simultaneous estimation of aboveground biomass and tree diversity across Neotropical forests: a comparison of field inventory methods. *Biotropica*, 45(3): 288–298, 2013.

R. A. Betts, P. M. Cox, S. E. Lee, and F. I. Woodward. Contrasting physiological and structural vegetation feedbacks in climate change simulations. *Nature*, 387(6635):796–799, 1997.

R. A. Betts, O. Boucher, M. Collins, P. M. Cox, P. D. Falloon, N. Gedney, D. L. Hemming, C. Huntingford, C. D. Jones, D. M. H. Sexton, and M. J. Webb. Projected increase in continental runoff due to plant responses to increasing carbon dioxide. *Nature*, 448(7157): 1037–1041, 2007.

G. B. Bonan. Forests and climate change: forcings, feedbacks, and the climate benefits of forests. *Science*, 320:1444–1449, 2008.

G. B. Bonan, P. J. Lawrence, K. W. Oleson, S. Levis, M. Jung, M. Reichstein, D. M. Lawrence, and S. C. Swenson. Improving canopy processes in the Community Land Model version 4 (CLM4) using global flux fields empirically inferred from FLUXNET data. *Journal of Geophysical Research*, 116(G2):G02014, 2011.

G. B. Bonan, K. W. Oleson, R. A. Fisher, G. Lasslop, and M. Reichstein. Reconciling leaf physiological traits and canopy flux data: Use of the TRY and FLUXNET databases in the Community Land Model version 4. *Journal of Geophysical Research*, 117(G2), 2012.

O. Boucher, A. Jones, and R. A. Betts. Climate response to the physiological impact of carbon dioxide on plants in the Met Office Unified Model HadCM3. *Climate Dynamics*, 32(2-3):237–249, 2009.

L. Bounoua, F. G. Hall, P. J. Sellers, A. Kumar, G. J. Collatz, C. J. Tucker, and M. L.

Imhoff. Quantifying the negative feedback of vegetation to greenhouse warming: A modeling approach. *Geophysical Research Letters*, 37(23), 2010.

R. J. W. Brienen, O. L. Phillips, T. R. Feldpausch, E. Gloor, T. R. Baker, J. Lloyd, G. Lopez-Gonzalez, A. Monteagudo-Mendoza, Y. Malhi, S. L. Lewis, R. Vasquez Martinez, M. Alexiades, E. Alvarez Davila, P. Alvarez-Loayza, A. Andrade, L. E. O. C. Aragao, A. Araujo-Murakami, E. J. M. M. Arets, L. Arroyo, G. A. Aymard C, O. S. Banki, C. Baraloto, J. Barroso, D. Bonal, R. G. A. Boot, J. L. C. Camargo, C. V. Castilho, V. Chama, K. J. Chao, J. Chave, J. A. Comiskey, F. Cornejo Valverde, L. da Costa, E. A. de Oliveira, A. Di Fiore, T. L. Erwin, S. Fauset, M. Forsthofer, D. R. Galbraith, E. S. Grahame, N. Groot, B. Herault, N. Higuchi, E. N. H. Coronado, H. Keeling, T. J. Killeen, W. F. Laurance, S. Laurance, J. Licona, W. E. Magnussen, B. S. Marimon, B. H. Marimon-Junior, C. Mendoza, D. A. Neill, E. M. Nogueira, P. Nunez, N. C. Pallqui Camacho, A. Parada, G. Pardo-Molina, J. Peacock, M. Pena-Claros, G. C. Pickavance, N. C. A. Pitman, L. Poorter, A. Prieto, C. A. Quesada, F. Ramirez, H. Ramirez-Angulo, Z. Restrepo, A. Roopsind, A. Rudas, R. P. Salomao, M. Schwarz, N. Silva, J. E. Silva-Espejo, M. Silveira, J. Stropp, J. Talbot, H. ter Steege, J. Teran-Aguilar, J. Terborgh, R. Thomas-Caesar, M. Toledo, M. Torello-Raventos, R. K. Umetsu, G. M. F. Van der Heijden, P. Van der Hout, I. C. G. Vieira, S. A. Vieira, E. Vilanova, V. A. Vos, and R. J. Zagt. Long-term decline of the Amazon carbon sink. *Nature*, 519, 2015.

W. S. Broecker, T. Takahashi, H. J. Simpson, and T. H. Peng. Fate of Fossil Fuel Carbon Dioxide and the Global Carbon Budget. *Science*, 206(4417):409–418, 1979.

E. E. Butler, A. Datta, H. Flores-Moreno, M. Chen, K. R. Wythers, F. Fazayeli, A. Banerjee, O. K. Atkin, J. Kattge, B. Amiaud, and others. Mapping local and global variability in plant trait distributions. *Proceedings of the National Academy of Sciences of the United States of America*, 114(51):E10937–E10946, 2017.

L. Cao, G. Bala, K. Caldeira, R. Nemani, and G. Ban-Weiss. Importance of carbon dioxide

physiological forcing to future climate change. *Proceedings of the National Academy of Sciences of the United States of America*, 107(21):9513–9518, 2010.

F. E. Carswell, P. Meir, E. V. Wandelli, L. Bonates, B. Kruijt, E. M. Barbosa, A. D. Nobre, J. Grace, and P. G. Jarvis. Photosynthetic capacity in a central Amazonian rain forest. *Tree Physiology*, 20(3):179–186, 2000.

L. A. Cernusak, K. Winter, J. W. Dalling, J. A. M. Holtum, C. Jaramillo, C. Koerner, A. D. B. Leakey, R. J. Norby, B. Poulter, B. L. Turner, and S. J. Wright. Tropical forest responses to increasing atmospheric CO_2: current knowledge and opportunities for future research. *Functional Plant Biology*, 40(6):531–551, 2013.

L. A. Cernusak, V. Haverd, O. Brendel, D. Le Thiec, J.-M. Guehl, and M. Cuntz. Robust Response of Terrestrial Plants to Rising CO_2. *Trends in Plant Science*, 2019.

P. Ciais, C. Sabine, G. Bala, L. Bopp, V. Brovkin, J. Canadell, A. Chhabra, R. DeFries, J. Galloway, M. Heimann, and others. Carbon and Other Biogeochemical Cycles. In *Climate change 2013: the physical science basis. Contribution of Working Group I to the Fifth Assessment Report of the Intergovernmental Panel on Climate Change*, pages 465–570. Cambridge University Press, 2013.

Computational and Information Systems Laboratory. Cheyenne: HPE/SGI ICE XA System (University Community Computing). *National Center for Atmospheric Research, Boulder, CO*, 2017.

R. Condit. *Tropical forest census plots*. Springer-Verlag and R. G. Landes Company, Berlin, Germany, and Georgetown, Texas, 1998.

R. Condit, S. Lao, R. Pérez, S. B. Dolins, R. Foster, and S. Hubbell. Barro Colorado forest census plot data (version 2012). *Center for Tropical Forest Science Databases. https://dx. doi. org/10.5479/data. bci*, 2012.

R. S. Condit, S. Aguilar, R. Perez, S. Lao, S. P. Hubbell, and R. B. Foster. Barro Colorado 50-ha Plot Taxonomy as of 2017. 2017.

P. M. Cox, R. A. Betts, C. B. Bunton, R. Essery, P. R. Rowntree, and J. Smith. The impact of new land surface physics on the GCM simulation of climate and climate sensitivity. *Climate Dynamics*, 15(3):183–203, 1999.

P. M. Cox, R. A. Betts, C. D. Jones, S. A. Spall, and I. J. Totterdell. Acceleration of global warming due to carbon-cycle feedbacks in a coupled climate model. *Nature*, 408(6809): 184–187, 2000.

U. Cubasch, D. Wuebbles, D. Chen, M. C. Facchini, D. Frame, N. Mahowald, and J. G. Winther. Introduction. In T. F. Stocker, D. Qin, G. K. Plattner, M. Tignor, S. K. Allen, J. Boschung, A. Nauels, Y. Xia, V. Bex, and P. M. Midgley, editors, *Climate Change 2013: The Physical Science Basis. Contribution of Working Group I to the Fifth Assessment Report of the Intergovernmental Panel on Climate Change*, pages 121–158. Cambridge University Press, Cambridge, UK, 2013.

D. F. Cusack, J. Karpman, D. Ashdown, Q. Cao, M. Ciochina, S. Halterman, S. Lydon, and A. Neupane. Global change effects on humid tropical forests: Evidence for biogeochemical and biodiversity shifts at an ecosystem scale. *Reviews of Geophysics*, 54(3):523–610, 2016.

E. L. Davin and N. de Noblet-Ducoudré. Climatic Impact of Global-Scale Deforestation: Radiative versus Nonradiative Processes. *Journal of Climate*, 23(1):97–112, 2010.

M.-A. De Graaff, K. J. Van Groenigen, J. Six, B. Hungate, and C. van Kessel. Interactions between plant growth and soil nutrient cycling under elevated CO_2: a meta-analysis. *Global Change Biology*, 12(11):2077–2091, 2006.

M. G. De Kauwe, B. E. Medlyn, S. Zaehle, A. P. Walker, M. C. Dietze, T. Hickler, A. K. Jain, Y. Luo, W. J. Parton, I. C. Prentice, B. Smith, P. E. Thornton, S. Wang, Y.-P. Wang, D. Wårlind, E. Weng, K. Y. Crous, D. S. Ellsworth, P. J. Hanson, H. Seok Kim,

J. M. Warren, R. Oren, and R. J. Norby. Forest water use and water use efficiency at elevated CO_2: a model-data intercomparison at two contrasting temperate forest FACE sites. *Global Change Biology*, 19(6):1759–1779, 2013.

M. G. De Kauwe, B. E. Medlyn, S. Zaehle, A. P. Walker, M. C. Dietze, Y.-P. Wang, Y. Luo, A. K. Jain, B. El-Masri, T. Hickler, D. Wårlind, E. Weng, W. J. Parton, P. E. Thornton, S. Wang, I. C. Prentice, S. Asao, B. Smith, H. R. McCarthy, C. M. Iversen, P. J. Hanson, J. M. Warren, R. Oren, and R. J. Norby. Where does the carbon go? A model-data intercomparison of vegetation carbon allocation and turnover processes at two temperate forest free-air CO_2 enrichment sites. *New Phytologist*, 203:883–899, 2014.

M. Detto, G. P. Asner, H. C. Muller-Landau, and O. Sonnentag. Spatial variability in tropical forest leaf area density from multireturn lidar and modeling. *Journal of Geophysical Research: Biogeosciences*, 120(2):294–309, 2015.

M. Detto, S. J. Wright, O. Calderón, and H. C. Muller-Landau. Resource acquisition and reproductive strategies of tropical forest in response to the El Niño–Southern Oscillation. *Nature Communications*, 9(1):913, 2018.

C. A. Deutsch, J. J. Tewksbury, M. Tigchelaar, D. S. Battisti, S. C. Merrill, R. B. Huey, and R. L. Naylor. Increase in crop losses to insect pests in a warming climate. *Science*, 361 (6405):916–919, 2018.

R. C. Dewar, L. Tarvainen, K. Parker, G. Wallin, and R. E. McMurtrie. Why does leaf nitrogen decline within tree canopies less rapidly than light? An explanation from optimization subject to a lower bound on leaf mass per area. *Tree Physiology*, 32(5):520–534, 2012.

C. E. Doughty, P. E. Santos-Andrade, A. Shenkin, G. R. Goldsmith, L. P. Bentley, B. Blonder, S. Díaz, N. Salinas, B. J. Enquist, R. E. Martin, and others. Tropical forest leaves may darken in response to climate change. *Nature Ecology & Evolution*, 2(12):1918–1924, 2018.

B. G. Drake, M. A. Gonzàlez-Meler, and S. P. Long. More efficient plants: a consequence of rising atmospheric CO_2? *Annual Review of Plant Physiology and Plant Molecular Biology*, 48(1):609–639, 1997.

R. A. Duursma and D. S. Falster. Leaf mass per area, not total leaf area, drives differences in above-ground biomass distribution among woody plant functional types. *New Phytologist*, 2016.

B. Efron and G. Gong. A Leisurely Look at the Bootstrap, the Jackknife, and Cross-Validation. *The American Statistician*, 37(1):36–48, 1983.

B. Efron and R. J. Tibshirani. *An introduction to the bootstrap*. CRC press, 1994.

D. S. Ellsworth and P. B. Reich. Canopy structure and vertical patterns of photosynthesis and related leaf traits in a deciduous forest. *Oecologia*, 96(2):169–178, 1993.

J. R. Evans and H. Poorter. Photosynthetic acclimation of plants to growth irradiance: the relative importance of specific leaf area and nitrogen partitioning in maximizing carbon gain. *Plant, Cell and Environment*, 24(8):755–767, 2001.

M. R. Evans. Modelling ecological systems in a changing world. *Philosophical Transactions of the Royal Society B: Biological Sciences*, 367(1586):181–190, 2012.

B. Faybishenko, S. Paton, T. Powell, R. Knox, G. Pastorello, C. Varadharajan, D. Christianson, and D. Agarwal. QA/QC-ed BCI meteorological drivers. Next-Generation Ecosystem Experiments Tropics; STRI; LBNL, 2018.

K. J. Feeley, S. J. Davies, P. S. Ashton, S. Bunyavejchewin, M. N. Supardi, A. R. Kassim, S. Tan, and J. Chave. The role of gap phase processes in the biomass dynamics of tropical forests. *Proceedings of the Royal Society of London B: Biological Sciences*, 274(1627): 2857–2864, 2007.

R. Fisher, N. McDowell, D. Purves, P. Moorcroft, S. Sitch, P. Cox, C. Huntingford, P. Meir, and F. Ian Woodward. Assessing uncertainties in a second-generation dynamic vegetation model caused by ecological scale limitations. *New Phytologist*, 187(3):666–681, 2010.

R. A. Fisher, S. Muszala, M. Verteinstein, P. Lawrence, C. Xu, N. G. McDowell, R. G. Knox, C. Koven, J. Holm, B. M. Rogers, D. Lawrence, and G. Bonan. Taking off the training wheels: the properties of a dynamic vegetation model without climate envelopes. *Geoscientific Model Development Discussions*, 8(4):3293–3357, 2015.

R. A. Fisher, C. D. Koven, W. R. Anderegg, B. O. Christoffersen, M. C. Dietze, C. E. Farrior, J. A. Holm, G. C. Hurtt, R. G. Knox, P. J. Lawrence, and others. Vegetation demographics in Earth System Models: A review of progress and priorities. *Global Change Biology*, 24(1):35–54, 2018.

P. Friedlingstein, M. Meinshausen, V. K. Arora, C. D. Jones, A. Anav, S. K. Liddicoat, and R. Knutti. Uncertainties in CMIP5 Climate Projections due to Carbon Cycle Feedbacks. *Journal of Climate*, 27(2):511–526, 2014.

N. M. Fyllas, S. Patiño, T. R. Baker, G. Bielefeld Nardoto, L. A. Martinelli, C. A. Quesada, R. Paiva, M. Schwarz, V. Horna, L. M. Mercado, and others. Basin-wide variations in foliar properties of Amazonian forest: phylogeny, soils and climate. *Biogeosciences*, 6: 2677–2708, 2009.

J. E. Hansen, M. Sato, A. Lacis, R. Ruedy, I. Tegen, and E. Matthews. Climate forcings in the Industrial era. *Proceedings of the National Academy of Sciences of the United States of America*, 95(22):12753–12758, 1998.

T. Hickler, B. Smith, I. C. Prentice, K. Mjöfors, P. Miller, A. Arneth, and M. T. Sykes. CO_2 fertilization in temperate FACE experiments not representative of boreal and tropical forests. *Global Change Biology*, 14(7):1531–1542, 2008.

S. P. Hubbell, R. B. Foster, S. T. O'Brien, K. E. Harms, R. Condit, B. Wechsler, S. J. Wright, and S. L. De Lao. Light-gap disturbances, recruitment limitation, and tree diversity in a neotropical forest. *Science*, 283(5401):554–557, 1999.

B. A. Hungate, J. S. Dukes, M. R. Shaw, Y. Luo, and C. B. Field. Nitrogen and climate change. *Science*, 302:1512–1513, 2003.

E. C. Hunke and W. H. Lipscomb. CICE: the Los Alamos Sea Ice Model Documentation and Software User's Manual Version 4.1 LA-CC-06-012. pages 1–76, 2010.

A. Ishida and T. Toma. Leaf gas exchange and cholorphyll fluorescence in relation to leaf angle, azimuth, and canopy position in the tropical pioneer tree, Macaranga conifera. *Tree Physiology*, 19(2):117–124, 1999.

S. Ishizaki, K. Hikosaka, and T. Hirose. Increase in leaf mass per area benefits plant growth at elevated CO_2 concentration. *Annals of Botany*, 91(7):905–914, 2003.

J. Kattge and W. Knorr. Temperature acclimation in a biochemical model of photosynthesis: a reanalysis of data from 36 species. *Plant, Cell and Environment*, 30(9):1176–1190, 2007.

J. Kattge, W. Knorr, T. Raddatz, and C. Wirth. Quantifying photosynthetic capacity and its relationship to leaf nitrogen content for global-scale terrestrial biosphere models. *Global Change Biology*, 15(4):976–991, 2009.

J. Kattge, S. Diaz, S. Lavorel, I. C. Prentice, P. Leadley, G. Bonisch, E. Garnier, M. Westoby, P. B. Reich, I. J. Wright, J. H. C. Cornelissen, C. Violle, S. P. Harrison, P. M. Van Bodegom, M. Reichstein, B. J. Enquist, N. A. Soudzilovskaia, et al. TRY–a global database of plant traits. *Global Change Biology*, 17:2905–2935, 2011.

C. Körner and J. A. Arnone. Responses to elevated carbon dioxide in artificial tropical ecosystems. *Science*, 257(5077):1672–1675, 1992.

C. Körner, M. Diemer, B. Schäppi, P. Niklaus, and J. Arnone. The responses of alpine grassland to four seasons of CO_2 enrichment: a synthesis. *Acta Oecologica*, 18(3):165–175, 1997.

C. D. Koven, D. M. Lawrence, and W. J. Riley. Permafrost carbon-climate feedback is sensitive to deep soil carbon decomposability but not deep soil nitrogen dynamics. *Proceedings of the National Academy of Sciences of the United States of America*, 112(12):3752–3757, 2015.

C. D. Koven et al. Benchmarking and Parameter Sensitivity of Predictions of Ecophysiological and Vegetation Dynamics using the Functionally Assembled Terrestrial Ecosystem Simulator (FATES) at Barro Colorado Island, Panama. *Unpublished*.

M. Kovenock and A. L. S. Swann. Leaf Trait Acclimation Amplifies Simulated Climate Warming in Response to Elevated Carbon Dioxide. *Global Biogeochemical Cycles*, 32, Oct. 2018.

D. Lawrence, R. A. Fisher, C. D. Koven, K. W. Oleson, S. C. Swenson, M. Vertenstein, B. Andre, G. B. Bonan, B. Ghimire, L. van Kampenhout, D. Kennedy, E. Kluzek, R. G. Knox, P. Lawrence, F. Li, H. Li, D. L. Lombardozzi, Y. Lu, J. Perket, W. J. Riley, W. Sacks, M. Shi, W. R. Wieder, and C. Xu. Technical Description of version 5.0 of the Community Land Model (CLM). 2018.

C. Le Quéré, R. M. Andrew, J. G. Canadell, S. Sitch, J. I. Korsbakken, G. P. Peters, A. C. Manning, T. A. Boden, P. P. Tans, R. A. Houghton, R. F. Keeling, S. Alin, O. D. Andrews, P. Anthoni, L. Barbero, L. Bopp, F. Chevallier, L. P. Chini, P. Ciais, K. Currie, C. Delire, S. C. Doney, P. Friedlingstein, T. Gkritzalis, I. Harris, J. Hauck, V. Haverd, M. Hoppema, K. Klein Goldewijk, A. K. Jain, E. Kato, A. Körtzinger, P. Landschützer, N. Lefèvre, A. Lenton, S. Lienert, D. Lombardozzi, J. R. Melton, N. Metzl, F. Millero, P. M. S. Monteiro, D. R. Munro, J. E. M. S. Nabel, S.-i. Nakaoka, K. O amp apos Brien, A. Olsen, A. M. Omar, T. Ono, D. Pierrot, B. Poulter, C. Rödenbeck, J. Salisbury, U. Schuster,

J. Schwinger, R. Séférian, I. Skjelvan, B. D. Stocker, A. J. Sutton, T. Takahashi, H. Tian, B. Tilbrook, I. T. van der Laan-Luijkx, G. R. van der Werf, N. Viovy, A. P. Walker, A. J. Wiltshire, and S. Zaehle. Global Carbon Budget 2016. *Earth System Science Data*, 8(2): 605–649, 2016.

A. D. Leakey, K. A. Bishop, and E. A. Ainsworth. A multi-biome gap in understanding of crop and ecosystem responses to elevated CO_2. *Current Opinion in Plant Biology*, 15(3): 228–236, 2012a.

A. D. B. Leakey, E. A. Ainsworth, C. J. Bernacchi, X. Zhu, S. P. Long, and D. R. Ort. Photosynthesis in a CO_2-Rich Atmosphere. In *Photosynthesis in silico*, pages 733–768. Springer Netherlands, Dordrecht, 2012b.

N. M. Levine, K. Zhang, M. Longo, A. Baccini, O. L. Phillips, S. L. Lewis, E. Alvarez-Dávila, A. C. Segalin de Andrade, R. J. W. Brienen, T. L. Erwin, T. R. Feldpausch, A. L. Monteagudo Mendoza, P. Nuñez Vargas, A. Prieto, J. E. Silva-Espejo, Y. Malhi, and P. R. Moorcroft. Ecosystem heterogeneity determines the ecological resilience of the Amazon to climate change. *Proceedings of the National Academy of Sciences of the United States of America*, 113(3):793–797, 2016.

J. Lloyd and G. D. Farquhar. Effects of rising temperatures and [CO_2] on the physiology of tropical forest trees. *Philosophical Transactions of the Royal Society B: Biological Sciences*, 363(1498):1811–1817, 2008.

J. Lloyd, S. Patiño, R. Q. Paiva, C. A. N. Quesada, G. B. Nardoto, A. J. B. Santos, T. R. Baker, W. A. Brand, I. Hilke, H. Gielmann, M. Raessler, F. J. Luizao, L. A. Martinelli, and L. M. Mercado. Optimisation of photosynthetic carbon gain and within-canopy gradients of associated foliar traits for Amazon forest trees. *Biogeosciences*, 7(6):1833–1859, 2010.

D. L. Lombardozzi, G. B. Bonan, N. G. Smith, J. S. Dukes, and R. A. Fisher. Temperature

acclimation of photosynthesis and respiration: A key uncertainty in the carbon cycle-climate feedback. *Geophysical Research Letters*, 42(20):8624–8631, 2015.

C. E. Lovelock, K. Winter, R. Mersits, and M. Popp. Responses of communities of tropical tree species to elevated CO_2 in a forest clearing. *Oecologia*, 116(1-2):207–218, 1998.

N. S. Lovenduski and G. B. Bonan. Reducing uncertainty in projections of terrestrial carbon uptake. *Environmental Research Letters*, 12(4):044020, 2017.

Y. Luo, C. B. Field, and H. A. Mooney. Predicting responses of photosynthesis and root fraction to elevated $[CO_2]_a$: interactions among carbon, nitrogen, and growth. *Plant, Cell and Environment*, 17(11):1195–1204, 1994.

Y. Luo, B. Su, W. S. Currie, J. S. Dukes, A. C. Finzi, U. Hartwig, B. Hungate, R. E. McMurtrie, R. Oren, W. J. Parton, D. E. Pataki, M. R. Shaw, D. R. Zak, and C. B. Field. Progressive nitrogen limitation of ecosystem responses to rising atmospheric carbon dioxide. *BioScience*, 54(8):731–739, 2004.

Y. Luo, D. Hui, and D. Zhang. Elevated CO_2 stimulates net accumulations of carbon and nitrogen in land ecosystems: A meta-analysis. *Ecology*, 87(1):53–63, 2006.

C. H. Lusk, P. B. Reich, R. A. Montgomery, D. D. Ackerly, and J. Cavender-Bares. Why are evergreen leaves so contrary about shade? *Trends in Ecology & Evolution*, 23(6):299–303, 2008.

N. Mahowald, F. Lo, Y. Zheng, L. Harrison, C. Funk, D. Lombardozzi, and C. Goodale. Projections of leaf area index in earth system models. *Earth System Dynamics*, 7(1): 211–229, 2016.

R. E. McMurtrie, R. J. Norby, B. E. Medlyn, R. C. Dewar, D. A. Pepper, P. B. Reich, and C. V. Barton. Why is plant-growth response to elevated CO_2 amplified when water is limiting, but reduced when nitrogen is limiting? A growth-optimisation hypothesis. *Functional Plant Biology*, 35(6):521–534, 2008.

V. Meakem, A. J. Tepley, E. B. Gonzalez-Akre, V. Herrmann, H. C. Muller-Landau, S. J. Wright, S. P. Hubbell, R. Condit, and K. J. Anderson-Teixeira. Role of tree size in moist tropical forest carbon cycling and water deficit responses. *New Phytologist*, 219:947–958, 2018.

B. E. Medlyn, F. W. Badeck, D. De Pury, C. Barton, M. Broadmeadow, R. Ceulemans, P. De Angelis, M. Forstreuter, M. E. Jach, S. Kellomaki, E. Laitat, M. Marek, S. Philippot, A. Rey, J. Strassemeyer, K. Laitinen, R. Liozon, B. Portier, P. Roberntz, K. Wang, and P. G. Jarvis. Effects of elevated [CO_2] on photosynthesis in European forest species: a meta-analysis of model parameters. *Plant, Cell and Environment*, 22:1475–1495, 1999.

B. E. Medlyn, R. A. Duursma, D. Eamus, D. S. Ellsworth, I. C. Prentice, C. V. M. Barton, K. Y. Crous, P. De Angelis, M. Freeman, and L. Wingate. Reconciling the optimal and empirical approaches to modelling stomatal conductance. *Global Change Biology*, 17(6): 2134–2144, 2011.

B. E. Medlyn, S. Zaehle, M. G. De Kauwe, A. P. Walker, M. C. Dietze, P. J. Hanson, T. Hickler, A. K. Jain, Y. Luo, W. Parton, I. C. Prentice, P. E. Thornton, S. Wang, Y.-P. Wang, E. Weng, C. M. Iversen, H. R. McCarthy, J. M. Warren, R. Oren, and R. J. Norby. Using ecosystem experiments to improve vegetation models. *Nature Climate Change*, 5 (6):528–534, 2015.

J. Meyerholt and S. Zaehle. The role of stoichiometric flexibility in modelling forest ecosystem responses to nitrogen fertilization. *New Phytologist*, 208:1042–1055, 2015.

P. R. Moorcroft. How close are we to a predictive science of the biosphere? *Trends in Ecology & Evolution*, 21(7):400–407, 2006.

P. R. Moorcroft, G. C. Hurtt, and S. W. Pacala. A method for scaling vegetation dynamics: the ecosystem demography model (ED). *Ecological monographs*, 71:557–586, 2001.

G. Myhre, E. J. Highwood, K. P. Shine, and F. Stordal. New estimates of radiative forcing due to well mixed greenhouse gases. *Geophysical Research Letters*, 25(14):2715–2718, 1998.

R. B. Neale, C.-C. Chen, A. Gettelman, P. H. Lauritzen, S. Park, D. L. Williamson, and Coauthors. Description of the NCAR Community Atmosphere Model (CAM 5.0). NCAR Technical Note. NCAR/TN-486+STR. pages 1–289, 2012.

Ü. Niinemets. Global-scale climatic controls of leaf dry mass per area, density, and thickness in trees and shrubs. *Ecology*, 82(2):453–469, 2001.

Ü. Niinemets, T. F. Keenan, and L. Hallik. A worldwide analysis of within-canopy variations in leaf structural, chemical and physiological traits across plant functional types. *New phytologist*, 205(3):973–993, 2015.

NOAA Earth System Research Laboratory. Atmospheric Carbon Dioxide at Mauna Loa Observatory (1958-2019), 2018.

R. J. Norby, M. F. Cotrufo, P. Ineson, E. G. O'Neill, and J. G. Canadell. Elevated CO_2, litter chemistry, and decomposition: a synthesis. *Oecologia*, 127(2):153–165, 2001.

R. J. Norby, J. D. Sholtis, C. A. Gunderson, and S. S. Jawdy. Leaf dynamics of a deciduous forest canopy: no response to elevated CO_2. *Oecologia*, 136(4):574–584, 2003.

R. J. Norby, J. M. Warren, C. M. Iversen, B. E. Medlyn, and R. E. McMurtrie. CO_2 enhancement of forest productivity constrained by limited nitrogen availability. *Proceedings of the National Academy of Sciences of the United States of America*, 107(45):19368–19373, 2010.

R. J. Norby, M. G. De Kauwe, and T. F. Domingues. Model–data synthesis for the next generation of forest free-air CO_2 enrichment (FACE) experiments. *New Phytologist*, 209 (1):17–28, 2016.

R. J. Norby, L. Gu, I. C. Haworth, A. M. Jensen, B. L. Turner, A. P. Walker, J. M. Warren, D. J. Weston, C. Xu, and K. Winter. Informing models through empirical relationships

between foliar phosphorus, nitrogen and photosynthesis across diverse woody species in tropical forests of Panama. *New Phytologist*, 215(4):1425–1437, 2017.

K. W. Oleson, D. M. Lawrence, G. B. Bonan, B. Drewniak, M. Huang, C. D. Koven, S. Levis, F. Li, W. J. Riley, Z. M. Subin, S. C. Swenson, and P. E. Thornton. Technical Description of the version 4.5 of the Community Land Model (CLM). NCAR Technical Note. NCAR/TN-503+STR. 2013.

S. V. Ollinger. Sources of variability in canopy reflectance and the convergent properties of plants. *New Phytologist*, 189(2):375–394, 2011.

A. Patton. Automatic Block Length Selection Procedure, 2007.

A. Patton, D. N. Politis, and H. White. Correction to "Automatic block-length selection for the dependent bootstrap" by D. Politis and H. White. *Econometric Reviews*, 2009.

R. Pavlick, D. T. Drewry, K. Bohn, B. Reu, and A. Kleidon. The Jena Diversity-Dynamic Global Vegetation Model (JeDi-DGVM): a diverse approach to representing terrestrial biogeography and biogeochemistry based on plant functional trade-offs. *Biogeosciences*, 10(6):4137–4177, 2013.

A. G. Peterson, J. T. Ball, Y. Luo, C. B. Field, P. S. Curtis, K. L. Griffin, C. A. Gunderson, R. J. Norby, D. T. Tissue, M. Forstreuter, and others. Quantifying the response of photosynthesis to changes in leaf nitrogen content and leaf mass per area in plants grown under atmospheric CO_2 enrichment. *Plant, Cell and Environment*, 22(9):1109–1119, 1999.

D. N. Politis and J. P. Romano. The Stationary Bootstrap. *Journal of the American Statistical Association*, 89(428):1303–1313, 1994.

D. N. Politis and H. White. Automatic Block-Length Selection for the Dependent Bootstrap. *Econometric Reviews*, 23(1):53–70, 2004.

J. Pongratz, C. H. Reick, T. Raddatz, and M. Claussen. Biogeophysical versus biogeochemical climate response to historical anthropogenic land cover change. *Geophysical Research Letters*, 37:L08702, 2010.

H. Poorter, Y. v. Berkel, R. Baxter, J. d. Hertog, P. Dijkstra, R. M. Gifford, K. L. Griffin, C. Roumet, J. Roy, and S. C. Wong. The effect of elevated CO_2 on the chemical composition and construction costs of leaves of 27 C_3 species. *Plant, Cell and Environment*, 20 (4):472–482, 1997.

H. Poorter, Ü. Niinemets, L. Poorter, I. J. Wright, and R. Villar. Causes and consequences of variation in leaf mass per area (LMA): a meta-analysis. *New Phytologist*, 182:565–588, 2009.

L. Poorter, S. F. Oberbauer, and D. B. Clark. Leaf optical properties along a vertical gradient in a tropical rain forest canopy in Costa Rica. *American Journal of Botany*, 82 (10):1257–1263, 1995.

I. C. Prentice, N. Dong, S. M. Gleason, V. Maire, and I. J. Wright. Balancing the costs of carbon gain and water transport: testing a new theoretical framework for plant functional ecology. *Ecology Letters*, 17(1):82–91, 2014.

S. H. Pritchard, H. O. Rogers, S. A. Prior, and C. M. Peterson. Elevated CO_2 and plant structure: a review. *Global Change Biology*, 5(7):807–837, 1999.

B. Pu and R. E. Dickinson. Examining vegetation feedbacks on global warming in the Community Earth System Model. *Journal of Geophysical Research*, 117:D20110, 2012.

D. Purves and S. Pacala. Predictive models of forest dynamics. *Science*, 320(5882):1452–1453, 2008.

D. W. Purves, J. W. Lichstein, N. Strigul, and S. W. Pacala. Predicting and understanding forest dynamics using a simple tractable model. *Proceedings of the National Academy of Sciences of the United States of America*, 105(44):17018–17022, 2008.

E. M. Quilis. Bootstrapping Time Series. Version 1.0., 2015.

E. G. Reekie and F. A. Bazzaz. Competition and patterns of resource use among seedlings of five tropical trees grown at ambient and elevated CO_2. *Oecologia*, 79(2):212–222, 1989.

P. B. Reich, D. S. Ellsworth, and M. B. Walters. Leaf Structure (Specific Leaf Area) Modulates Photosynthesis-Nitrogen Relations: Evidence from within and Across Species and Functional Groups. *Functional Ecology*, 12(6):948–958, 1998.

P. B. Reich, M. G. Tjoelker, K. S. Pregitzer, I. J. Wright, J. Oleksyn, and J.-L. Machado. Scaling of respiration to nitrogen in leaves, stems and roots of higher land plants. *Ecology Letters*, 11(8):793–801, 2008.

P. B. Reich, R. L. Rich, X. Lu, Y.-P. Wang, and J. Oleksyn. Biogeographic variation in evergreen conifer needle longevity and impacts on boreal forest carbon cycle projections. *Proceedings of the National Academy of Sciences of the United States of America*, 111(38): 13703–13708, 2014.

M. Reichstein, M. Bahn, M. D. Mahecha, J. Kattge, and D. D. Baldocchi. Linking plant and ecosystem functional biogeography. *Proceedings of the National Academy of Sciences of the United States of America*, 111(38):13697–13702, 2014.

A. Rogers, B. E. Medlyn, J. S. Dukes, G. Bonan, S. von Caemmerer, M. C. Dietze, J. Kattge, A. D. B. Leakey, L. M. Mercado, Ü. Niinemets, I. C. Prentice, S. P. Serbin, S. Sitch, D. A. Way, and S. Zaehle. A roadmap for improving the representation of photosynthesis in Earth system models. *New phytologist*, 213(1):22–42, 2017.

C. Roumet, G. Laurent, and J. Roy. Leaf structure and chemical composition as affected by elevated CO_2: genotypic responses of two perennial grasses. *New Phytologist*, 143(1): 73–81, 1999.

S. E. Said and D. A. Dickey. Testing for Unit Roots in Autoregressive-Moving Average Models of Unknown Order. *Biometrika*, 71(3):599–607, 1984.

S. Scheiter, L. Langan, and S. I. Higgins. Next-generation dynamic global vegetation models: learning from community ecology. *New Phytologist*, 198(3):957–969, 2013.

D. Schimel, B. B. Stephens, and J. B. Fisher. Effect of increasing CO_2 on the terrestrial carbon cycle. *Proceedings of the National Academy of Sciences of the United States of America*, 112(2):436–441, 2015.

P. J. Sellers, L. Bounoua, G. J. Collatz, D. A. Randall, D. A. Dazlich, S. O. Los, J. A. Berry, I. Fung, C. J. Tucker, C. B. Field, and T. G. Jensen. Comparison of radiative and physiological effects of doubled atmospheric CO_2 on climate. *Science*, 271(5254): 1402–1406, 1996.

N. G. Smith and J. S. Dukes. Plant respiration and photosynthesis in global-scale models: incorporating acclimation to temperature and CO_2. *Global Change Biology*, 19(1):45–63, 2013.

N. G. Smith, D. Lombardozzi, A. Tawfik, G. Bonan, and J. S. Dukes. Biophysical consequences of photosynthetic temperature acclimation for climate. *Journal of Advances in Modeling Earth Systems*, 2017.

N. G. Smith, T. F. Keenan, I. Colin Prentice, H. Wang, I. J. Wright, Ü. Niinemets, K. Y. Crous, T. F. Domingues, R. Guerrieri, F. Yoko Ishida, and others. Global photosynthetic capacity is optimized to the environment. *Ecology Letters*, 22(3):506–517, 2019.

R. P. Souza and I. F. Válio. Leaf optical properties as affected by shade in saplings of six tropical tree species differing in successional status. *Brazilian Journal of Plant Physiology*, 15(1):49–54, 2003.

F. Sterck, L. Markesteijn, F. Schieving, and L. Poorter. Functional traits determine trade-offs and niches in a tropical forest community. *Proceedings of the National Academy of Sciences of the United States of America*, 108(51):20627–20632, 2011.

M. Stitt and A. Krapp. The interaction between elevated carbon dioxide and nitrogen nutrition: the physiological and molecular background. *Plant, Cell and Environment*, 22 (6):583–621, 1999.

B. R. Strain and F. A. Bazzaz. Terrestrial plant communities. In E. R. Lemon, editor, *CO2 and plants*, pages 177–222. Am. Assoc. Adv. Sci., Symp.;(United States), Boulder, Colorado, 1983.

A. L. S. Swann, F. M. Hoffman, C. D. Koven, and J. T. Randerson. Plant responses to increasing CO_2 reduce estimates of climate impacts on drought severity. *Proceedings of the National Academy of Sciences of the United States of America*, 113(36):10019–10024, 2016.

G. Taylor, M. J. Tallis, C. P. Giardina, K. E. Percy, F. Miglietta, P. S. Gupta, B. Gioli, C. Calfapietra, B. Gielen, M. E. Kubiske, G. E. Scarascia-Mugnozza, K. Kets, S. P. Long, and D. F. Karnosky. Future atmospheric CO_2 leads to delayed autumnal senescence. *Global Change Biology*, 14(2):264–275, 2008.

P. E. Thornton and N. E. Zimmermann. An improved canopy integration scheme for a land surface model with prognostic canopy structure. *Journal of Climate*, 20(15):3902–3923, 2007.

K. Tully and D. Lawrence. Declines in leaf litter nitrogen linked to rising temperatures in a wet tropical forest. *Biotropica*, 42(5):526–530, 2010.

P. M. Van Bodegom, J. C. Douma, J. P. M. Witte, J. C. Ordoñez, R. P. Bartholomeus, and R. Aerts. Going beyond limitations of plant functional types when predicting global ecosystem-atmosphere fluxes: exploring the merits of traits-based approaches. *Global Ecology and Biogeography*, 21(6):625–636, 2012.

P. van der Sleen, P. Groenendijk, M. Vlam, N. P. R. Anten, A. Boom, F. Bongers, T. L.

Pons, G. Terburg, and P. A. Zuidema. No growth stimulation of tropical trees by 150 years of CO_2 fertilization but water-use efficiency increased. *Nature*, 8(1):24–28, 2015.

L. M. Verheijen, V. Brovkin, R. Aerts, G. Bonisch, J. H. C. Cornelissen, J. Kattge, P. B. Reich, I. J. Wright, and P. M. Van Bodegom. Impacts of trait variation through observed trait–climate relationships on performance of an Earth system model: a conceptual analysis. *Biogeosciences*, 10(8):5497–5515, 2013.

L. M. Verheijen, R. Aerts, V. Brovkin, J. Cavender-Bares, J. H. C. Cornelissen, J. Kattge, and P. M. van Bodegom. Inclusion of ecologically based trait variation in plant functional types reduces the projected land carbon sink in an earth system model. *Global Change Biology*, 21(8):3074–3086, 2015.

A. P. Walker, A. P. Beckerman, L. Gu, J. Kattge, L. A. Cernusak, T. F. Domingues, J. C. Scales, G. Wohlfahrt, S. D. Wullschleger, and F. I. Woodward. The relationship of leaf photosynthetic traits–Vcmax and Jmax–to leaf nitrogen, leaf phosphorus, and specific leaf area: a meta-analysis and modeling study. *Ecology and Evolution*, 4(16):3218–3235, 2014.

A. P. Walker, T. Quaife, P. M. van Bodegom, M. G. De Kauwe, T. F. Keenan, J. Joiner, M. R. Lomas, N. MacBean, C. Xu, X. Yang, and others. The impact of alternative trait-scaling hypotheses for the maximum photosynthetic carboxylation rate (Vcmax) on global gross primary production. *New Phytologist*, 215(4):1370–1386, 2017.

D. A. Way, R. Oren, and Y. Kroner. The space-time continuum: the effects of elevated CO_2 and temperature on trees and the importance of scaling. *Plant, Cell and Environment*, 38 (6):991–1007, 2015.

Z. Wei, K. Yoshimura, L. Wang, D. G. Miralles, S. Jasechko, and X. Lee. Revisiting the contribution of transpiration to global terrestrial evapotranspiration. *Geophysical Research Letters*, 44(6):2792–2801, 2017.

M. A. White, P. E. Thornton, S. W. Running, and R. R. Nemani. Parameterization and sensitivity analysis of the BIOME-BGC terrestrial ecosystem model: net primary production controls. *Earth Interactions*, 4(3):1–85, 2000.

W. R. Wieder, C. C. Cleveland, W. K. Smith, and K. Todd-Brown. Future productivity and carbon storage limited by terrestrial nutrient availability. *Nature*, 8(6):441–444, 2015.

K. Winter and C. E. Lovelock. Growth responses of seedlings of early and late successional tropical forest trees to elevated atmospheric CO_2. *Flora*, 194(2):221–227, 1999.

K. Winter, M. Garcia, C. E. Lovelock, R. Gottsberger, and M. Popp. Responses of model communities of two tropical tree species to elevated atmospheric CO_2: growth on unfertilized soil. *Flora*, 195(4):289–302, 2000.

K. Winter, M. Garcia, R. Gottsberger, and M. Popp. Marked growth response of communities of two tropical tree species to elevated CO_2 when soil nutrient limitation is removed. *Flora*, 196(1):47–58, 2001.

I. J. Wright, P. B. Reich, M. Westoby, D. D. Ackerly, Z. Baruch, F. Bongers, J. Cavender-Bares, T. Chapin, J. Cornelissen, M. Diemer, J. Flexas, E. Garnier, P. K. Groom, J. Gulias, K. Hikosaka, B. B. Lamont, T. Lee, W. Lee, C. Lusk, J. J. Midgley, M. L. Navas, Ü. Niinemets, J. Oleksyn, N. Osada, H. Poorter, P. Poot, L. Prior, V. I. Pyankov, C. Roumet, S. C. Thomas, M. G. Tjoelker, E. J. Veneklaas, and R. Villar. The worldwide leaf economics spectrum. *Nature*, 428(6985):821–827, 2004.

C. Xu, R. Fisher, S. D. Wullschleger, C. J. Wilson, M. Cai, and N. G. McDowell. Toward a mechanistic modeling of nitrogen limitation on vegetation dynamics. *PLoS ONE*, 7(5): e37914, 2012.

S. Zaehle and A. D. Friend. Carbon and nitrogen cycle dynamics in the O-CN land surface model: 1. Model description, site-scale evaluation, and sensitivity to parameter estimates. *Global Biogeochemical Cycles*, 24:GB1005, 2010.

S. Zaehle, B. E. Medlyn, M. G. De Kauwe, A. P. Walker, M. C. Dietze, T. Hickler, Y. Luo, Y.-P. Wang, B. El-Masri, P. Thornton, A. Jain, S. Wang, D. Wårlind, E. Weng, W. Parton, C. M. Iversen, A. Gallet-Budynek, H. McCarthy, A. Finzi, P. J. Hanson, I. C. Prentice, R. Oren, and R. J. Norby. Evaluation of 11 terrestrial carbon-nitrogen cycle models against observations from two temperate Free-Air CO_2 Enrichment studies. *New Phytologist*, 202 (3):803–822, 2014.

K. Zhang, J. S. Kimball, R. R. Nemani, S. W. Running, Y. Hong, J. J. Gourley, and Z. Yu. Vegetation Greening and Climate Change Promote Multidecadal Rises of Global Land Evapotranspiration. *Scientific Reports*, 5:15956, 2015.

B. Zhou and W. H. Wong. A Bootstrap-Based Non-Parametric Anova Method with Applications to Factorial Microarray Data. *Statistica Sinica*, 21(2):495–514, 2011.

Z. Zhu, S. Piao, R. B. Myneni, M. Huang, Z. Zeng, J. G. Canadell, P. Ciais, S. Sitch, P. Friedlingstein, A. Arneth, C. Cao, L. Cheng, E. Kato, C. Koven, Y. Li, X. Lian, Y. Liu, R. Liu, J. Mao, Y. Pan, S. Peng, J. Peñuelas, B. Poulter, T. A. M. Pugh, B. D. Stocker, N. Viovy, X. Wang, Y. Wang, Z. Xiao, H. Yang, S. Zaehle, and N. Zeng. Greening of the Earth and its drivers. *Nature Climate Change*, 2016.

Appendix A

SUPPORTING INFORMATION FOR CHAPTER 2

Marlies Kovenock[1] and Abigail L.S. Swann[2,1]

[1]Department of Biology, University of Washington, Seattle, WA; [2]Department of Atmospheric Sciences, University of Washington, Seattle, WA.

Supporting Information for:

Kovenock, M., and Swann, A. L. S. (2018). Leaf trait acclimation amplifies simulated climate warming in response to elevated carbon dioxide. *Global Biogeochemical Cycles, 32,* 1437-1448. https://doi.org/10.1029/2018GB005883

A.1 Materials and Methods

A.1.1 Nitrogen Cycle

As the default model's interactive nitrogen cycle breaks the relationship between transpiration fluxes and gross primary productivity [De Kauwe et al., 2013] we disabled it and represented nitrogen limitation with a fractional reduction in the rate of photosynthesis for each plant functional type following the methods of Koven et al. [2015].

A.1.2 CO_2 Acclimation of Leaf Mass per Area Estimation and Implementation

We estimated the plausible extent of leaf mass per area acclimation using Poorter et al. [2009]'s meta-analysis of approximately 200 studies of leaf mass per area response to CO_2 level. Specifically, we added the approximate interquartile range for the response of leaf mass per area to a doubling of CO_2 in all plants (no interquartile range for C_3 plants was reported) to the median response for C_3 plants. The resulting level of change, a one-third increase in leaf mass per area, was implemented by directly modifying the model parameter controlling leaf mass per area at the top of the canopy. This model parameter, SLA_o, represents specific leaf area (m^2 leaf area/g leaf carbon), the inverse of leaf mass per area. We therefore multiplied the SLA_o parameter for all C_3 plant types by 0.75 to implement a one-third increase in leaf mass per area.

As formulated by default, increasing leaf mass per area in this Earth system model raises area-based maximum photosynthetic rates (μmol/m^2/s) as follows:

$$V_{cmax25} = \frac{\alpha \cdot LMA}{CN_{leaf}} \tag{A.1}$$

where V_{cmax25} is the maximum rate of carboxylation at 25°C (μmol C/m^2/s), LMA is the leaf mass per area (gC/m^2 leaf area), CN_{leaf} is the leaf carbon-to-nitrogen ratio (gC/gN), and α accounts for the amount of nitrogen in Rubisco and the specific activity of Rubisco.

Other area-based maximum photosynthetic rate parameters (J_{max25}, T_{p25}) are calculated in proportion to V_{cmax25}. In all but one simulation (CCLMAPS), we maintained control levels of area-based maximum photosynthetic rates by increasing the parameter values for CN_{leaf} (leaf gC/gN) for each C_3 plant type by one third. This change encompasses both increases in CN_{leaf} and decreases in the fraction of nitrogen in Rubisco, which have been observed in response to elevated CO_2 in manipulation experiments [reviewed in Ainsworth and Long, 2005, Leakey et al., 2012b, Way et al., 2015]. Prior studies have identified trait-climate relationships in the literature that suggest that V_{cmax25} and J_{max25} decrease with CO_2 [Ainsworth and Rogers, 2007, Medlyn et al., 1999]. However, estimating an exact magnitude of acclimation remains challenging because empirical relationships conflate the physiological effects of CO_2, nitrogen limitation, and altered within-plant nitrogen allocation [Rogers et al., 2017, Smith and Dukes, 2013]. We chose here to make a conservative estimate that maximum photosynthetic rates stay constant as CO_2 increases. This approach is conservative as most estimates predict a decrease in maximum photosynthetic rates which would enhance the climate impacts of leaf mass per area acclimation by further reducing the increase in leaf area in response to elevated CO_2. The CCLMAPS simulation tested the sensitivity of climate impacts to a simultaneous one-third increase in maximum photosynthetic rates.

A.1.3 Temperature Acclimation of Leaf Mass per Area Estimation and Implementation

We estimated the potential extent of leaf mass per area acclimation to temperature using biome-specific acclimation relationships from Poorter et al. [2009]'s meta-analysis of 40 studies and the growing season temperature change due to doubling CO_2 (CC - CTRL; northern hemisphere JJA and southern hemisphere DJF) at each gridcell. We estimated the upper bound of leaf mass per area response to temperature by adding the interquartile range for all plant types reported by Poorter et al. [2009] to the biome-specific median response (biome-specific interquartile ranges were not reported). The magnitude of temperature acclimation was not sensitive to interannual variability in CC - CTRL growing season temperature.

We found that temperature could be an influential driver of leaf mass per area acclima-

tion in boreal and arctic biomes (Figure A.5a). This is because temperature acclimation occurs when leaves warm from growth-limiting cold temperatures to temperatures suitable for growth [Poorter et al., 2009]. The acclimation response declines to zero when warming begins from temperatures closer to those suitable for growth [Poorter et al., 2009]. Growing season temperatures below this threshold occur primarily in boreal and arctic biomes in our simulation. Using a threshold of at least 10% response we found that four plant functional types - boreal needleleaf evergreen and deciduous trees, boreal deciduous shrubs, and C_3 arctic grasses - cover 90% of the vegetated area that we estimate could be impacted by leaf mass per area acclimation to temperature (Figure A.5b).

To test the climate influence of temperature acclimation on our results, we use an experiment (TCCLMA) that includes a conservative estimate of the upper bound of leaf mass per area acclimation to both temperature and CO_2. The TCCLMA simulation is identical to CCLMA ($2xCO_2$; +1/3 leaf mass per area in C_3 plants) except that leaf mass per area of four plant functional types — boreal needleleaf evergreen and deciduous trees, boreal deciduous shrubs, and C_3 arctic grasses — were held at control (CTRL) levels. The corresponding average response of leaf mass per area acclimation to temperature alone was -15% for grid-cells with temperature acclimation. Combining the acclimation of leaf mass per area to CO_2 (+33%) with the decrease due to temperature acclimation (average value -15%) results in an average overall increase of +13%. We therefore conservatively left leaf mass per area values at control levels for these four plant types, representing an implied 25% decrease in leaf mass per area due to temperature.

This approach included a number of assumptions but offered the best estimate of leaf mass per area temperature acclimation influences on climate and carbon cycling given the options. It assumes that the temperature acclimation relationship reported by Poorter et al. [2009] holds at temperatures below 7°C, despite lack of data below this point; that as shown by Poorter et al. [2009] (Figure 5j) there is no response above 18°C; and, based on the underlying mechanisms of temperature limiting leaf expansion and sink growth [Poorter et al., 2009], that growing season rather than annual mean temperature is the driver. It also

assumes that temperature and CO_2 acclimation are additive (no interaction effect).

A.1.4 Statistical Analysis

Several variables had time series that were non-normally distributed and temporally autocorrelated. We therefore used stationary bootstrap methods [Politis and Romano, 1994, Quilis, 2015] with n = 50,000 to test for differences. The optimal block length for each stationary bootstrap was determined by automatic estimation [Patton, 2007, Patton et al., 2009, Politis and White, 2004]. Time series that failed the Augmented Dickey-Fuller test for stationarity [Said and Dickey, 1984, and Matlab version 2015b *adftest* function] were detrended prior to bootstrap analysis. Differences were considered significant at the 95% level using the percentile method [Efron and Gong, 1983, Efron and Tibshirani, 1994]. Confidence intervals for average annual means and differences were constructed from their bootstrap distributions. T-test and Non-parametric Analysis of Variance [Zhou and Wong, 2011, modified to use stationary bootstrap] analyses support the reported findings and conclusions.

We tested for spatial relationships between variables at the gridcell scale using simple, multiple, and stepwise linear regression methods on annual mean values (CCLMA - CC). Only continental land gridcells (no ocean or coast) that were a least 40% vegetated were included in the regression analysis. Results were not sensitive to the selected percentage vegetation. Relationships were considered significant at the 95% level.

A.2 Results

A.2.1 Temperature Acclimation of Leaf Mass per Area

Observations of leaf acclimation show that warming temperatures and rising CO_2 levels have opposing influences on leaf mass per area. As such, warming temperatures could be hypothesized to offset the influence of CO_2 on leaf mass per area and the resulting climate and carbon cycling impacts. However, temperature acclimation of leaf mass per area only occurs at low temperatures [Poorter et al., 2009] and is therefore limited to boreal and arctic

regions.

We quantified the influence of temperature acclimation on our CO_2 acclimation results using a simulation that represents the potential extent of leaf mass per area acclimation to both temperature and CO_2 (TCCLMA). Specifically, we compared the differences in the change from the climate change control between two leaf mass per area acclimation cases: leaf mass per area acclimation to CO_2 alone (CCLMA - CC) and leaf mass per area acclimation to both CO_2 and temperature (TCCLMA - CC).

We found that temperature acclimation of leaf mass per area did not significantly alter the additional warming beyond the climate change control induced by CO_2 acclimation of leaf mass per area. Physical warming was unaltered at the global and latitude band scales (TCCLMA - CC $\approx$ CCLMA - CC) because temperature acclimation of leaf mass per area did not significantly offset changes in evapotranspiration and solar radiation absorbed at the surface, despite slightly compensating for changes in leaf area index (Figure A.1). Furthermore, temperature acclimation offset only a small portion ($\sim$1 PgC/yr) of the net primary productivity change induced by CO_2 acclimation (TCCLMA - CC; -5.0 PgC/yr, $CI_{95\%}$ -4.7 to -5.3). Thus, our estimate of additional biogeochemical warming due to leaf mass per area acclimation was also similar (+0.1 to +0.9°C over 100 years for TCCLMA - CC compared to +0.1 to +1.0°C over 100 years for CCLMA - CC).

A.2.2 Historical Climate Sensitivity to Leaf Mass per Area Change

We found that the influence of historical leaf mass per area acclimation on climate is likely to be small. From the relationship reported by Poorter et al. [2009], we estimated that the largest potential extent of historical leaf mass per area change compared to the pre-industrial period (from 280ppm CO_2 to 355ppm) is +8%. We tested a much larger one-third increase in leaf mass per area for historical simulations at the control CO_2 concentration of 355ppm (LMA: 1xCO_2, +1/3 leaf mass per area). This experiment showed that a stronger than expected increase in leaf mass per area did not significantly alter historical temperature over land (LMA - CTRL; -0.1°C over land, $CI_{95\%}$ 0 to -0.2; -0.2°C globally, $CI_{95\%}$ -0.1 to

-0.2).

The effect of leaf mass per area change in the historical period is limited for two reasons. First, the decrease in leaf area in response to a one-third increase in leaf mass per area was smaller at historical CO_2 (LMA - CTRL: -0.67 m^2/m^2, $CI_{95\%}$ -0.65 to 0.69) than at future CO_2 (CCLMA - CTRL). This smaller change in leaf area when beginning from low initial leaf area is consistent with our findings under future CO_2 conditions (see main text Results, Figure A.2). The small change in leaf area at historical CO_2 levels muted the decrease in evapotranspiration (LMA - CTRL: -0.6 W/m^2, $CI_{95\%}$ -0.4 to -0.8) compared to the change at future CO_2 levels (CCLMA - CC). Second, the change in solar radiation absorbed at the surface was reduced in the historical simulations (LMA - CTRL; -0.3 W/m^2, $CI_{95\%}$ -0.1 to -0.6) compared to future simulations (CCLMA - CC), as reduced leaf area increased albedo (as measured by a change in clear-sky shortwave radiation absorbed at the surface of -0.2 W/m^2, $CI_{95\%}$ -0.1 to -0.4). Overall, the small decrease in solar radiation absorbed at the surface and small increase in evapotranspiration resulted in a near zero change in temperature.

Historical net primary productivity was significantly decreased in response to the one-third leaf mass per area increase (-6.9 PgC/yr, $CI_{95\%}$ -6.6 to -7.2). However, this value likely overestimates the decrease in productivity by a factor of four, as the predicted 8% increase in leaf mass per area for historical climate change is approximately one fourth of the experimental change of 33%. We therefore suggest that -2 PgC/yr is a more reasonable ballpark estimate for the sensitivity of simulated productivity to leaf mass per area change at historical CO_2. We also note that while the LMA experiment (355ppm CO_2, +1/3 leaf mass per area) is useful for testing the model sensitivity to changes in leaf mass per area at a historical CO_2 concentration, we do not expect leaf mass per area to differ from the control values at 355ppm because these values are based on observations of leaf mass per area during the present day [White et al., 2000].

A.2.3 Acclimation Altered Balance between Biogeophysical and Biogeochemical Warming

Leaf mass per area represents the conversion factor between carbon available for leaf growth and leaf area. Thus increasing leaf mass per area in response to rising CO_2 alters the balance between biogeophysical and biogeochemical warming by altering the total leaf area displayed for a given amount of productivity. Plants could overcome this reduced leaf area by increasing maximum photosynthetic rates. We quantified the approximate increase in maximum photosynthetic rates and productivity required to offset the biogeophysical warming induced by leaf acclimation to CO_2 using a simulation that simultaneously increased area-based maximum photosynthetic rates (V_{cmax25}, J_{max25}, T_{p25},) and leaf mass per area by one third (CCLMAPS) compared to the control climate change simulation (CC).

The greater photosynthetic capacity increased global net primary productivity by +9 PgC/yr ($CI_{95\%}$ 8 to 9) compared to the control climate change simulation (CCLMAPS - CC) and +14 PgC/yr ($CI_{95\%}$ 14 to 15) compared to the leaf acclimation simulation (CCLMAPS - CCLMA). This large increase in productivity mitigated approximately half of the decline in global leaf area index incurred due to leaf mass per area acclimation (leaf area index decreased by -14% in CCLMAPS - CC compared to -26% in CCLMA - CC). While leaf area decline was not fully compensated for by increasing photosynthetic rates, total evapotranspiration was no longer significantly reduced compared to the control climate change simulation (CCLMAPS - CC). Transpiration remained unchanged and decreased evaporation from leaf surfaces (CCLMAPS - CC; -0.4 W/m^2, $CI_{95\%}$ -0.4 to -0.5) was compensated for by an increase in evaporation from the soil (+0.4 W/m^2, $CI_{95\%}$ +0.2 to +0.5). The albedo of the land surface increased slightly globally (-0.3 W/m^2, $CI_{95\%}$ -0.1 to -0.4) compared to the climate change control consistent with the change in leaf area but did not significantly alter the amount of solar radiation absorbed at the surface (-0.2 W/m^2, $CI_{95\%}$ -0.6 to +0.1). As a result, the biogeophysical warming of the land surface due to a one-third increase in leaf mass per area (CCLMA - CC) was mitigated by a proportional increase in maximum photosynthetic rates (CCLMAPS - CC; -0.1°C, $CI_{95\%}$ 0 to -0.2;). Thus, a large increase in

productivity above that estimated in our control climate change simulation offset the biogeophysical warming due to leaf acclimation. However, leaf mass per area acclimation altered the balance between productivity and biogeophysical land surface processes.

A.3 Figures and Tables

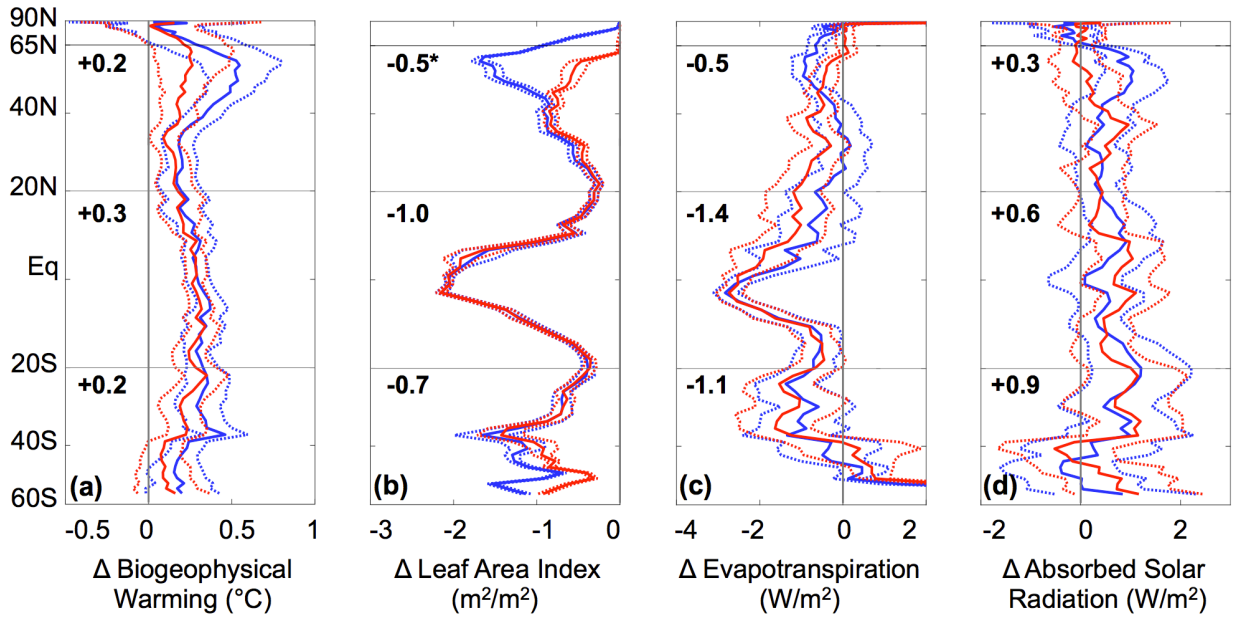

Figure A.1: Zonal annual mean change over land due to leaf mass per area acclimation to temperature and CO_2 (red, TCCLMA - CC) and leaf mass per area acclimation to CO_2 alone (blue, CCLMA - CC) of (a) biogeophysical warming (°C); (b) leaf area index (m^2/m^2); (c) evapotranspiration (W/m^2); and (d) net solar radiation absorbed at the surface (W/m^2). Mean differences are shown as solid lines, along with the 95% bootstrap confidence interval (dashed lines). Average zonal mean change on land due to leaf acclimation to temperature and CO_2 (bold numbers) for each latitude band (bounded by gray lines). Latitude band differences between (CCLMA - CC) and (TCCLMA - CC) significant at the 95% level indicated with asterisk ($*$).

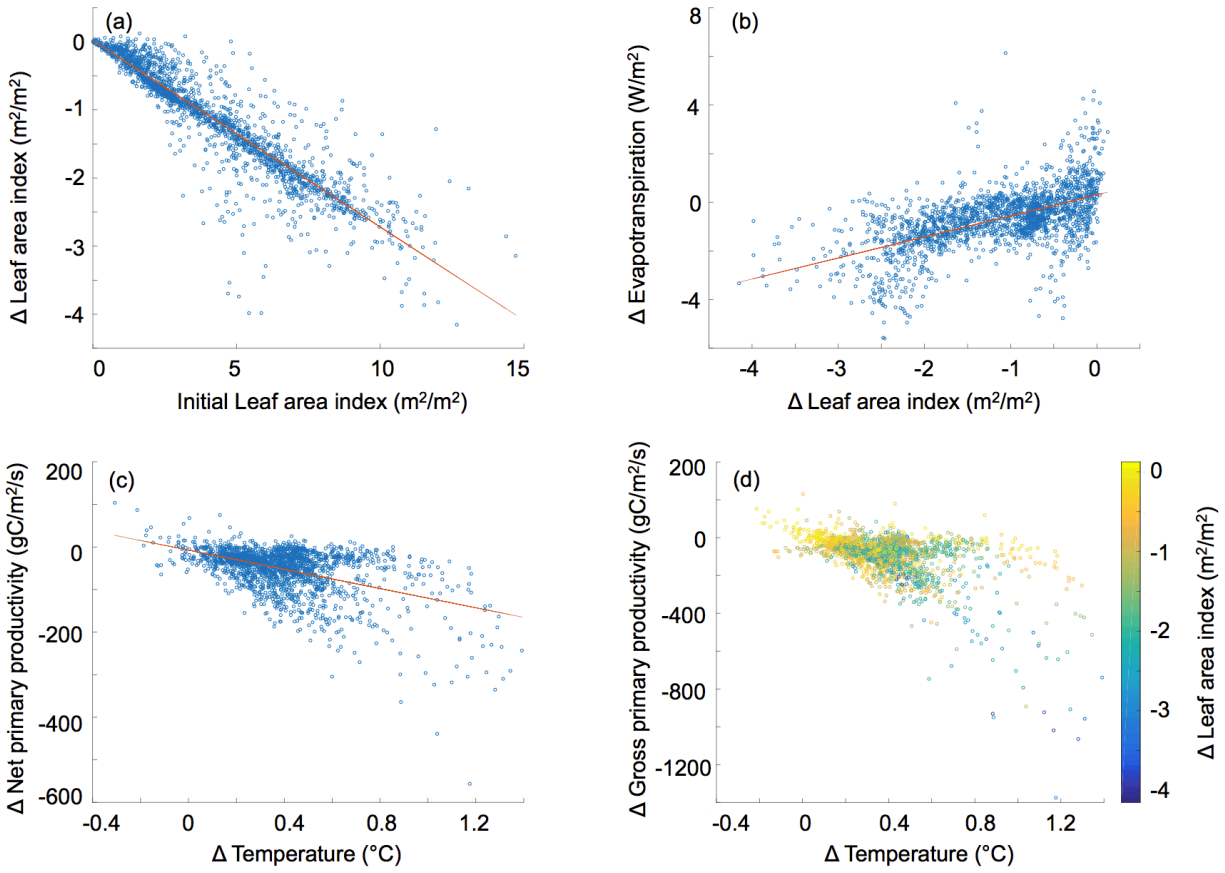

Figure A.2: Scatterplot of gridcell level (a) initial leaf area index (CC) and the change in leaf area in response to leaf acclimation to CO_2 (r = -0.91, R^2 = 0.83); (b) the changes in leaf area and evapotranspiration (r = 0.57, R^2 = 0.32); (c) the changes in temperature and net primary productivity (r = -0.49, R^2 = 0.24); and (d) the changes in temperature, leaf area index, and gross primary productivity (multiple regression R^2 = 0.32). Ordinary least squares regression lines plotted in red (a-c). All changes are CCLMA - CC.

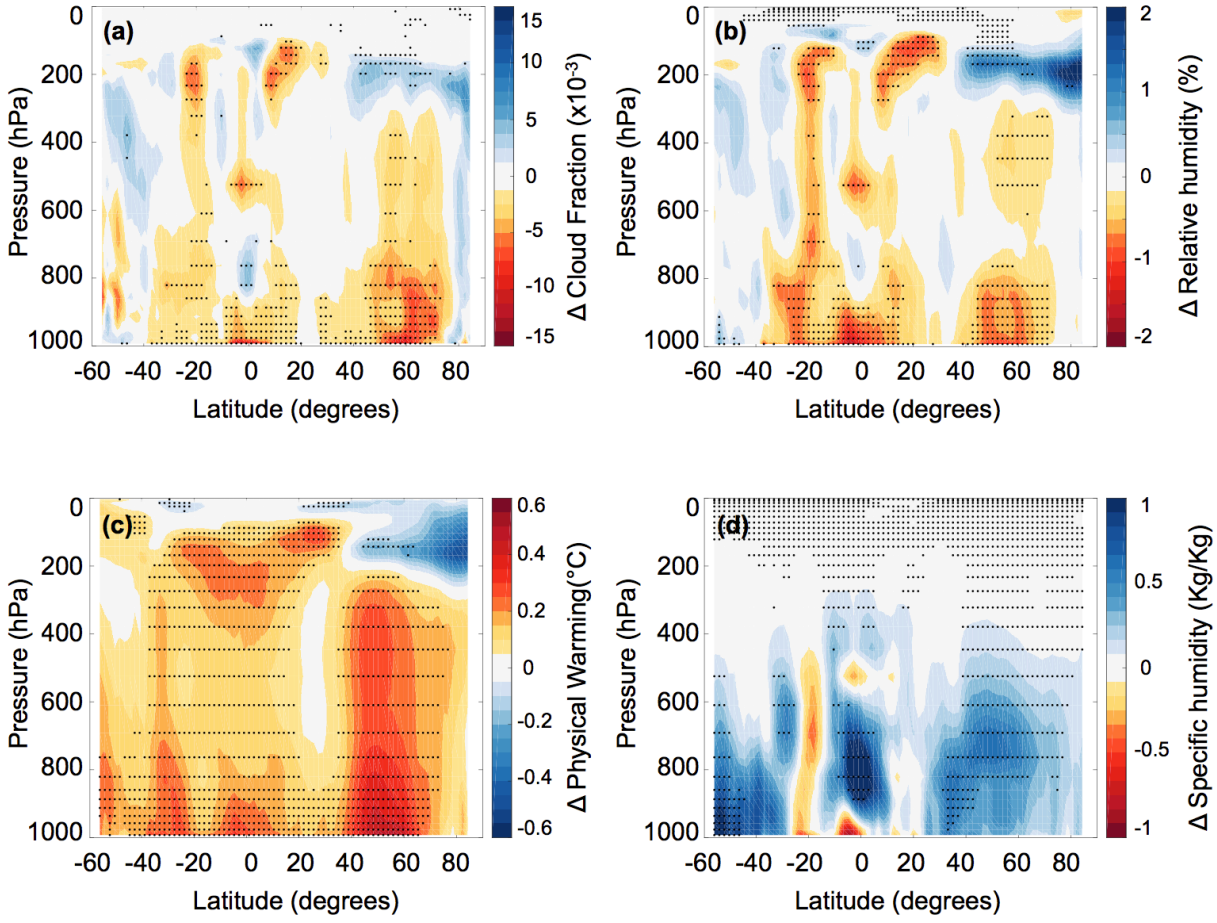

Figure A.3: Zonal annual mean change over land due to leaf acclimation to CO_2 of (a) cloud fraction; (b) relative humidity (%); (c) biogeophysical warming (°C); and (d) specific humidity (Kg Water/Kg). Stippling indicates significance at the 95% level.

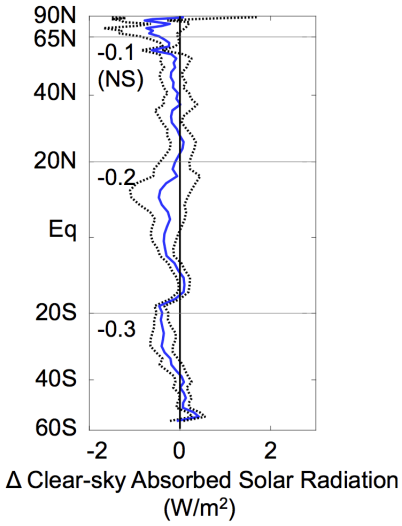

Figure A.4: Zonal annual mean change over land due to leaf acclimation (CCLMA - CC) of clear-sky solar radiation absorbed at the surface (W/m^2). The mean difference is shown in blue, along with the 95% bootstrap confidence interval (dashed black) and average zonal mean change on land (bold numbers) for each latitude band (bounded by gray lines).

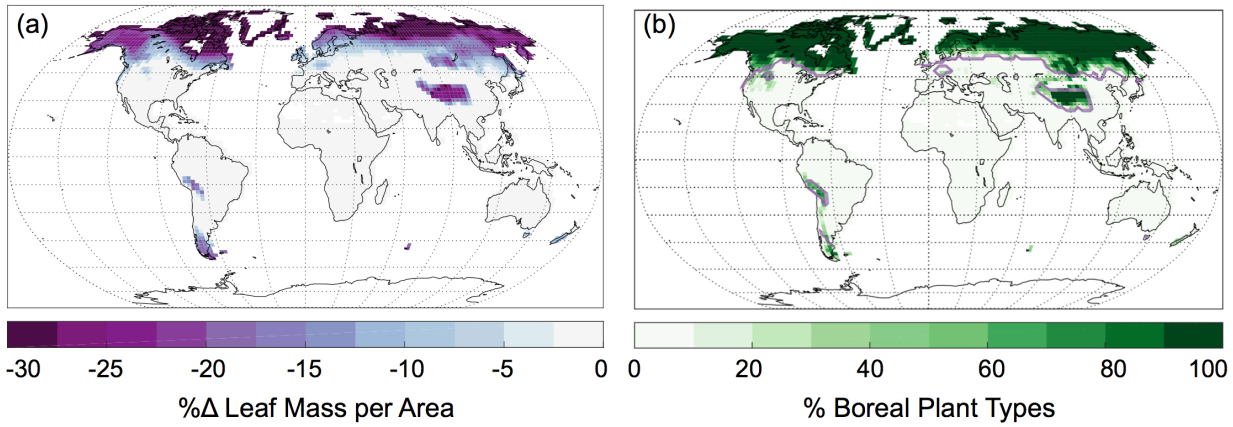

Figure A.5: (a) Potential extent of leaf mass per area change (%) due to temperature acclimation estimated from growing season temperature change (CC - CTRL) and biome-specific acclimation relationships from Poorter et al. [2009]. (b) Percent of simulated vegetated area covered by boreal plant types (boreal needleleaf evergreen and deciduous trees, boreal deciduous shrubs, and C_3 arctic grasses). Purple contours indicate -5% threshold for change in leaf mass per area due to temperature acclimation.

Table A.1: List of Earth system model simulations

Name	[CO_2]	ΔLMA	ΔPS Rates	Description
CTRL	1xCO_2	-	-	*control*
LMA	1xCO_2	+1/3	-	*historical climate + leaf mass per area change*
CC	2xCO_2	-	-	*climate change only*
CCLMA	2xCO_2	+1/3	-	*climate change + upper range of leaf mass per area acclimation to CO_2*
CCLMAPS	2xCO_2	+1/3	+1/3	*climate change + upper range of leaf mass per area acclimation to CO_2 + greater photosynthetic rates*
TCCLMA	2xCO_2	+1/3, no Δ boreal & arctic	-	*climate change + upper range of leaf mass per area acclimation to CO_2 & temperature*

Note. [CO_2], prescribed atmospheric CO_2 concentration (1xCO_2 = 355ppm, 2xCO_2 = 710ppm); ΔLMA, prescribed change in leaf mass per area for C_3 plants; ΔPS Rates, prescribed change in maximum photosynthetic rates per area for C_3 plants.

Table A.2: Confidence intervals for annual mean changes over land due to leaf trait acclimation (CCLMA - CC)

	Global	S. extratropics	Tropics	N. extratropics	N. high latitudes
	Mean (95%CI)	Mean (95%CI)	Mean (95%CI)	Mean (95%CI)	Mean (95%CI)
Biogeophysical Warming (°C)	0.3 (0.2, 0.4)	0.3 (0.2, 0.4)	0.3 (0.2, 0.4)	0.4 (0.2, 0.5)	0.2 (0.0, 0.5)
Net primary productivity (PgC/yr)	-5.8 (-5.5, -6.0)	-0.8 (-0.7, -1.0)	-2.5 (-2.3, -2.8)	-2.1 (-1.9, -2.3)	-0.3 (-0.2, -0.3)
Leaf area index (m^2/m^2)	-0.9 (-0.9, -1.0)	-0.8 (-0.7, -0.8)	-1.0 (-1.0, -1.1)	-1.0 (-0.9, -1.0)	-0.6 (-0.5, -0.6)
Evapotranspiration (W/m^2)	-0.7 (-0.5, -0.9)	-0.9 (-0.2, -1.6)	-1.2 (-0.8, -1.5)	-0.4 (-0.1, -0.6)	-0.5 (-0.3, -0.7)
Transpiration (W/m^2)	-1.4 (-1.2, -1.5)	-1.9 (-1.4, -2.4)	-1.7 (-1.5, -1.9)	-1.1 (-1.0, -1.3)	-0.6 (-0.4, -0.7)
Leaf Evaporation (W/m^2)	-0.8 (-0.7, -0.8)	-0.7 (-0.5, -0.8)	-1.3 (-1.2, -1.5)	-0.5 (-0.5, -0.6)	-0.3 (-0.3, -0.4)
Soil Evaporation (W/m^2)	1.4 (1.3, 1.6)	1.6 (1.3, 1.9)	1.9 (1.8, 2.1)	1.3 (1.1, 1.4)	0.4 (0.3, 0.5)
Absorbed Solar Radiation (W/m^2)	0.6 (0.3, 0.8)	0.8 (0.1, 1.5)	0.6 (0.3, 1.0)	0.6 (0.3, 0.9)	-0.1 (-0.4, 0.2)

Appendix B

SUPPORTING INFORMATION FOR CHAPTER 3

Marlies Kovenock[1], Charles D. Koven[2], Ryan G. Knox[2], Rosie A. Fisher[3], and Abigail L.S. Swann[4,1]

[1]Department of Biology, University of Washington, Seattle, WA; [2]Lawrence Berkeley National Laboratory, Berkeley, CA; [3]National Center for Atmospheric Research, Boulder, CO; [4]Department of Atmospheric Sciences, University of Washington, Seattle, WA.

B.1 Materials and Methods

B.1.1 Background Parameter Selection and Sensitivity Tests

We select baseline parameters for the model from an evaluation of the model's performance against observations at our tropical forest site, Barro Colorado Island, Panama, across a plant trait parameter ensemble (see Chapter 4 for details). Briefly, the benchmarking study in Chapter 4 sampled 287 plausible parameterizations from the tropical tree trait space for 12 parameters, following Koven et al., [unpublished]. In the sampling process, values for six parameters — leaf mass per area at the top of the canopy, maximum rate of carboxylation at the top of the canopy ($V_{cmax25top}$), wood density, leaf carbon to nitrogen ratio, leaf longevity, and background mortality rate — were sampled from the observed trait space for tropical trees at Barro Colorado Island and two nearby sites, Parque Natural Metropolitano and Bosque Protector San Lorenzo, Panama. Values for the remaining six parameters were sampled from plausible distributions as observational constraints are lacking. These parameters include the slope parameter in the Ball-Berry stomatal conductance model and several allometric parameters: parameters that control the intercepts in the relationships between diameter at breast height and plant crown area, as well as diameter at breast height and target allometric leaf biomass; a parameter that controls the exponential in the relationships between diameter at breast height and both plant crown area and target allometric leaf biomass; the ratio of target leaf biomass to target fine root biomass; and the intercept of the relationship between sapwood area to leaf area. Parameter sampling maintained observed covariance between traits.

The performance of each ensemble member was evaluated against six observed variables at our test site: leaf area index [Detto et al., 2018], above-ground biomass [Meakem et al., 2018, Feeley et al., 2007, Baraloto et al., 2013], basal area [Condit et al., 2017, 2012, Condit, 1998, Hubbell et al., 1999], and gross primary productivity, latent heat, and sensible heat fluxes from eddy covariance measurements [Koven et al., unpublished].

Three parameter sets performed particularly well when benchmarked against these ob-

servations across several formulations of model skill. The main text of this paper reports results from the highest performing parameter set. We test the sensitivity of the results in the main text to parameter selection using the next two highest performing parameter sets, and report results in Section B.2. These parameter sets are described in further detail in Chapter 4 and made publicly available through the University of Washington Libraries ResearchWorks digital repository. The URL for the parameter files in the ResearchWorks system is http://hdl.handle.net/1773/43779. Two changes were made to the publicly available parameter sets prior to running our competition experiments. First, we allowed the simulation of two plant functional types by changing the parameter controlling initial seedling density (recruit_initd) from 0 to 0.2 for the second plant type in the parameter file; and 2) we changed the competitive exclusion parameter (comp_excln) from -1 to 3 to minimize random stochastic influences on competitive outcomes in our simulations. Parameter set numbers 1, 2, and 3 herein correspond to parameter set numbers 86, 151, and 260 in the publicly available files, respectively.

B.1.2 Leaf Trait Plasticity Implementation

We implemented 13 combinations of leaf mass per area (LMA) and leaf carbon to nitrogen ratio (C:N_{leaf}) responses to a doubling of carbon dioxide (CO_2) in the FATES model by directly manipulating the parameters that control these traits. In the FATES model, LMA is controlled by a parameter for specific leaf area at the top of the canopy (fates_leaf_slatop, m^2 leaf area g^{-1} C), which is the inverse of LMA. C:N_{leaf} is set by a separate parameter (fates_leaf_cn_ratio, g C g^{-1} N). In our experiments, we scaled the parameters controlling LMA and C:N_{leaf} so that these traits changed by magnitudes we sampled from the observed trait space. These levels of change included no change and one-twelfth, one-sixth, one-fourth, and one-third increases (gray squares in main text Figure 3.1).

Together LMA and C:N_{leaf} control the amount of nitrogen present per leaf area (N_{area}, g N m^{-2} leaf area) in the FATES model, as described by Equation 3.1 in the main text. As leaves gain more mass per area (increase LMA), the amount of leaf nitrogen per leaf area

increases. As leaves increase the ratio of carbon to nitrogen in leaves (increase C:N_{leaf}), less nitrogen is present per leaf area.

As photosynthetic enzymes require nitrogen, the magnitude of leaf nitrogen per area is closely associated with area-based maximum photosynthetic and respiration rates [Drake et al., 1997, Kattge et al., 2009, 2011, Walker et al., 2014, Norby et al., 2017, Reich et al., 2008]. FATES explicitly represents this relationship between leaf nitrogen per area and leaf maintenance respiration rates as follows:

$$R_{m25} = R_m \cdot N_{area} \tag{B.1}$$

where R_{m25} is the rate of leaf maintenance respiration at the top of the canopy at 25°C (μ mol CO_2 m^{-2} s^{-1}), R_m is a baseline leaf maintenance respiration rate at 25°C at the top of the canopy, and N_{area} is the nitrogen per leaf area (g N m^{-2} leaf area). As leaf maintenance respiration per area scales with leaf N_{area} following Equation B.1, it too increases with LMA. On the other hand, increasing the C:N_{leaf} lowers leaf N_{area} and leaf maintenance respiration rates. As FATES does not explicitly represent the relationship between leaf N_{area} and maximum photosynthetic rates (V_{cmax25}, J_{max25}, T_{pmax25}), we impose this dependency in our simulations by scaling the maximum photosynthetic rates by the proportional change in leaf N_{area} resulting from our experimental changes in LMA and C:N_{leaf} (following Equation 3.1 in the main text). In our experiments, we scale the parameter for V_{cmax25} at the top of the canopy by the proportional change in N_{area} using the following relationship (based on Equation B.1):

$$V_{cmax25,plasticity} = V_{cmax25} \cdot \Delta N_{area} \tag{B.2}$$

where $V_{cmax25,plasticity}$ is the maximum rate of carboxylation at the top of the canopy at 25°C in our leaf trait plasticity experiments, V_{cmax25} is the control parameter value representing

the maximum rate of carboxylation at the top of the canopy at 25°C, and ΔN_{area} is the proportional change in leaf nitrogen per area due to changes in LMA and $C{:}N_{leaf}$ in each of our leaf trait plasticity experiments. In the model, other maximum photosynthetic rates J_{max25} and T_{pmax25} are calculated in proportion to V_{cmax25} and thus change in proportion to leaf N_{area} in our experiments as well. Experimental evidence shows that plants can alter the fraction of leaf nitrogen used for photosynthetic enzymes, and the partitioning between the different photosynthetic enzymes that carry out the different photosynthetic rates [e.g., V_{cmax}, J_{max}; Xu et al., 2012, Leakey et al., 2012b]. Here we test the baseline assumption that this does not occur. Future work could investigate these changes in nitrogen allocation.

B.1.3 Allometric Assumptions and Sensitivity Tests

We test the sensitivity of our results to two alternative assumptions about tree allometry, described below. We report the results of these sensitivity tests in Section B.2.

Conserve Leaf Area vs. Leaf Biomass

The model set up for the experiments reported in the main text assumes that tropical trees conserve target leaf area, rather than a target leaf biomass, when LMA changes in response to elevated CO_2. In the default version of the model, all trees have a target "on allometry" leaf biomass that is determined by the allometry parameters for that plant functional type and the tree size as measured by diameter at breast height. Trees in the model try to maintain this leaf biomass when enough carbon is available, and if leaf layers remain in positive carbon balance (i.e., leaf layer annual productivity is greater or equal to the carbon cost of building and maintaining the leaf layer). This explicit target leaf biomass corresponds with an implicit target leaf area index. Experiments presented in the main text assume that trees can attempt to maintain their control target leaf area index by allocating additional carbon to leaves when a unit of leaf area becomes more expensive in terms of carbon to build as a result of increasing LMA. Meta-analysis of observations across over 650 woody plant

species support this "conserve leaf area" allometry assumption [Duursma and Falster, 2016], which we use in our main text experiments.

We implement the conserved leaf area allometry assumption in the model by increasing the target "on allometry" leaf biomass in proportion with changes in LMA. More specifically, we increase the parameter that directly scales target leaf biomass in proportion with the changes we make to LMA in each experiment. This parameter is called the diameter to leaf biomass parameter (allom_d2bl1) and linearly scales target leaf biomass in the FATES model. This approach allows us to test the sensitivity of our results to the allometry scheme chosen by allowing higher LMA trees to approximately maintain control levels of leaf area, when they have enough carbon to do so. However, it is an estimation of the target leaf area (not necessarily exactly equal to the control target leaf area) because several other factors influence the amount of leaf area that can be produced from a given amount of carbon. First, LMA decreases with overlying leaf area index in our model, following observations [e.g., Lloyd et al., 2010]. Thus the actual cost of building leaf area depends on the overlying leaf area index, which could vary between simulations. Second, the rate of LMA decrease through the canopy depends on the maximum rate of carboxylation, following an empirical formula [Lloyd et al., 2010]. Thus, the overall cost of building leaf area also depends on the maximum rate of carboxylation, which can differ between simulations, as it is one of the trait changes we test herein. Third, the actual amount of biomass plants allocate toward leaf growth in our model can differ from the target amount based on their productivity and whether leaves at the bottom of the canopy are able to achieve carbon balance. If leaves are in negative carbon balance (i.e., require more carbon to build and maintain then they bring in through photosynthesis each year), trees allocate less carbon to leaves until they reach a positive carbon balance for each leaf layer in the canopy.

We test the sensitivity of our results to the "conserve leaf area" allometric assumption by repeating all simulations with the alternative assumption that trees "conserve leaf biomass." Under the "conserve leaf biomass" assumption leaf area is more limited when LMA is increased because leaf area becomes more expensive to build in terms of carbon but trees do

not increase the overall target amount of leaf biomass they attempt to allocate to leaves. Thus, leaf area index is expected to decrease with increases in LMA under this allometry assumption. This is the default allometric assumption in the FATES model, and does not require model modifications to implement. This assumption also conserves the relationship between leaf and fine root biomass (details below).

Conserve Area- vs. Mass-Based Relationship between Leaves and Fine Roots

Our main text experiments assume that trees conserve the relationship between leaf area and fine root surface area, which we refer to as the "area-based" relationship. This area-based relationship between leaves and roots could be driven by the need for root surface area to match leaf area for water transport. In the default model set up, target fine root biomass is calculated in proportion to target leaf biomass. In order to test the influence of instead conserving the area-based relationship between leaves and fine roots when leaf traits respond to elevated CO_2 we alter this relationship for the experiments reported in the main text. To conserve the target fine root biomass while altering the target leaf biomass (in order to conserve the target leaf area and root area when LMA changes), we make a simultaneous and inversely proportional change to the ratio of fine root to leaf area parameter (allom_l2fr), which linearly scales target leaf biomass to calculate target fine root biomass.

Alternatively, trees could conserve the mass-based (rather than area-based) relationship between leaves and fine roots to support water transport. We therefore test the sensitivity of our main text results, which conserve the area-based relationship, to conserving the mass-based relationship instead by repeating all simulations with the mass-based relationship. This is the default assumption in our model setup and therefore does not require changes to implement. Under this assumption trees can increase carbon allocation to leaves to attempt to conserve leaf area as LMA increases but, they must also pay a carbon cost to additionally allocate more carbon to fine roots. We refer to this case as the "conserved leaf area, with mass-based leaf to root relationship."

B.1.4 Statistical Analysis

Several variables have time series that are non-normally distributed, have unequal variances, and temporal autocorrelation. Thus, we tested for differences between means using stationary bootstrap methods [Politis and Romano, 1994, Quilis, 2015] with n=50,000. We used automatic estimation [Patton, 2007, Patton et al., 2009, Politis and White, 2004] to determine the optimal block length for each stationary bootstrap. Time series that failed the Augmented Dickey-Fuller test for stationarity [Said and Dickey, 1984, and Matlab version 2015b *adftest* function] were de-trended prior to statistical analysis. We used the percentile method [Efron and Gong, 1983, Efron and Tibshirani, 1994] to determine differences significant at the 95% level. Confidence intervals for average annual means and differences were constructed from their bootstrap distributions.

B.2 Results

B.2.1 Sensitivity to Background Parameterization and Allometric Assumptions

Ecosystem Properties

We find that the qualitative influence of leaf trait plasticity on biomass, carbon uptake, and evapotranspiration is not generally sensitive to the parameterizations and allometry assumptions we tested (Figures B.1, B.4, B.5).

The influence of leaf trait plasticity on leaf area index is also qualitatively robust across our sensitivity tests with one exception. The response pattern for leaf area index differs when the alternative allometric assumption is made that trees conserve a target leaf biomass rather than a target leaf area when LMA changes. Under this alternative allometric assumption increasing LMA no longer consistently enhances leaf area index (Figure B.2). This result is expected given that increasing LMA raises the carbon cost of building leaf area but, trees do not increase their target leaf biomass to compensate for this additional cost under the alternative "conserve leaf biomass" assumption. However, a meta-analysis of observations [Duursma and Falster, 2016] suggests that trees adhere to the allometric assumption we

use in our main text experiments by conserving leaf area across variation in LMA, lending support to the robustness of our main text results.

Competitive Ability

Our finding that the control leaf (no leaf trait plasticity) is more competitively advantageous than leaf trait plasticity levels that result in decreases in N_{area} (-N_{area}) is qualitatively robust to the background parameterizations and allometry assumptions we tested (Figure B.3).

However, whether increasing LMA enhances competitive ability, as found in our main text experiments, is sensitive to assumptions about tree allometry. Notably, increasing LMA no longer consistently enhances competitive ability when the assumption is made that trees conserve the mass-based relationship between leaves and fine roots (rather than area-based relationship as in the main text results; Figure B.3). Under this assumption, trees increase target root mass in proportion with increases in LMA. This increase in root mass with leaf mass could occur to support water transport or the additional nutrient requirements for leaves with greater LMA. The additional root mass requirement under this assumption makes it even more costly to increase LMA, which we expect should reduce the competitive advantage of doing so. In this case, we find that the control plant type is always at a competitive advantage, and the benefit of increasing LMA that we saw in our primary results no longer consistently occurs (Figure B.3). We hypothesize that higher baseline photosynthetic rates, as occur in parameterization #2 (Table B.1), could enable plants to offset this additional cost of root mass and allow them to enhance competitive advantage through increases in LMA despite the higher root mass requirement (parameterization #2, Figure B.3).

Total Canopy Nitrogen

Total canopy nitrogen can be calculated from the inverse of C:N_{leaf}, which describes the amount of nitrogen required to support each unit of leaf carbon biomass (g N g^{-1} C leaf), and the total carbon leaf biomass (g C). In our main text experiments changes in LMA

can influence total canopy nitrogen by altering the target total carbon leaf biomass (details in Section B.1), as is supported by observations [Duursma and Falster, 2016]. Under this allometric assumption, we find that a decrease in leaf N_{area}, which incorporates information about both $C{:}N_{leaf}$ and LMA (main text Equation 3.1), is required to maintain the total canopy nitrogen requirement at the 1xCO_2 level (Figure B.3).

This finding is robust across our sensitivity tests with one notable exception. $C{:}N_{leaf}$ rather than N_{area} is the dominant driver of changes in total canopy nitrogen under the "conserve leaf biomass" allometric assumption (Figure B.3). Under this assumption, trees conserve their target leaf biomass rather than their target leaf area and changes in LMA no longer directly alter target leaf biomass. As target leaf biomass no longer varies with LMA, changes in $C{:}N_{leaf}$ become the dominant driver of total canopy nitrogen under this allometric assumption. However, it is important to note that while this alternative allometric assumption provides an interesting sensitivity test, observations support the allometric assumption used in our main text experiments [Duursma and Falster, 2016].

B.3 Figures and Tables

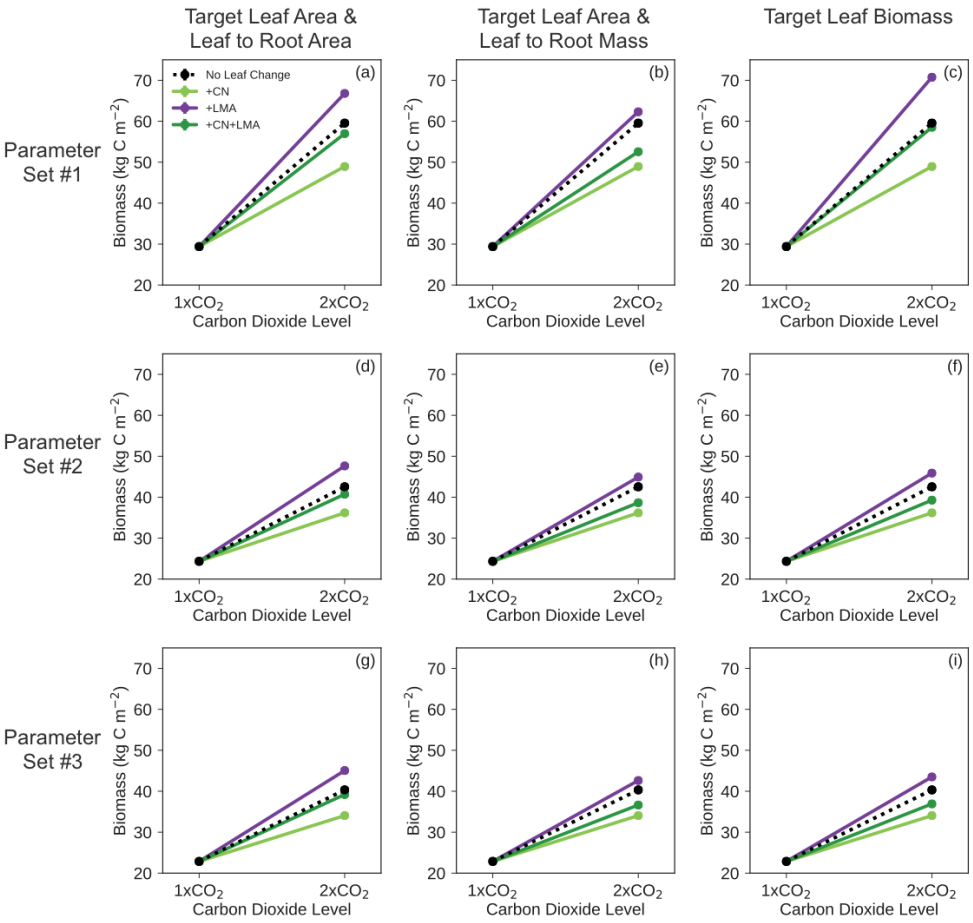

Figure B.1: Annual mean biomass (kg C m^{-2}) for the 1xCO$_2$ control, 2xCO$_2$ control (black), and the following leaf trait plasticity levels in the absence of competition: a one-third increase in leaf C:N alone (+CN, light green), a one-third increase in leaf mass per area alone (+LMA, purple), and a one-third increase in both leaf C:N and leaf mass per area (+CN+LMA, dark green). Error bars show bootstrap 95% confidence intervals for the mean value. Main text results shown in panel (a). Rows group results by the three background parameterizations tested. Columns group results by allometry assumption: experiments that conserve target leaf area and the area-based leaf to fine root relationship (a, d, g), experiments that conserve target leaf area and the mass-based leaf to fine root relationship (b, e, h), and experiments that conserve target leaf biomass (c, f, i).

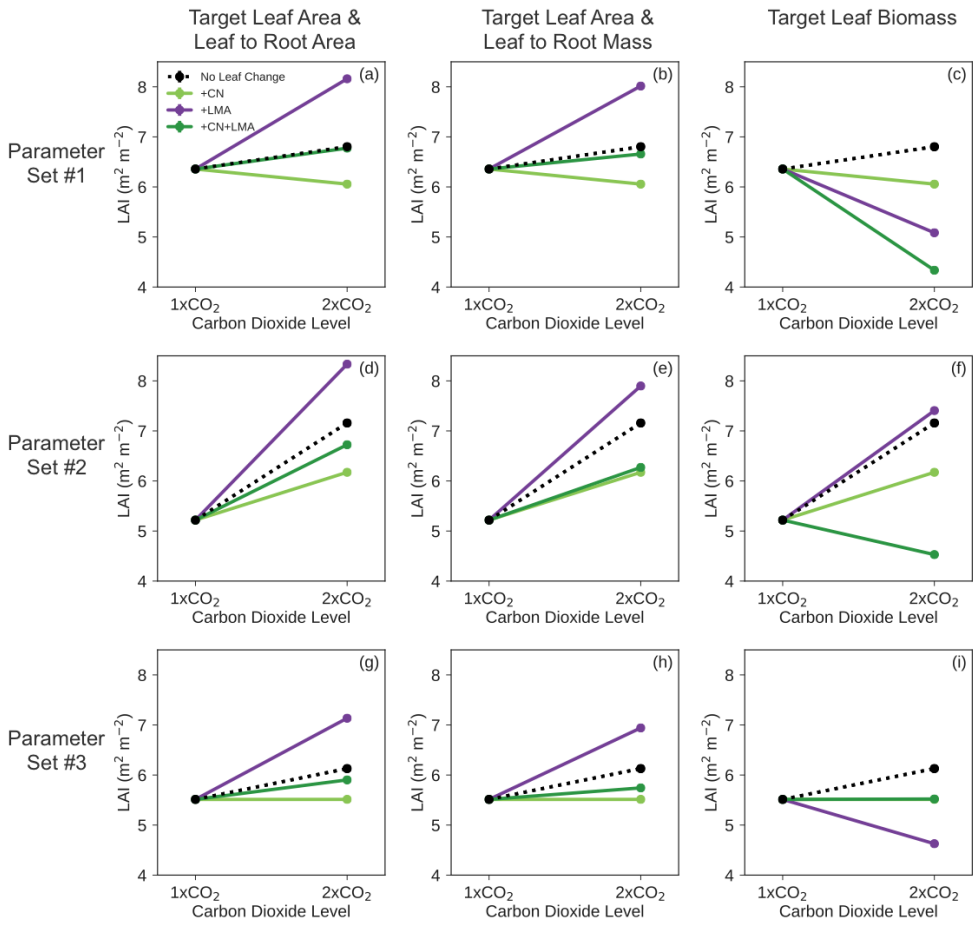

Figure B.2: Annual mean leaf area index (LAI, m^2 m^{-2}) for the $1xCO_2$ control, $2xCO_2$ control (black), and the following leaf trait plasticity levels in the absence of competition: a one-third increase in leaf C:N alone (+CN, light green), a one-third increase in leaf mass per area alone (+LMA, purple), and a one-third increase in both leaf C:N and leaf mass per area (+CN+LMA, dark green). Error bars show bootstrap 95% confidence intervals for the mean value. Main text results shown in panel (a). Rows group results by the three background parameterizations tested. Columns group results by allometry assumption: experiments that conserve target leaf area and the area-based leaf to fine root relationship (a, d, g), experiments that conserve target leaf area and the mass-based leaf to fine root relationship (b, e, h), and experiments that conserve target leaf biomass (c, f, i). +CN+LMA and +CN overlap in panel (i).

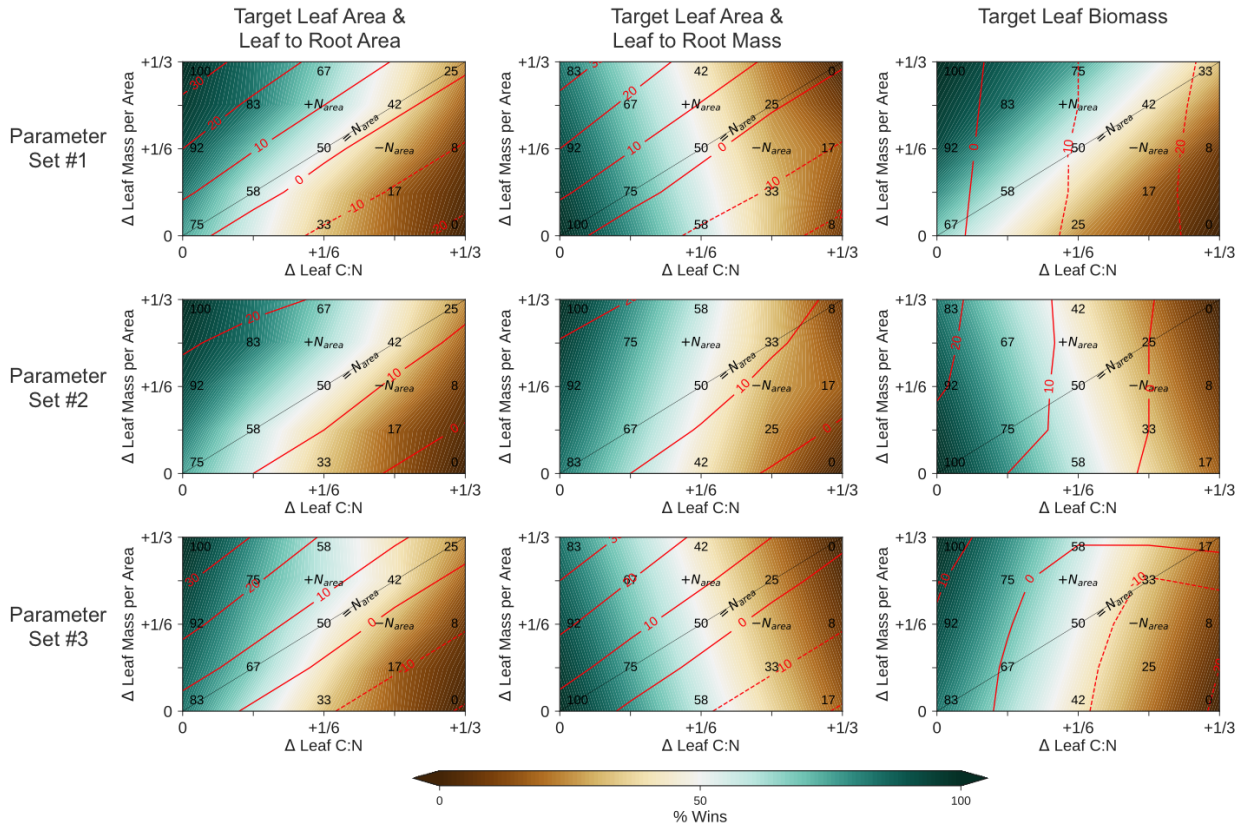

Figure B.3: The percent of pairwise competitions won (% Wins, color shading and black numbers) and percent change in total canopy nitrogen compared to the 1xCO_2 control (red contours) for each leaf trait plasticity level of leaf C:N and leaf mass per area. Percent wins for sampled trait changes (black numbers). Diagonal line (dashed black) indicates where nitrogen per area (N_{area}, g N m^{-2} leaf area) remains at control levels (=N_{area}). Leaf trait plasticity levels below the diagonal line reduce N_{area} (-N_{area}) compared to the control plant type. Leaf trait plasticity levels above the diagonal line enhance N_{area} (+N_{area}) compared to the control plant type. Linear interpolation used to estimate percent wins and change in total canopy nitrogen between sampled trait changes. Main text results shown in panel (a). Rows group results by the three background parameterizations tested. Columns group results by allometry assumption: experiments that conserve target leaf area and the area-based leaf to fine root relationship (a, d, g), experiments that conserve target leaf area and the mass-based leaf to fine root relationship (b, e, h), and experiments that conserve target leaf biomass (c, f, i).

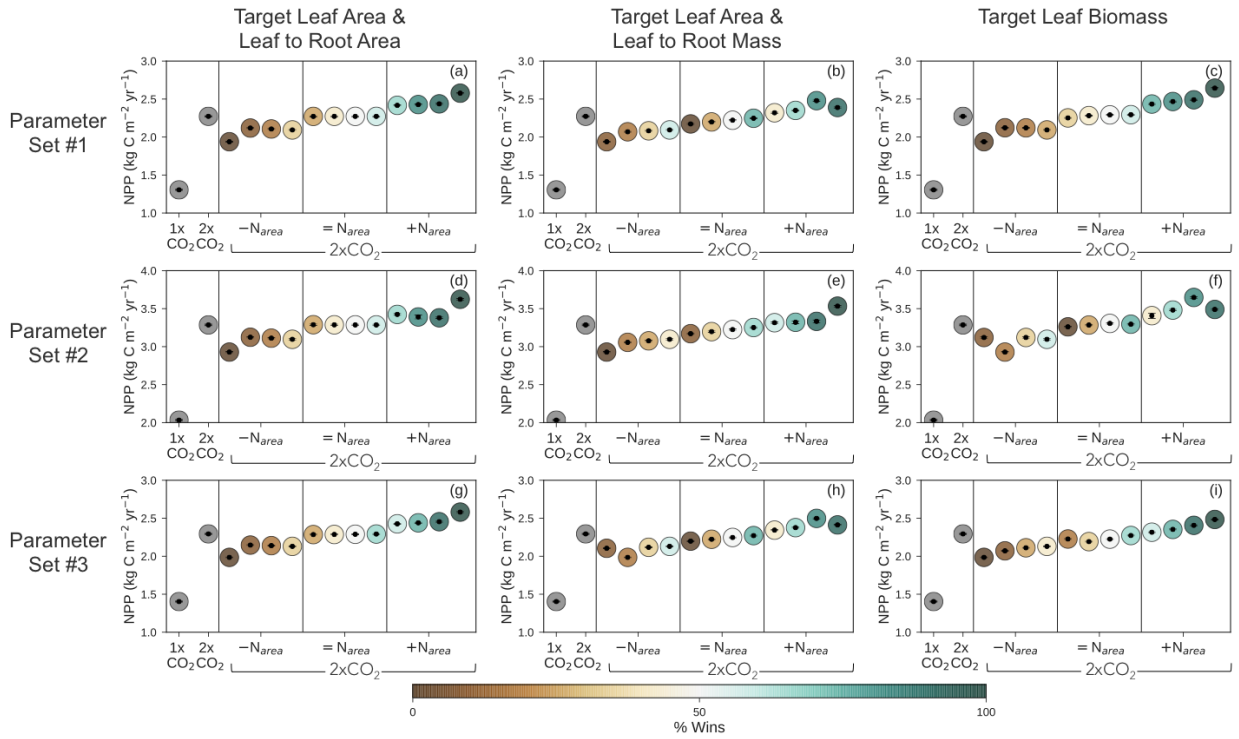

Figure B.4: Annual mean net primary productivity (NPP, kg C m^{-2} yr^{-1}) for the 1xCO_2 control, 2xCO_2 control (no leaf trait plasticity), and 12 ecosystems each consisting entirely of one plant type with a different level of leaf trait plasticity sampled from the -N_{area}, =N_{area}, and +N_{area} plasticity spaces. Color indicates the percentage of all pairwise competitions won by each level of leaf trait plasticity (% Wins). Error bars show bootstrap 95% confidence intervals for the mean value. Main text results shown in panel (a). Rows group results by the three background parameterizations tested. Columns group results by allometry assumption: experiments that conserve target leaf area and the area-based leaf to fine root relationship (a, d, g), experiments that conserve target leaf area and the mass-based leaf to fine root relationship (b, e, h), and experiments that conserve target leaf biomass (c, f, i).

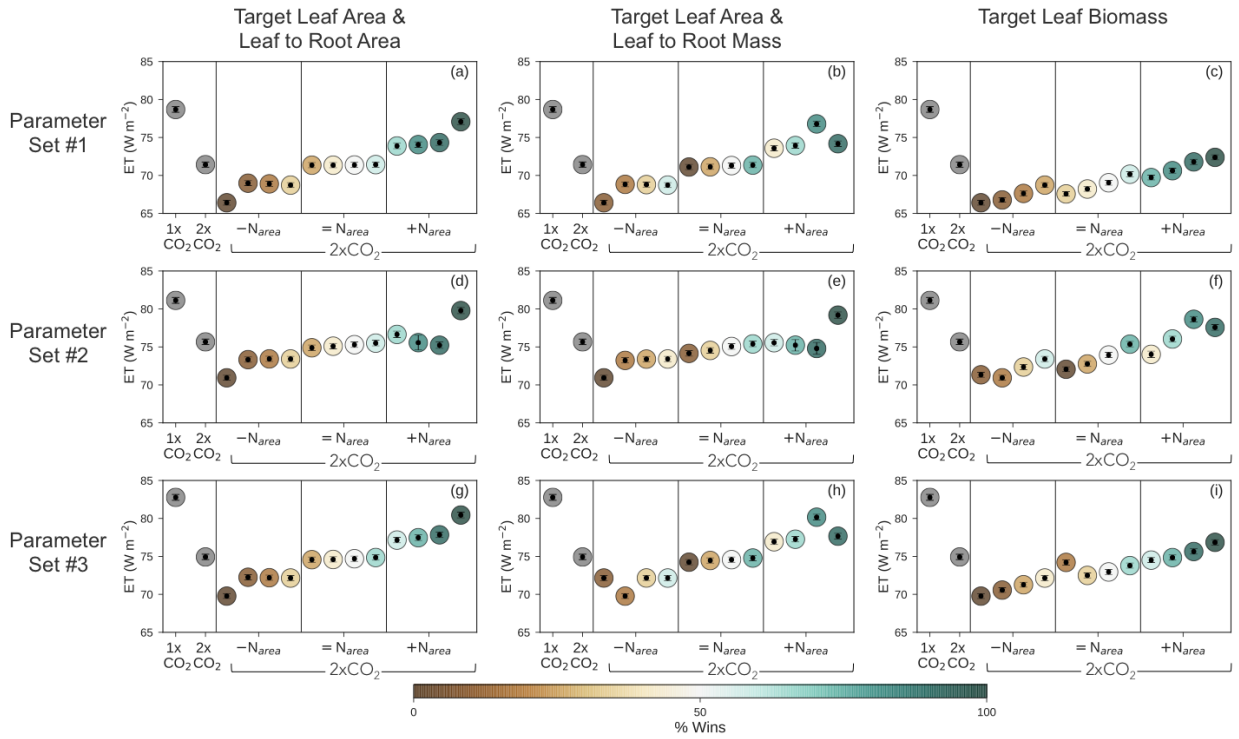

Figure B.5: Annual mean evapotranspiration (ET, W m^{-2}) for the 1xCO_2 control, 2xCO_2 control (no leaf trait plasticity), and 12 ecosystems each consisting entirely of one plant type with a different level of leaf trait plasticity sampled from the -N_{area}, =N_{area}, and +N_{area} plasticity spaces. Color indicates the percentage of all pairwise competitions won by each level of leaf trait plasticity (% Wins). Error bars show bootstrap 95% confidence intervals for the mean value. Main text results shown in panel (a). Rows group results by the three background parameterizations tested. Columns group results by allometry assumption: experiments that conserve target leaf area and the area-based leaf to fine root relationship (a, d, g), experiments that conserve target leaf area and the mass-based leaf to fine root relationship (b, e, h), and experiments that conserve target leaf biomass (c, f, i).

Table B.1: Baseline values for parameter sensitivity test

Trait Parameter	**Set #1** Main Results	**Set #2** Sensitivity Test	**Set #3** Sensitivity Test
Leaf C:N ratio (g C g^{-1} N)	20.9	24.1	21.3
Leaf mass per area (g C m^{-2})	44.4	70.4	54.3
V_{cmax25} (μmol CO_2 m^{-2} s^{-1})	62.6	106.6	52.1

Notes. Maximum rate of carboxylation at 25°C (V_{cmax25}) and leaf mass per area values are at top of canopy.

Appendix C

SUPPORTING INFORMATION FOR CHAPTER 4

This appendix describes the code changes made to the Functionally Assembled Terrestrial Ecosystem Simulator (FATES) to implement the canopy profile of specific leaf area described in Chapter 4.

C.1 Tree Leaf Area Index Function

The following code was implemented in the FatesAllometryMod.F90 file of the FATES code to calculate leaf area index using dynamic values of specific leaf area that increase with overlying leaf area index.

```
real(r8) function tree_lai( bl, pft, c_area, nplant, cl, canopy_lai)

  ! ------------------------------------------------------------------------
  ! LAI of individual trees is a function of the total leaf area
  ! and the total canopy area.
  ! ------------------------------------------------------------------------

  ! !ARGUMENTS
  real(r8), intent(in) :: bl                      ! plant leaf biomass [kg]
  integer, intent(in)  :: pft                     ! plant functional type index
  real(r8), intent(in) :: c_area                  ! areal extent of canopy (m2)
  real(r8), intent(in) :: nplant                  ! number individuals in cohort/ha
  integer, intent(in)  :: cl                      ! canopy layer index
  real(r8), intent(in) :: canopy_lai(nclmax)      ! total leaf area index of
                                                  ! each canopy layer

  ! !LOCAL VARIABLES:
  real(r8) :: leafc_per_unitarea ! KgC of leaf per m2 area of ground.
  real(r8) :: slat               ! the sla of the top leaf layer. m2/kgC
  real(r8) :: canopy_lai_above   ! total LAI of canopy layer overlying this tree
  real(r8) :: vai_per_lai        ! ratio of vegetation area index (ie. sai+lai)
                                 ! to lai for individual tree
```

```
real(r8) :: kn                ! coefficient for exponential decay of 1/sla and
                              ! vcmax with canopy depth
real(r8) :: sla_max           ! Observational constraint on how large sla
                              ! (m2/gC) can become
real(r8) :: leafc_slamax      ! Leafc_per_unitarea at which sla_max is reached
real(r8) :: clim              ! Upper limit for leafc_per_unitarea in exponential
                              ! tree_lai function
!---------------------------------------------------------------------

if( bl  <  0._r8 .or. pft  ==  0 ) then
   write(fates_log(),*) 'problem␣in␣treelai',bl,pft
endif

slat = g_per_kg * EDPftvarcon_inst%slatop(pft) ! m2/g to m2/kg
leafc_per_unitarea = bl/(c_area/nplant) !KgC/m2

if(leafc_per_unitarea > 0.0_r8)then


   if (cl==1) then ! if in we are in the canopy (top) layer)
      canopy_lai_above = 0._r8
   else
      canopy_lai_above = sum(canopy_lai(1:cl-1))
   end if

   ! Coefficient for exponential decay of 1/sla with canopy depth:
   kn = decay_coeff_kn(pft)

   ! take PFT-level maximum SLA value,
   ! even if under a thick canopy (which has units of m2/gC),
   ! and put into units of m2/kgC
   sla_max = g_per_kg *EDPftvarcon_inst%slamax(pft)

   ! Leafc_per_unitarea at which sla_max is reached
   ! due to exponential sla profile in canopy:
   leafc_slamax = (slat - sla_max * exp(-1.0_r8 * kn * canopy_lai_above)) / &
        (-1.0_r8 * kn * slat * sla_max)
   if(leafc_slamax < 0.0_r8)then
      leafc_slamax = 0.0_r8
   endif

   ! Calculate tree_lai (m2 leaf area /m2 ground) = unitless LAI
```

```
!-----------------------------------------------------------------------
! If leafc_per_unitarea is less than leafc_slamax,
! sla with depth in the canopy will not exceed sla_max.
! In this case, we can use an exponential profile for
! sla throughout the entire canopy.
! The exponential profile for sla is given by:
! sla(at a given canopy depth) = slat / exp(-kn (canopy_lai_above + tree_lai)
!
! We can solve for tree_lai using the above function for the sla profile
! and first setting
! leafc_per_unitarea = integral of e^(-kn(x + canopy_lai_above)) / slatop
! over x = 0 to tree_lai
! Then, rearranging the equation to solve for tree_lai.

if (leafc_per_unitarea <= leafc_slamax)then
   tree_lai = (log(exp(-1.0_r8 * kn * canopy_lai_above) - &
        kn * slat * leafc_per_unitarea) + &
        (kn * canopy_lai_above)) / (-1.0_r8 * kn)

   ! If leafc_per_unitarea becomes too large,
   ! tree_lai becomes an imaginary number
   ! (because the tree_lai equation requires us to
   ! take the natural log of something >0)
   ! Thus, we include the following error message
   ! in case leafc_per_unitarea becomes too large.
   clim = (exp(-1.0_r8 * kn * canopy_lai_above)) / (kn * slat)
   if (leafc_per_unitarea >= clim) then
      write(fates_log(),*) 'too␣much␣leafc_per_unitarea' , &
           leafc_per_unitarea, clim, pft, canopy_lai_above
      write(fates_log(),*) 'Aborting'
      call endrun(msg=errMsg(sourcefile, __LINE__))
   endif

   ! When leafc_per_unitarea is greater than leafc_slamax,
   ! tree_lai could become so great that the sla profile
   ! surpasses sla_max at depth.
   ! In this case, we use the exponential profile to calculate tree_lai until
   ! we reach the maximum allowed value for sla (sla_max).
   ! Then, calculate the remaining tree_lai using a linear function of
   ! sla_max and the remaining leafc.

else if(leafc_per_unitarea > leafc_slamax)then
```

```
        ! Add exponential and linear portions of tree_lai
        ! Exponential term for leafc = leafc_slamax;
        ! Linear term (static sla = sla_max) for portion of leafc > leafc_slamax
        tree_lai = ((log(exp(-1.0_r8 * kn * canopy_lai_above) - &
             kn * slat * leafc_slamax) + &
             (kn * canopy_lai_above)) / (-1.0_r8 * kn)) + &
             (leafc_per_unitarea - leafc_slamax) * sla_max

        ! if leafc_slamax becomes too large,
        ! tree_lai_exp becomes an imaginary number
        ! (because the tree_lai equation requires us to
        ! take the natural log of something >0)
        ! Thus, we include the following error message
        ! in case leafc_slamax becomes too large.
        clim = (exp(-1.0_r8 * kn * canopy_lai_above)) / (kn * slat)
        if(leafc_slamax >= clim)then
           write(fates_log(),*) 'too much leafc_slamax' , &
                leafc_per_unitarea, leafc_slamax, clim, pft, canopy_lai_above
           write(fates_log(),*) 'Aborting'
           call endrun(msg=errMsg(sourcefile, __LINE__))
        endif
     end if ! (leafc_per_unitarea  > leafc_slamax)
  else
     tree_lai = 0.0_r8
  endif ! (leafc_per_unitarea > 0.0_r8)

  return
end function tree_lai
```

C.2 Decay Coefficient Function

The following code was implemented in the FatesAllometryMod.F90 file of the FATES code to calculate the decay coefficient used to estimate the profiles of specific leaf area and maximum photosynthetic rates.

```
real(r8) function decay_coeff_kn(pft)
  ! ------------------------------------------------------------------------
  ! This function estimates the decay coefficient used to estimate vertical
  ! attenuation of properties in the canopy.
  !
```

```
    ! Decay coefficient (kn) is a function of vcmax25top for each pft.
    !
    ! Currently, this decay is applied to vcmax attenuation, and SLA (optionally)
    !
    ! ------------------------------------------------------------------------

    !ARGUMENTS
    integer, intent(in) :: pft

    !LOCAL VARIABLES
    ! ------------------------------------------------------------------------

    ! Bonan et al (2011) JGR, 116, doi:10.1029/2010JG001593 used
    ! kn = 0.11. Here, we derive kn from vcmax25 as in Lloyd et al
    ! (2010) Biogeosciences, 7, 1833-1859

    decay_coeff_kn = exp(0.00963_r8 * EDPftvarcon_inst%vcmax25top(pft) - 2.43_r8)

    return
end function decay_coeff_kn
```

C.3 Canopy Trimming Function

The trim_canopy subroutine within the EDPhysiologyMod.F90 file of the FATES source code was modified to account for increasing values of specific leaf area through the canopy. This subroutine determines if each leaf layer is in positive carbon balance. Specific leaf area is used to determine the carbon cost of each leaf layer.

```
  subroutine trim_canopy( currentSite )
    !
    ! !DESCRIPTION:
    ! Canopy trimming / leaf optimisation.
    ! Removes leaves in negative annual carbon balance.
    !
    ! !USES:

    ! !ARGUMENTS
    type (ed_site_type),intent(inout), target :: currentSite
    !
    ! !LOCAL VARIABLES:
```

```
type (ed_cohort_type) , pointer :: currentCohort
type (ed_patch_type)  , pointer :: currentPatch

integer  :: z               ! leaf layer
integer  :: ipft            ! pft index
logical  :: trimmed         ! was this layer trimmed in this year?
                               !If not expand the canopy.
real(r8) :: tar_bl          ! target leaf biomass       (leaves flushed, trimmed)
real(r8) :: tar_bfr         ! target fine-root biomass  (leaves flushed, trimmed)
real(r8) :: bfr_per_bleaf   ! ratio of fine root per leaf biomass
real(r8) :: sla_levleaf     ! sla at leaf level z
real(r8) :: nscaler_levleaf ! nscaler value at leaf level z
integer  :: cl              ! canopy layer index
real(r8) :: kn              ! nitrogen decay coefficient
real(r8) :: sla_max         ! Observational constraint on how large
                               ! sla (m2/gC) can become

real(r8) :: leaf_inc           ! LAI-only portion of the vegetation increment of dinc_ed
real(r8) :: lai_canopy_above   ! the LAI in the canopy layers above the layer of interest
real(r8) :: lai_layers_above   ! the LAI in the leaf layers, within the current canopy,
                               ! above the leaf layer of interest
real(r8) :: lai_current        ! the LAI in the current leaf layer
real(r8) :: cumulative_lai     ! the cumulative LAI, top down,
                               ! to the leaf layer of interest

!------------------------------------------------------------------------

currentPatch => currentSite%youngest_patch
do while(associated(currentPatch))

   currentCohort => currentPatch%tallest
   do while (associated(currentCohort))

      trimmed = .false.
      ipft = currentCohort%pft
      call carea_allom(currentCohort%dbh,currentCohort%n,currentSite%spread, &
                                    currentCohort%pft,currentCohort%c_area)
      currentCohort%treelai = tree_lai(currentCohort%bl, currentCohort%pft, &
                                    currentCohort%c_area, currentCohort%n, &
                                    currentCohort%canopy_layer, &
                                    currentPatch%canopy_layer_tlai )
```

```
currentCohort%treesai = tree_sai(currentCohort%pft, currentCohort%dbh, &
                                 currentCohort%canopy_trim, &
                                 currentCohort%c_area, currentCohort%n, &
                                 currentCohort%canopy_layer, &
                                 currentPatch%canopy_layer_tlai, &
                                 currentCohort%treelai )

currentCohort%nv      = ceiling((currentCohort%treelai+ &
                                    currentCohort%treesai)/dinc_ed)

if (currentCohort%nv > nlevleaf)then
   write(fates_log(),*) 'nv␣>␣nlevleaf',currentCohort%nv, &
         currentCohort%treelai,currentCohort%treesai, &
         currentCohort%c_area,currentCohort%n,currentCohort%bl
   call endrun(msg=errMsg(sourcefile, __LINE__))
endif

call bleaf(currentcohort%dbh,ipft,currentcohort%canopy_trim,tar_bl)

if ( int(EDPftvarcon_inst%allom_fmode(ipft)) .eq. 1 ) then
   ! only query fine root biomass if using a fine root allometric model
   ! that takes leaf trim into account
   call bfineroot(currentcohort%dbh,ipft,currentcohort%canopy_trim,tar_bfr)
   bfr_per_bleaf = tar_bfr/tar_bl
endif

! Identify current canopy layer (cl)
cl = currentCohort%canopy_layer

! PFT-level maximum SLA value, even if under a thick canopy (same units as slatop)
sla_max = EDPftvarcon_inst%slamax(ipft)

!Leaf cost vs netuptake for each leaf layer.
do z = 1, currentCohort%nv

   ! Calculate the cumulative total vegetation area index
   ! (no snow occlusion, stems and leaves)

   leaf_inc    = dinc_ed * &
         currentCohort%treelai/(currentCohort%treelai+currentCohort%treesai)

   ! Now calculate the cumulative top-down lai of the current layer's midpoint
```

```
lai_canopy_above  = sum(currentPatch%canopy_layer_tlai(1:cl-1))
lai_layers_above  = leaf_inc * (z-1)
lai_current       = min(leaf_inc, currentCohort%treelai - lai_layers_above)
cumulative_lai    = lai_canopy_above + lai_layers_above + 0.5*lai_current

if (currentCohort%year_net_uptake(z) /= 999._r8)then
! there was activity this year in this leaf layer.


   ! Calculate sla_levleaf following the sla profile with overlying leaf area
   ! Scale for leaf nitrogen profile
   kn = decay_coeff_kn(ipft)
   ! Nscaler value at leaf level z
   nscaler_levleaf = exp(-kn * cumulative_lai)
   ! Sla value at leaf level z after nitrogen profile scaling (m2/gC)
   sla_levleaf = EDPftvarcon_inst%slatop(ipft)/nscaler_levleaf

   if(sla_levleaf > sla_max)then
      sla_levleaf = sla_max
   end if

   !Leaf Cost kgC/m2/year-1
   !decidous costs.
   if (EDPftvarcon_inst%season_decid(ipft) == 1.or. &
        EDPftvarcon_inst%stress_decid(ipft) == 1)then

      ! Leaf cost at leaf level z accounting for sla profile (kgC/m2)
      currentCohort%leaf_cost =  1._r8/(sla_levleaf*1000.0_r8)

      if ( int(EDPftvarcon_inst%allom_fmode(ipft)) .eq. 1 ) then
         ! if using trimmed leaf for fine root biomass allometry,
         ! add the cost of the root increment
         ! to the leaf increment; otherwise do not.
         currentCohort%leaf_cost = currentCohort%leaf_cost + &
              1.0_r8/(sla_levleaf*1000.0_r8) * &
              bfr_per_bleaf / EDPftvarcon_inst%root_long(ipft)
      endif

      currentCohort%leaf_cost = currentCohort%leaf_cost * &
            (EDPftvarcon_inst%grperc(ipft) + 1._r8)
   else !evergreen costs
      ! Leaf cost at leaf level z accounting for sla profile
```

```
            currentCohort%leaf_cost = 1.0_r8/(sla_levleaf* &
                 EDPftvarcon_inst%leaf_long(ipft)*1000.0_r8)
                 ! convert from sla in m2g-1 to m2kg-1
            if ( int(EDPftvarcon_inst%allom_fmode(ipft)) .eq. 1 ) then
               ! if using trimmed leaf for fine root biomass allometry,
               ! add the cost of the root increment
               ! to the leaf increment; otherwise do not.
               currentCohort%leaf_cost = currentCohort%leaf_cost + &
                    1.0_r8/(sla_levleaf*1000.0_r8) * &
                    bfr_per_bleaf / EDPftvarcon_inst%root_long(ipft)
            endif
            currentCohort%leaf_cost = currentCohort%leaf_cost * &
                  (EDPftvarcon_inst%grperc(ipft) + 1._r8)
         endif
         if (currentCohort%year_net_uptake(z) < currentCohort%leaf_cost)then
            if (currentCohort%canopy_trim > EDPftvarcon_inst%trim_limit(ipft))then

               if ( DEBUG ) then
                  write(fates_log(),*) 'trimming␣leaves', &
                        currentCohort%canopy_trim,currentCohort%leaf_cost
               endif

               ! keep trimming until none of the canopy is
               ! in negative carbon balance.
               if (currentCohort%hite > EDPftvarcon_inst%hgt_min(ipft))then
                  currentCohort%canopy_trim = currentCohort%canopy_trim - &
                        EDPftvarcon_inst%trim_inc(ipft)
                  if (EDPftvarcon_inst%evergreen(ipft) /= 1)then
                     currentCohort%laimemory = currentCohort%laimemory * &
                           (1.0_r8 - EDPftvarcon_inst%trim_inc(ipft))
                  endif
                  trimmed = .true.
               endif
            endif
         endif
      endif !leaf activity?
   enddo !z

   currentCohort%year_net_uptake(:) = 999.0_r8
   if ( (.not.trimmed) .and.currentCohort%canopy_trim < 1.0_r8)then
      currentCohort%canopy_trim = currentCohort%canopy_trim + &
                               EDPftvarcon_inst%trim_inc(ipft)
```

```
        endif

        if ( DEBUG ) then
           write(fates_log(),*) 'trimming',currentCohort%canopy_trim
        endif

        ! currentCohort%canopy_trim = 1.0_r8 !FIX(RF,032414)
        ! this turns off ctrim for now.
        currentCohort => currentCohort%shorter
      enddo
      currentPatch => currentPatch%older
   enddo

end subroutine trim_canopy
```